DISTRIBUTION OF SEISMICITY ON THE MEGATHRUST: CHARACTERIZING THE SEISMOGENIC ZONE IN THE SHUMAGIN GAP, ALASKA WITH PRECISE EARTHQUAKE LOCATIONS

A Thesis

Presented to the Faculty of the Graduate School

of Cornell University

In Partial Fulfillment of the Requirements for the Degree of

Master of Science

by

Stephanie Michelle Nale

August 2017

ABSTRACT

The fortuitous location of the Shumagin Islands above the seismogenic zone in the Alaska-Aleutian subduction zone provides an ideal opportunity to study seismic waves directly from the megathrust interface. Double-difference relative relocation of hypocenters are performed on a catalog of earthquakes from the Shumagin Gap spanning nearly a decade. Relocation results show an abrupt transition in seismicity along the plate interface at 44 km depth, from a distinct 4 – 8 km thick plane to a broad zone of sparse seismicity. In the eastern area of the network, deeply rooted faults appear to cut into the downgoing plate, dipping steeply trenchward. Active faults within the upper plate seem to correlate with the strike of mapped normal faults and a splay fault imaged within an MCS reflection profile in the Eastern Sanak Basin. Further investigation of these splay faults may provide important information relating to tsunamigensis in the Shumagin Gap.

BIOGRAPHICAL SKETCH

Stephanie Nale was born and raised in California. Beginning at a young age, she spent a lot of time outside, running amok and exploring the world around her. She loved climbing trees, exploring the forests and fields, and playing in the creek with her brother and sister. In high school, Stephanie spent two summers conducting research in an immunology lab at the City of Hope Beckman Research Institute.

Stephanie moved to the San Francisco Bay Area and started classes at Skyline College studying anthropology. In her final semester before transferring to San Francisco State University she took a general geology course and within the first month of classes she realized she wanted to be a geologist. She disinclined her acceptance to SFSU and changed her major. While continuing classes at Skyline College, Stephane was accepted into the Environmental Leadership Pathway program at UC Berkeley, a year-long fellowship that included classes in teaching and learning science as well as a summer internship in forest and fire ecology in the Eastern Sierras. As Stephanie prepared to graduate, again, from Skyline College she applied to multiple universities in California. To her amazement, she was awarded the Karl S. Pister Leadership Opportunity Award at U.C. Santa Cruz, which covered the majority of tuition costs.

While at UCSC, Stephanie had opportunities to tutor and teach her peers. It was incredibly challenging and immensely rewarding. Stephanie completed her senior thesis research with Prof. Emily Brodsky, which modeled the potential stability under different stress regimes and rock properties of a bore-hole for the planned research drill into the megathrust fault that produced the massive March 11, 2011 Tohoku-oki earthquake and tsunami. She was awarded honors for her

thesis work and graduated *cum laude* from UCSC. After graduation, Stephanie convinced one of her professors, Prof. Eli Silver, to hire her as a researcher in his lab and soon after she was also hired to work on another project with Prof. Emily Brodsky. Stephanie spent the next couple years working full time as a researcher. After the completion of these projects, she was accepted to the Earth and Atmospheric Sciences at Cornell University.

In her life outside of academics, Stephanie has spent many years studying and performing belly dance throughout the SF Bay Area. She developed a strong foundation in Egyptian folk style and through active participation in the dance and music community she expanded her skills, experience and knowledge of different dance styles and music throughout the Middle East and beyond. Dance taught Stephanie much about her own creativity and strength. While in Ithaca she was able to continue this passion as a dancer and percussionist with the Cornell Middle Eastern Music Ensemble.

After earning her Master of Science degree, Stephanie will move back home with her precious little kitty-cat, Emma, to be with family and friends in the bountiful California sunshine. She plans to teach earth sciences, and will always keep dancing.

For Cecily. And Emma.

ACKNOWLEDGEMENTS

I want to first thank my committee members Katie Keranen, Geoff Abers, and Rick Allmendinger for their guidance. Thank you to the Earth and Atmospheric Science department at Cornell and especially Savannah Williams for being so very helpful and caring. I am grateful for funding provided by the McMullen Fellowship and the National Science Foundation. Thank you to my lab-mates, who all at different times and in different ways provided insight, advice and encouragement. I especially want to thank Cat, Dana, Nate, Kayla, Ryan and Diego. I am also grateful to Dana and Lenny for opening their home to me.

I am grateful for the lifetime of encouragement I've been given by my parents and my family. Pookie and Jimmy, thank you for everything; I am so glad we're family. Thank you to my friends for your encouragement, much-needed reality checks, many laughs and love from near and afar. Particularly Natalie, Heather, Katie, Alexander, Francis, Sharon and especially Katelyn for the plentiful encouragement, laughs and excursions. I can't wait for our family camping trips.

Huge thank you to the Cornell University Middle Eastern Ensemble and the dancers whom I had to opportunity to learn from and perform with, most especially Alicia, Joseph and Tessa. Collectively, you offered community and filled my life with creativity, music, dance, and joy.

And, last but not least, I am so grateful for Emma and her boundless snuggles and unconditional love, and to the SPCA of Tompkins County for bringing us together.

TABLE OF CONTENTS

LIST OF FIGURES

LIST OF TABLES

Chapter 1

Introduction and Motivation

The Alaska-Aleutian subduction zone is an active plate boundary, and the location of many great earthquakes including 1964 Great Alaska Earthquake (M_w 9.2) (Figure 1). The propensity for rupture of tsunamigenic earthquakes along the Alaska-Aleutian megathrust makes it an important area for studying the *in situ* properties and conditions that control seismicity of subduction zones. Great earthquakes and subsequent tsunamis of Alaska-Aleutian origin have historically lead to a relatively low number of casualties when compared to other subduction zone earthquakes due to the sparse population of the region, but have lead to an excess of $100 million in damage throughout the circum-Pacific (Lockridge and Smith, 1984). However, in the decades since the 1964 catastrophe, the population throughout Alaska has been on the rise and is projected to continue increasing from 732,298 in 2012 to 925,042 in 2042 (Alaska Department of Labor and Workforce Development, 2014). As the population of Alaska and coastal communities around the Pacific increase and more urban centers are developed, the hazards to both life and infrastructure from a great earthquake and tsunami escalate. Therefore, study of the Alaska-Aleutian subduction zone is of both scientific and societal merit.

Earthquake hypocenters in this study come from a legacy dataset of digital earthquake records spanning 1982 – 1991 from the Shumagin Island seismic network operated by the Lamont-Doherty Geological Observatory. In most subduction zones, the seismogenic

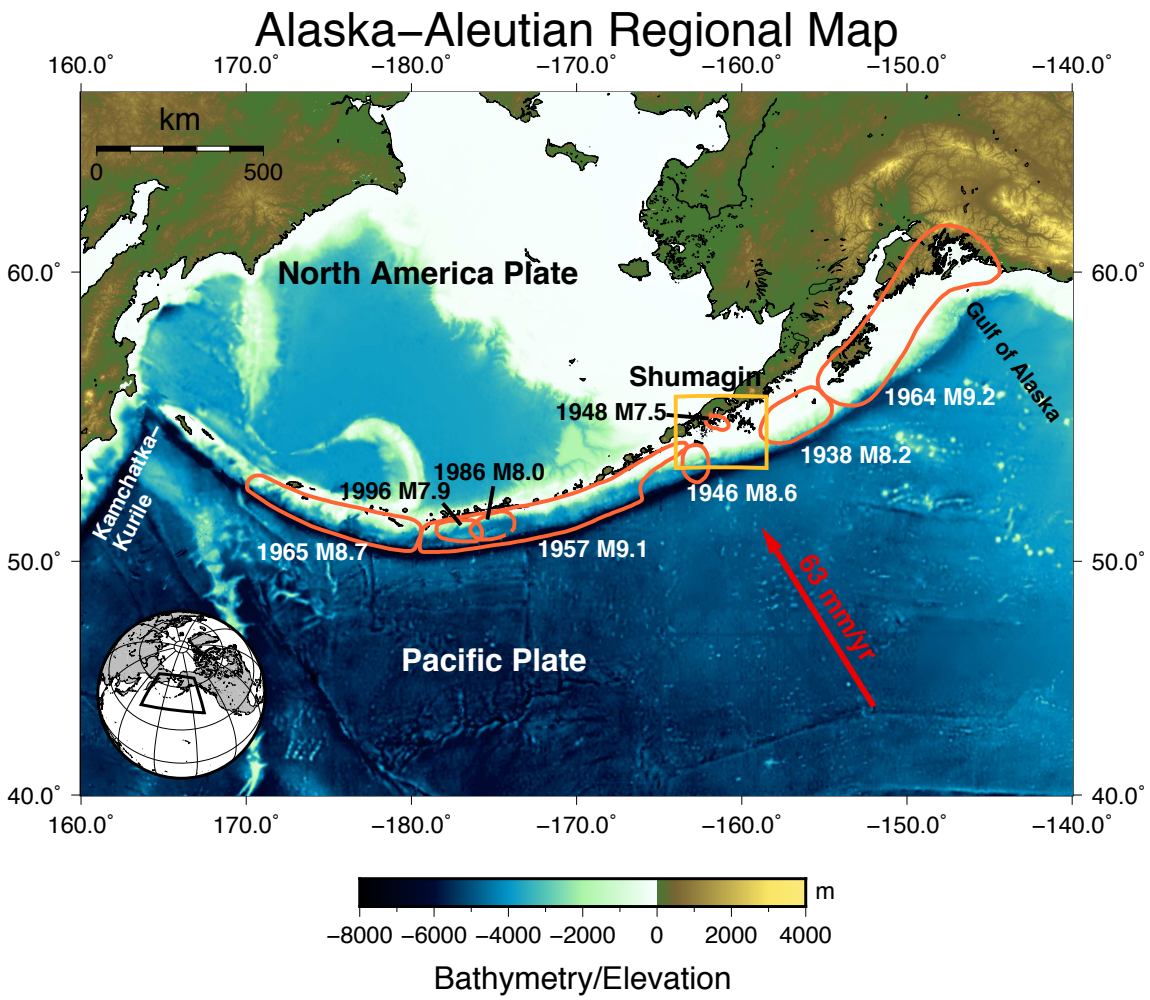

Figure 1: Map of the Alaska-Aleutian subduction zone showing bathymetry and elevation. Orange curves delineate the rupture areas of historic earthquakes, with the year and magnitude labeled in white or black text (Davies *et al.,* 1981). The yellow square outlines the study area in the Shumagin Gap; see Figure 4 for this inset. The red arrow indicates the orientation and rate of convergence in the area of the Shumagin Gap. The Semidi segment is labeled to the east of the study area. Inset shows regional location on globe. Bathymetry from ETOPO1 (Amante and Eakins, 2009). Topography from SRTM 90m Digital Elevation Data (Jarvis *et al.,* 2008).

zone has an updip limit >100 km trenchward of the volcanic arc and a downdip limit at depth beneath the coastline (Ruff and Tichelaar, 1996). Since this places the seismogenic zone offshore for most subduction zones, there are few locations globally that provide opportunity to directly sample the active megathrust, notable exceptions being events recorded by on-land seismometers in Costa Rica (e.g. Newman *et al.,* 2002; Norabuena *et al*., 2004) and Sumatra (e.g. Hill *et al*., 2012; Hsu *et al.,* 2006), seafloor geodetic data from Japan (e.g. Kido *et al.,* 2011; Iinuma *et al.,* 2012; Sun *et al*., 2014) and the Shumagin Islands (Davies and House, 1979; Reyners and Coles, 1982; Hauksson et al., 1984; Hauksson, 1985; Hudnut and Tabor, 1987; Boyd *et al.*, 1988; Abers, 1992; Abers, 1994; Bufe *et al,* 1994.; Abers, 1995b; Yang *et al.*, 1995). Due to the location of the Shumagin Islands, which extend ~100 km trenchward from the shoreline of the Alaskan Peninsula (Figure 2), events were recorded by on-land seismometers directly over the thrust zone providing high resolution for local seismic events and one of the better datasets for studying seismicity along the megathrust. Recent improvements in methodology and computational power make possible further investigation into this dataset.

Previous studies from the Shumagin network data show aftershock sequences, clustering, and evidence for streaks in the Shumagin segment (Abers, 1995b). Streaks, which are groupings of earthquakes that are spatially aligned as an approximately linear feature parallel to convergence, may indicate differences in slip behavior and physical properties on the fault. Abers *et al.*, (1995b) observed that the lineations have similar spacing (5-20 km) to the dimensions of rupture patches obtained from scaling of event pulse durations,

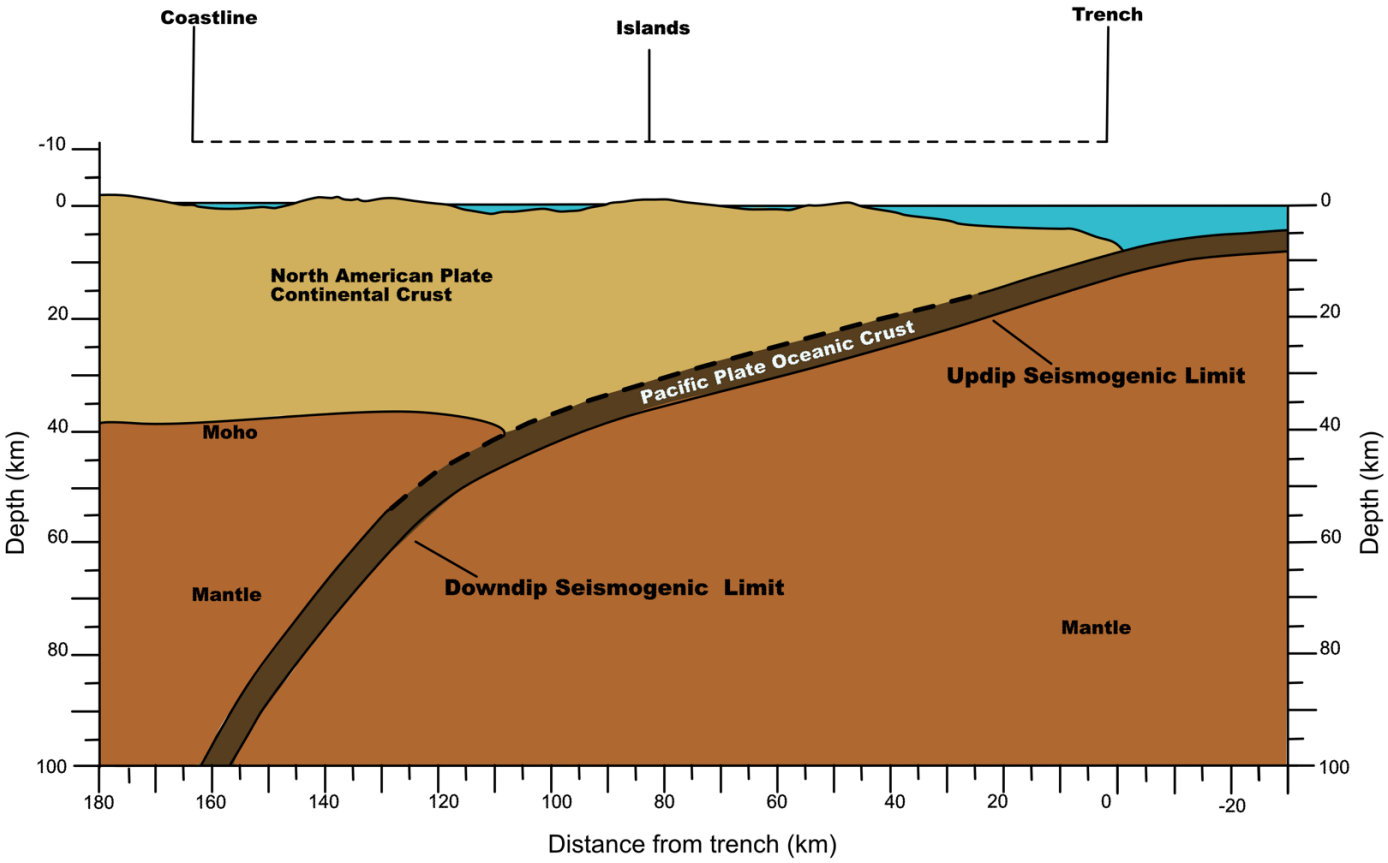

Figure 2: Schematic cross-section of the simplified structure of the Shumagin Gap. The Shumagin islands extend ~100 off the shoreline, placing them directly above the seismogenic zone. (Modified from Hyndman *et al*., 1997, Fig. 1).

and may reflect variations in seafloor topography, downgoing plate roughness, structural changes, or the effects of subducting sediments in valleys between abyssal hills on the seafloor. Schaff *et al*. (2002) found that streaks may have repeating earthquake sequences, as well as evidence of variability in stick-slip behavior of streaks on the Calaveras fault in California. Rubin *et al.* (1999) proposed that streaks of seismicity aligned with the direction of slip are common characteristics of creeping faults.

Precise earthquake locations indicate where a fault is seismogenic. Precise relocation of hypocenters is performed using double-difference relative relocation for earthquakes recorded near the Shumagin Islands, Alaska. The aim of this project is to improve the hypocentral locations of earthquakes recorded in the Shumagin region of the Alaska-Aleutian subduction zone to gain a better understanding of the structure and spatial distribution of seismicity. This understanding may provide insight into the physical properties controlling seismicity as well as the potential hazards of earthquakes and tsunamis generated at the Shumagin segment megathrust.

Chapter 2

Tectonic Background

The Alaska-Aleutian subduction zone is the convergent boundary between the Pacific plate and the North America plate, spanning ~ 3000 km from mainland Alaska in the east to the Kamchatka-Kurile subduction zone in the west (Figure 1). Major tectonic plate reorganizations, including the change in rotation of the Kula plate (56 - 55 Ma) and cessation of spreading of the Kula-Pacific junction (43 Ma), have shaped the margin and affected arc volcanism and plate orientations (Lonsdale, 1988). The accretionary character of the Alaska subduction zone is relatively young at 3 Ma; the tectonic history before that time indicates subduction erosion along the Alaska-Aleutian subduction zone until the margin was inundated by increased trench sediment that could not be accommodated by the subduction channel (Von Huene *et al*., 2012).

Some of the largest earthquakes globally ($M_w > 8.0$) originate in the Alaska-Aleutian subduction zone including the second largest earthquake in recorded history, the 1964 M_w 9.2 Great Alaska Earthquake (Kanamori, 1977; Ryan *et al.,* 2012). The resulting tsunami inundated shores around the circum-Pacific and caused 122 deaths across Alaska, Oregon and California (Haeussler *et al*., 2014). Nearly 20 years before, the $M_w > 8.6$ Unimak Island Earthquake of 1946 caused a tsunami that killed 164 people, was recorded around the Pacific including the U.S. west coast, Hawaii, the Marquesas Islands, and Antarctica (Lander and Lockridge, 1989; Shepard *et al*., 1950; Okal *et al*., 2002; Fuchs, 1982), and highlighted the necessity of a tsunami warning system (Igarashi *et al*., 2011).

Seismological analyses, tsunami-modeling, seismic reflection and multibeam bathymetric surveys indicate that ground shaking from the 1946 earthquake caused a submarine landslide on the continental slope which contributed to the magnitude of the resulting nearfield tsunami (Plafker 2002; Okal *et al*., 2003; López and Okal, 2006; Okal and Hébert, 2007; von Huene *et al*., 2014). Tsunami modeling by Thio *et al.* (2010) show that tsunamis generated along the Alaskan Peninsula pose the greatest risk of inundation to the California coastline.

In the Alaska Peninsula region, including the Shumagin Islands, the Pacific plate is subducting under the North America plate with a slab dip of ~45.0° and descent rate of 41.8 km/Ma (Syracuse *et al.,* 2010). The Pacific plate is 52.2 Ma (Syracuse and Abers, 2006) and converges normal to the trench at a rate of ~63 km/Ma with an azimuth of 148° at the Shumagin Islands (Sella *et al.,* 2002). Sediments on the incoming Pacific plate are ~500 – 700 m thick (Li *et al.,* 201). Gravity highs in the forearc correlate with seismic velocities obtained from a 3D velocity inversion, which are produced by shallow mass excesses in the upper plate (Abers, 1994). From these observations, Abers (1994) concluded that excess of mass in the strong upper plate compensate regionally for part of the downward flexure of the subducting plate.

The Sanak basement, between the Shumagin and Sanak Islands, contains late Miocene and younger sediment fill up to 8 km thick, above an acoustic basement (Bruns *et al*, 1985). The sedimentary cover of the upper slope ranges in thickness between 2 – 4 km, and possibly up to 6 km (Vallier *et al*, 1994). The landward trench slope includes a 35 km wide accretionary complex near the Shumagin Islands (Vallier *et al,* 1994). These Tertiary deposits overlay the Late Cretaceous Chugach Terrane consisting of volcaniclastic flysch, chert, pillow basalts, and

sandstone (Vallier *et al*., 1994).

The subducting Pacific plate beneath the Shumagin Islands dips 10-15° to the northwest (Abers, 1992). Seismicity studies indicate the interplate thrust zone from 25-45 km depth is narrow (5-10 km) and extends for 75 km downdip (Reyners and Coles, 1982; Abers, 1992). Below 45 km depth, Abers (1992) proposed a planar seismic zone of intraplate deformation extending to 120 km depth. This planar feature continues to approximately 250 km depth, dipping 30° in the east and 40° in the west (Abers, 1992). In the western part of the network a double seismic zone is observed, with a parallel zone of seismicity 20-25 km beneath the main zone of seismicity (Hudnut and Taber, 1987).

At the eastern edge of this study's field area (i.e., the western extent of the 1938 M_w 8.2 rupture area, Figure 3), Li *et al.* (2015) interpret shallowly dipping thin reflection band from about 13-20 km depth seen on multi-channel seismic (MCS) reflection profiles as the plate interface, where synthetic waveform modeling indicates the presence of a low velocity zone ~100 – 250 m thick. Receiver function analysis indicate a relatively constant continental crustal thickness of 37.5 ± 2.5 km across the Alaska-Aleutian arc, with a depth of 39 km for the continental Moho in the Shumagin region (Janiszewski *et al*., 2013). Between 120 km to ~170 landward from the trench, ~25 – 55 km depth, MCS studies indicate a thick band of reflections that Li *et al*. (2015) interpret as a broad deformation zone where the plate interface transitions from stick-slip sliding to slow slip and tremor. Based on MCS reflection data and seismicity, the plate interface downdip in the transition zone from the Semidi segment to the Shumagin segment can be described by three domains: (1) a ~ 500 m thick unconsolidated sediment layer beneath the accretionary wedge; (2)

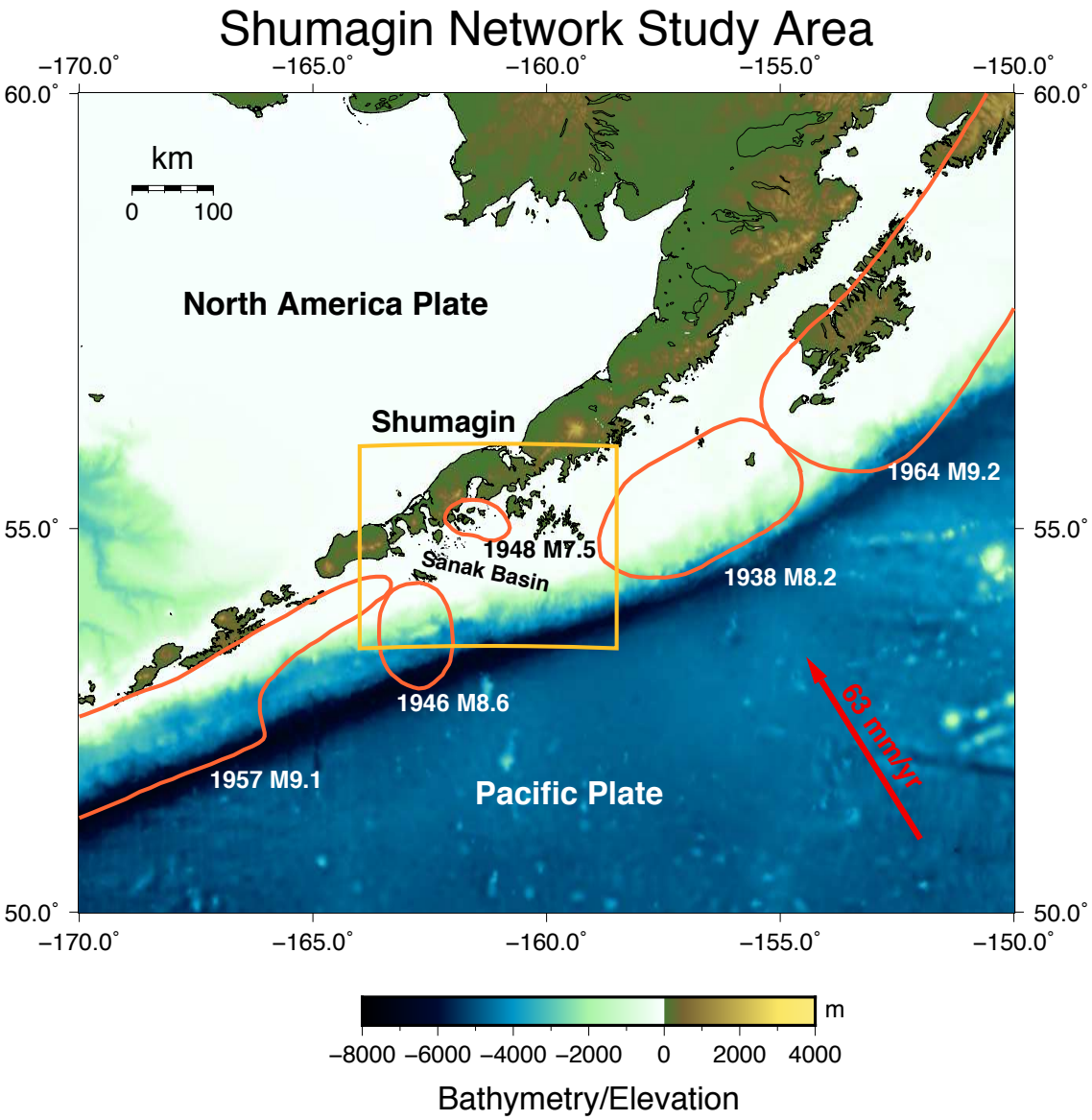

Figure 3: A closer look at the Shumagin regional geography, including the Sanak Basin. Labels as in Figure 1.

a thin (~ 100 - 250 m) area of localized shear of consolidated sediments exhibiting slip weakening and frictionally unstable behavior, which is capable of rupturing in a large earthquake but is otherwise relatively inactive; (3) a broadening (~ 100 - 250 m to 3 - 5 km) zone of deformation along the plate interface that is more seismically active, in which frictional stability increases downdip toward patches of tremor and slow slip events (SSE) (Li *et al.,* 2015).

The Shumagin Islands are located in the region known as the Shumagin Gap, a 200 km long segment where the movement along the megathrust appears to be stable (creeping) (Davies *et al*., 1981; Nishenko and Jacob, 1990). Within this region, there has not been a great earthquake ($M \geq 8$) in at least the past century, though the region does produce earthquakes of intermediate and smaller magnitudes (e.g. Kelleher, 1970; Davies *et al*., 1981; Hauksson *et al*.,1984; Bufe *et al*., 1994). The Shumagin Gap is adjacent to the Semidi segment (1938 M_w 8.2 rupture area) to the east and the rupture area of the 1946 M_w 8.6 earthquake (López and Okal, 2006) to the west (Figure 3). The Shumagin Gap appears to have a heterogeneous rupture style in which there is evidence of large earthquakes rupturing separately in one of three segments in the area (1899 M_w 7.2, southwest; 1917 M_w 7.4, northeast; 1948 M_w 7.5, center), as well as great earthquakes (1788, 1847) in which more than one segment of the Shumagin Gap may have ruptured during the events (Davies *et al*., 1981; Boyd *et al.*, 1988; Nishenko and Jacob, 1990; Estabrook and Boyd, 1992). These great earthquakes, however, are unlikely to have been generated solely in the Shumagin Gap, but instead ruptured during large events in adjacent segments and are not likely gap-filling events (Nishenko and Jacob, 1990; Estabrook and Boyd, 1992). Paleoseismic surveys of the Shumagin Islands indicated instances of wave-cut marine terraces, which Carver and Plafker (2008) interpreted as evidence of paleosubduction earthquakes large enough to cause

nearfield tsunamis. Witter *et al*., (2014), however, argue that field surveys, carbon isotope dating, and elastic dislocation modeling of Simeonof Island (the easternmost of the Shumagin Islands) do not show evidence of tectonic uplift or tsunami deposits; they conclude that the Shumagin region has experienced aseismic slip through the late Holocene, any stored strain is released in large (M 7 – M 8) rather than great earthquakes.

The Shumagin Gap has experienced a number of intermediate sized earthquakes (M ~ 3 – 7.5) including the earthquakes of April 1974 (m_b 5.8 and 6.0) (House and Boatwright, 1980; Mori, 1983; Abers *et al*., 1995a; Abers *et al.*, 1995b), the 1991 May sequence (mainshock M_w 6.7) which occurred after nearby stations of the Shumagin network were removed and was only recorded on the Shumagin Island station (Abers *et al*., 1995b), and the 1993 May sequence (mainshock M_w 6.9) directly beneath the Shumagin Islands, recorded on strong motion accelerographs (Abers *et al.,* 1995a).

The Semidi segment to the east, however, has a history of rupturing in great earthquakes with a recurrence rate of ~50 - 75 years (Davies *et al*., 1981), most recently in the 1938 great earthquake (M_w 8.2) (Fournier and Freymueller, 2007). Geodetic studies indicate that the Semidi segment is locked within the 1938 rupture zone, but locking decreases to 30% where the western edge of the rupture zone meets the Shumagin Gap, and further decreases to 0% locking beneath Sanak Island to the west (Fournier and Freymueller, 2007). The Semidi segment exhibits fewer intermediate-depth and interplate earthquakes than the seismicity of the Shumagin segment (Shillington *et al*., 2015). The abrupt transition (tens of km) in seismicity between the Shumagin and Semidi segments is likely controlled by differences in orientation and style of faulting and in

hydration of the subducting oceanic plate (Shillington *et al.,* 2015). The contrast in plate coupling and seismic history between the Shumagin Gap (weakly coupled) and Semidi segment (strongly coupled) compel investigation into the variations of physical properties and conditions that give rise to the differences in seismic behavior.

Chapter 3

Data and Methods

3.1 Data

From 1973 to 1991 Lamont Doherty Earth Observatory operated the East Aleutian (Shumagin) Seismic Network (EASN) in the Shumagin Islands, with digital records collected beginning in 1982 (Reyners and Coles, 1982; Hauksson *et al.,* 1984; Taber *et al.*, 1991; Abers, 1992; Abers 1994; Abers, 1995). This network is one of few globally where on-land seismometers recorded earthquakes directly over the active megathrust, due to the location of the Shumagin Islands trenchward of the Alaska Peninsula. Station coverage of the EASN is relatively good, with the exception of the southwest portion of the study area due to the absence of islands for instrument placement.

This legacy dataset of digital seismic records has recently been rediscovered and archived with the International Federation of Digital Seismograph Networks (doi:10.7914/SN/SH). The network consisted of 15 – 18 remote telemetered stations with 20 – 25 km spacing (Figure 4). Stations included 5 high-gain three-component seismometers, the rest being vertical short-period seismometers with 1 Hz natural frequency and force-balance accelerometers. Data were radio-telemetered to the central station at Sand Point. Signals are digitized at 100 samples per second by a 12-bit digitizer, recording events as low as magnitude 0.4, with uniform coverage above magnitude 2.0 – 2.5 within the network. The array recorded both upgoing and downgoing direct rays for earthquakes up to 125 km depth, and upgoing rays of deeper events (Abers, 1992).

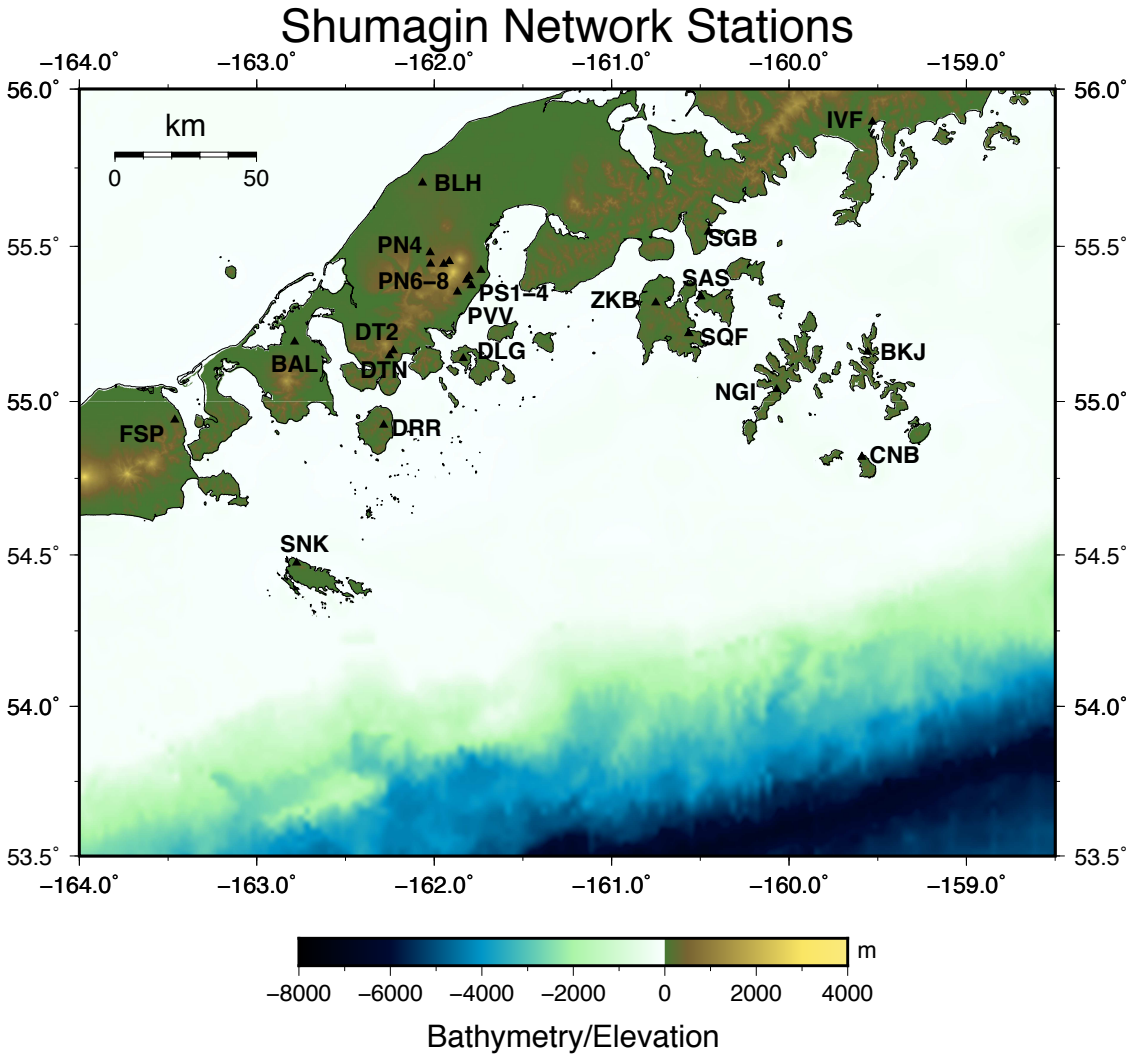

Figure 4: Map of the Shumagin Seismic Network, inset from Figure 1. Stations providing data for this study are shown as black triangles.

The Shumagin Island dataset consists of 5213 recorded events between 1982 – 1991, during which time digital recordings exits. Earthquakes predating digital recording, as well as ~2400 earthquakes for which tapes could not be read are not included in this study (Reyners and Coles, 1982). Analyst-picked P- and S- arrivals exist for 83% of the data (44626 P and 28686 S); S-arrivals make up ~ 39% of the picks. In the recent acquisition of the dataset, 143,925 waveforms were recovered. Approximately 5 % of the waveforms are clipped, having amplitude responses that exceed the limits of the receiver.

3.2 Methods

3.2.1 Additional S-picks

The original S-picks in the database are recorded on the vertical component of the seismograms, and therefore the accuracy of these picks is dubious. S-wave arrivals can give nearly the same accuracy of P-arrivals even though they are often obscured by P-wave coda, provided the S-arrivals are picked on the same phase for all seismograms at each station (Deichmann and Garcia-Fernandez, 1992). Gomberg *et al*. (1990) conclude that accurately picked S-wave arrivals greatly increase the accuracy of locations, even with good azimuthal coverage of the seismic network and good P-arrivals. Conversely, even a single incorrectly picked S-arrival can decrease the location accuracy by several kilometers (Gomberg *et al.,* 1990). Accurate S-wave arrival picks also better constrain depths in hypocenter locations (Schaff and Waldhauser, 2005). In order to obtain greater accuracy for our locations, 8437 new picks were made for S-arrivals on the horizontal channels of the three-component seismometers. Each pick is assigned an uncertainty (deltim), to be utilized in the data selection process for hypoDD relocation. S-phases

recorded on vertical component are downweighted to have a reduced influence on the double-difference calculations.

3.2.2 Data Selection

Data from mid 1983 through 1991 are used, as the recording instruments are more reliable during this period. See Section 3.2.5 (Tables 4 – 6) for a summary of data processing steps. Within the chosen time range 4349 earthquakes were used (68087 total arrivals; 37081 P and 31006 S). Earthquakes to be relocated are selected with the program db2ph, which finds events within a given range of times, latitude, longitude, depth and a minimum number associations (nass) and also defines the weighting scheme for pick deltim weights (Table 1). This processing step creates three files of (1) all events within the given parameters, (2) the stations recording phases and (3) the P- and S-phases at all stations for each of these events to be used in the next processing step.

Table 1 (a): Input parameters for db2ph.

Start time	1983231
End time	1991365
Min latitude	53.5
Max latitude	56
Min longitude	-164
Max longitude	-158.5
Min depth	0
Max depth	100
Weight type	D*
NASS	4

*deltim in arrival table

(b): Weighting scheme for deltim weighting.

Min	Max	Weight
0.0	0.05	1.0
0.05	0.1	0.8
0.1	0.2	0.5
0.2	10.0	0.1

The next step in data processing, ph2dt, calculates the travel-time differences at common stations for earthquake pairs from the events selected in db2ph. This travel-time information enhances the connectivity of events chosen for relocation. Earthquakes are selected within a minimum pick weight value, a maximum event-pair to station distance and maximum event-pair separation, maximum number of neighboring events, minimum number of event links per neighbor, and between a minimum and maximum number of links per pair (Table 2). The parameters in ph2dt are relaxed in this study to allow the maximum number of events through, to be further constrained in hypoDD.

Table 2: Input parameters for ph2dt.

Min Weight	Max Dist	Max Sep	Max Ngh	Min Link	Min Obs	Max Obs
0	500	200	50	4	4	200

Of the 3396 events selected in db2ph, 3395 are used to calculate 630340 P-phase and 524488 S-phase travel time pairs for events at common stations as input to hypoDD. Waldhauser and Ellsworth, 2001 and Waldhauser, 2001 provide a thorough explanation of the ph2dt and hypoDD processes and parameters.

3.2.3 Relative Relocation with hypoDD

Precise relative earthquake locations are calculated using the hypoDD Fortran computer program package (Waldhauser, 2001). Double difference relative relocation using hypoDD can improve locations by an order of magnitude (Waldhauser and Ellsworth, 2000). This program utilizes the double-difference algorithm of Waldhauser and Ellsworth (2000) and takes advantage of the fact

that if the distance between two hypocenters is small compared to the event-station distance and the length-scale of velocity heterogeneity, then the ray paths between the event sources and a common station are similar along most of the path (Frechet, 1985; Got *et al*., 1994). Therefore, differences in travel time between a hypocenter pair measured at a common station can be attributed to the event spatial offset (Waldhauser and Ellsworth, 2000). For a pair of events, the differential travel time of catalog P- and S-waves are differenced with the calculated differential travel time of the two events, resulting in the double-difference (Waldhauser and Ellsworth, 2000).

For a large earthquake dataset, hypoDD simultaneously determines the solution for the hypocenter adjustment for each event, linked to several neighboring events (Waldhauser and Ellsworth, 2002). For each event pair, the double-difference residuals are minimized by weighted least squares using the conjugate gradient method (LSQR) of Paige and Saunders (1982) (Waldhauser and Ellsworth, 2000). The final, high-resolution relative locations of all events are found by iteratively weighting and reweighting the data while simultaneously updating the locations and residuals of all events until a stable solution is reached (Waldhauser and Ellsworth, 2001). Through this iterative process, the catalog data are weighted to control the relative locations and events with large separation distances are down-weighted, with weights decreasing per event offset (Waldhauser and Ellsworth, 2000).

Errors in relative relocation of earthquakes may arise from multiple causes. As described by Pavlis (1992), poorly known earth structure results in systematic biases in hypocenter locations due to unmodeled anomalies that distort the relative positions. These errors increase with the

travel times between two events. Nonlinear effects during relocation calculations and errors in location estimates that propagate from measurement errors can also lead to uncertainty in relative hypocenter locations (Pavlis, 1992). Relative location errors commonly tend to be smaller than absolute location errors (Pavlis, 1992). However, the double-difference algorithm used in hypoDD is sensitive to errors in the absolute locations, which may result in systematic changes in the computed relative locations (Waldhauser and Ellsworth, 2000). Further, the hypoDD double-difference algorithm only relocates earthquakes relative to one another, and is sensitive to the accuracy of the absolute catalog locations and velocity model used to calculate the double–difference location algorithm.

The hypoDD parameters selected for this study are given in Table 3. Of the 3395 events input, 1798 events are linked and used in the relocations. Isolated events are not relocated. During the relocation process, 44 events are removed due to loss of links to other events in the event-pair chain, removal of outlier cutoff or after being relocated as 'airquakes' (hypocenters that are relocated above ground surface). See Appendix A: I for hypoDD output. Weighting and reweighting of the outlier threshold (WRCT) and maximum hypocentral distance (WDCT) are not implemented for the first two sets of iterations, so that all input data are used in the beginning iterative relocation calculations. Relocations are calculated using the three-dimensional tomography velocity model from Abers (1994). This velocity model is rotated 30° counter-clockwise from north, positioning one coordinate axis parallel to the arc (Abers, 1994).

Table 3: Input parameters for hypoDD relocations presented in this study.

--- DATA SELECTION:				
IDAT	IPHA	DIST		
2	3	400		
--- EVENT CLUSTERING:				
OBSCC	OBSCT	MINDS	MAXDS	MAXGAP
0	12	0	150	-999
--- SOLUTION CONTROL:				
ISTART	ISOLV	IAQ	NSET	
2	2	1	4	

DATA WEIGHTING AND REWEIGHTING:									
NITER	WTCCP	WTCCS	WRCC	WDCC	WTCTP	WTCTS	WRCT	WDCT	DAMP
3	-999	-999	-999	-999	1.00	0.80	-999	-999	55
5	-999	-999	-999	-999	1.00	0.80	-999	-999	65
3	-999	-999	-999	-999	1.00	0.80	6	50	90
5	-999	-999	-999	-999	1.00	0.80	6	20	100

3.2.4 hypoDD weighting parameters

Five of the hypoDD parameters were tested to see the effect on the final locations. With each test, all input parameters to hypoDD are as in Table 3, with the exception of one parameter being tested. The input parameters and hypoDD output for each test are given in Appendix A. Appendix B contains maps and cross-sections of resulting earthquakes locations.

Number of Neighbors

During relative relocation, event pairs of earthquakes are linked to nearest neighbors to form a continuous cluster. The minimum number of links per event pair is determined by the variable

OBSCT. Requiring more links per event pair can break up the data into multiple clusters. Waldhauser (2001) recommends using the number of degrees of freedom for each event pair, minimum 8, or more if both P phases and S phases are being used. In these data, more events are selected for the main cluster by using the minimum value of 8, fewer events are considered isolated and left out of relocations (Appendix A: II). This parameter test resulting in the most airquakes: 65, with 33 removed during the first iteration. This test resulted in an RMS residual of 87 ms, with changes in the last iterations of < 2%. The higher value of OBSCT=16 results in a greater number of isolated events (2281), and splits the events into a few more clusters, but with 5 or fewer events in each. The condition number in the final iterations is half that of when OBSCT = 8. In the final iteration, 96% of events and 63% of travel-time pairs are used for OBSCT=8, compared to 87% of events and 69% travel-time data.

P vs. S Weighting

The weight of S-phases compared to P-phases does not appear to have a great influence on the relocations of these data. Comparison of 0.5 S to P and 0.3 S to P have similar output from hypoDD (Appendix A: III). However, the higher weighting of S does result in smaller changes in hypocenter locations and origin times through the final iterations. The higher weight of 0.8 S is used in this study since the addition of repacked S-arrivals on the horizontal increase confidence in their reliability.

Outlier Cutoff

The parameter with the most significant effect on the output from hypoDD is the cutoff threshold for outliers, WRCT. In these tests, a dynamic cutoff is used as a factor to multiply the standard

deviation of the data during each iteration. A high value of WRCT=20 results in an output that is similar to the that from the parameters used in Table 3. The lower value of WRCT=1, however, gives very different results (Appendix A: IV), including absolute changes in hypocenter location and origin time of 0, a RMS residual of 0, and a low condition number below 100 by the final iterations. The percent RMS residual change between iterations in the last set are large (-70.5 ms, -83.9 ms, -86.3 ms, -60 ms). The percentage of travel-time data used drops significantly during iterations 15-18 and in the final iteration only 2% of travel-time data are used.

Hypocentral Separation

During each iteration, events that are located beyond the designated maximum hypocentral distance, WDCT, from other events in the event-pair chain are removed from the relocation process. Setting a smaller distance threshold allows only the closest events through to the final relocations. Lowering WDCT for the final two iteration sets from WDCT=100 km and WDCT=50, respectively, to WDCT=10 km and WDCT=5 km, respectively, results in fewer earthquakes being passed through the relocation calculations. With the higher separation-distance cutoff, more events lose linkage to others in the event chain, and are dropped from the calculations; for these tests the final output of relocated earthquakes decreases from 1774 to 1320. In Figure B VII.2, where the lower values of WDCT are used, the relocated earthquakes are more tightly clustered and there are large (10's of km) areas where no earthquakes have been located. Although the larger distance cutoffs of 100 km and 50 km do keep more events, the RMS residual and condition number are greater as well. The output of these tests are in Appendix A: V.

Damping

The damping of least squares is set by the parameter DAMP, which regulates solution fluctuations. In these tests, the selection of damping that decreases from initially high values results in a slightly smaller RMS residual and the percent change in residual between each iteration is lower through the final iteration sets than the results of the increasing DAMP values. The test of increased damping, however, does give an output that shows smaller adjustments to the three spatial and the temporal values (Appendix A: VI).

3.2.5 Summary of Data Processing Steps

The following four tables show the number of events and phases or phase pairs at each step of data processing through added picks (Table 4), db2ph (Table 5), ph2dt (Table 6) and hypoDD (Table 7).

Table 4: Additional picks, pre data processing

	Events	Total Phases	P-phases	S-phases
Starting	5213	73312	44626	28686
Added S-picks	5213	81749	44626	37123

Table 5: Data processing in db2ph

	Events	Total Phases	P-phases	S-phases
Time	4349	68087	37081	31006
Latitude	3857	60146	32518	27628
Longitude	3625	56535	30362	26173
Depth	3424	52830	28387	24443
nass	3396	52720	28326	24394

Table 6: Data processing in ph2dt

	Events	P-phase pairs	S-phase pairs
Ph2dt input	3396	666914	541674
Ph2dt selected	3395	630340	524488

Table 7: Data processing in hypoDD

	Events	P-phase pairs	S-phase pairs
hypoDD input	3395	630340	524488
After gap/distance check	3395	528167	458976
After dtime match	3383	528167	458976
Isolated	1585	188103	170121
Clustered	1798	340064	288855
Cluster 1	1794	340050	288842
Cluster 2	2	6	6
Cluster 3	2	8	7
hypoDD relocated**	1754	223278	162192

** 20 removed as airquakes, 24 lost connection to neighboring events or removed as outliers.

Chapter 4

Results

This study focuses primarily on the seismicity along the shallow interface, up to 60 km depth. The main thrust zone, as defined by Davies and House (1979), is the shallower portion of the Wadati-Benioff zone, above ~40 km depth. Figure 5 shows the relocated seismicity compared to the locations of the input data for earthquakes as well as the locations for all earthquakes in the study area up to 120 km depth. The subducting plate dips to the northwest. Few earthquakes at depths greater than 20 km are located beyond the coastline beneath the Alaskan Peninsula. There are clusters of earthquakes located within the upper plate, particularly in the western part of the field area. The overall distribution of earthquakes from the hypoDD relocations are not drastically changed from the input locations. However, there are some differences, as discussed below.

In map view, there are 10 – 50 km-long streaks of earthquakes that trend ~ 140° - 136°, decreasing westward (Figure 5). These features are seen in Abers, 1992 and Abers *et al*. 1995b. At depth, the streaks seen in map view in the central region of the study area also correspond with the area on the interface that is clearly defined in cross-section, with a downward dipping plane of tightly clustered earthquakes that broadens abruptly at around 44 km depth (Figure 6, 7). When viewed in profile parallel to convergence, linear features appear to extend down from the bottom of the interface about 30 – 40 km depth, dipping trenchward (Figures 6 and 7). These features range between ~ 5-10 km in length. Between the streaks in the central region, there is an area ~ 75 km long and up to 20 km wide with sparse seismicity (Figure 5).

The subduction interface is visible as a ~5 – 8 km thick plane that increases in dip from ~30° in the east to 40° toward the west, as seen by Abers (1992). In the region nearest the Shumagin Island stations, the seismicity forms a clearly defined, clustered linear trace dipping landward, from about 27 km depth to about 44 km depth. At 44 km depth, there is a transition in the seismicity (Figures 6 and 7), where earthquakes are sparser and more spread out over a wider plane down dip. This transition occurs below the depth of the Moho as interpreted from receiver function analyses, at approximately 40 km beneath the Shumagin Gap (Janiszewski *et al*., 2013). The double seismic zone described in previous studies of the Shumagin Gap (e.g. Reyners and Cole, 1982; Hudnut and Taber, 1987; Abers, 1992; Ratchovsky *et al*., 1997) is not clearly defined by the relocations presented here. However, the broadening of events downdip of the 44 km depth seismicity transition does still appear to follow a broadly spaced planar trend, which may coincide with upper and lower planes of the double seismic zone (Figures 6 and 9). In profiles parallel to the convergence orientation, the subducting plate dips shallowly until about 35 km depth, and gradually increases in dip from ~30° - 34° between 35 and 45 km depth (Figure7). The interface in Profile D – D' has a more consistent dip of ~35° but steepens to ~40° at 46 km depth (Figure 9). Further west, the band of seismicity broadens to ~16.5 km and the interface is difficult to discern (Figure 10).

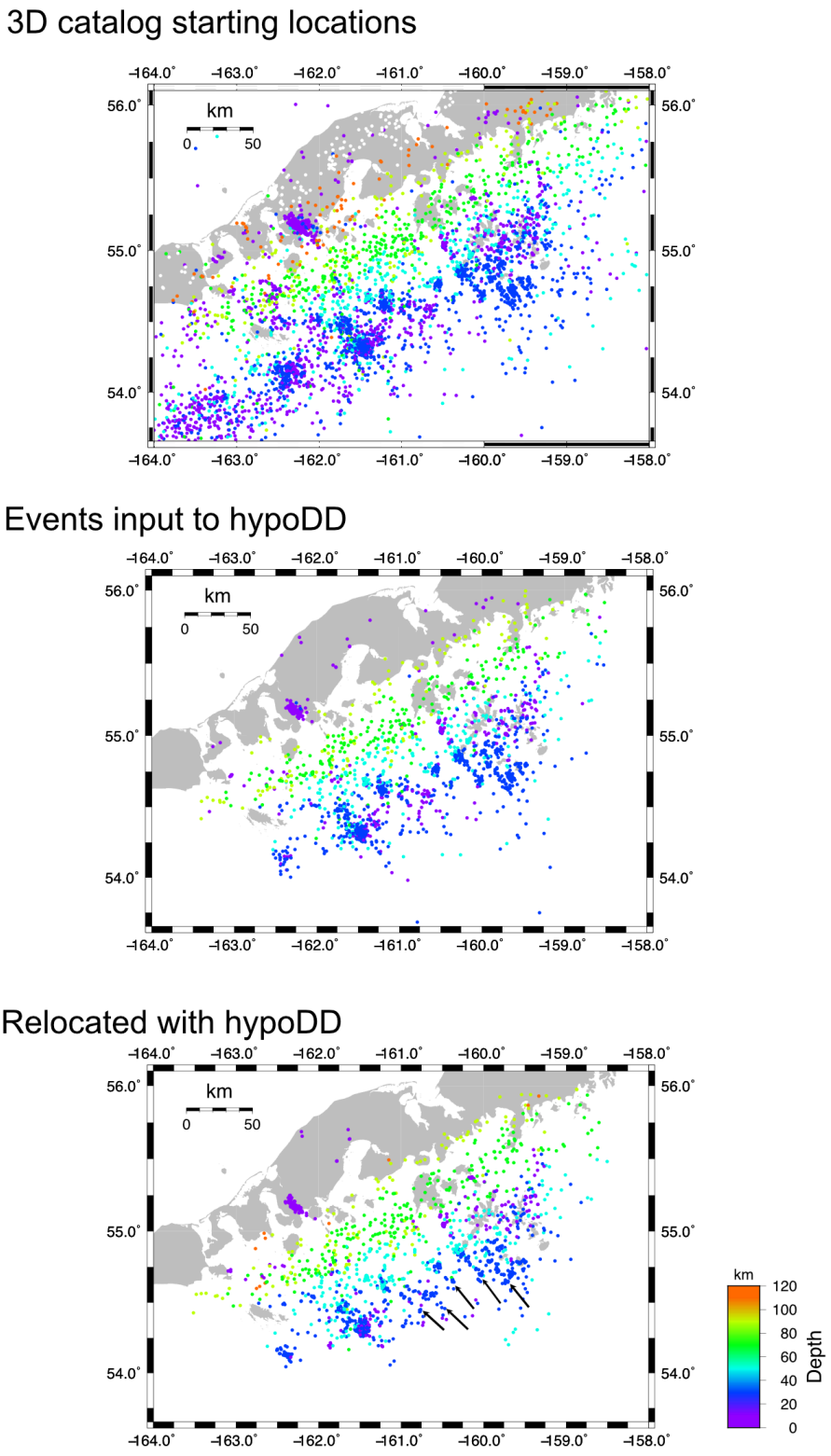

Figure 5: Three panels show a comparison of the 3D catalog starting locations (top), Input to hypoDD (middle), Events relocated with hypoDD (bottom). Black arrows in bottom panel indicate streaks of seismicity. Earthquakes are colored by depth.

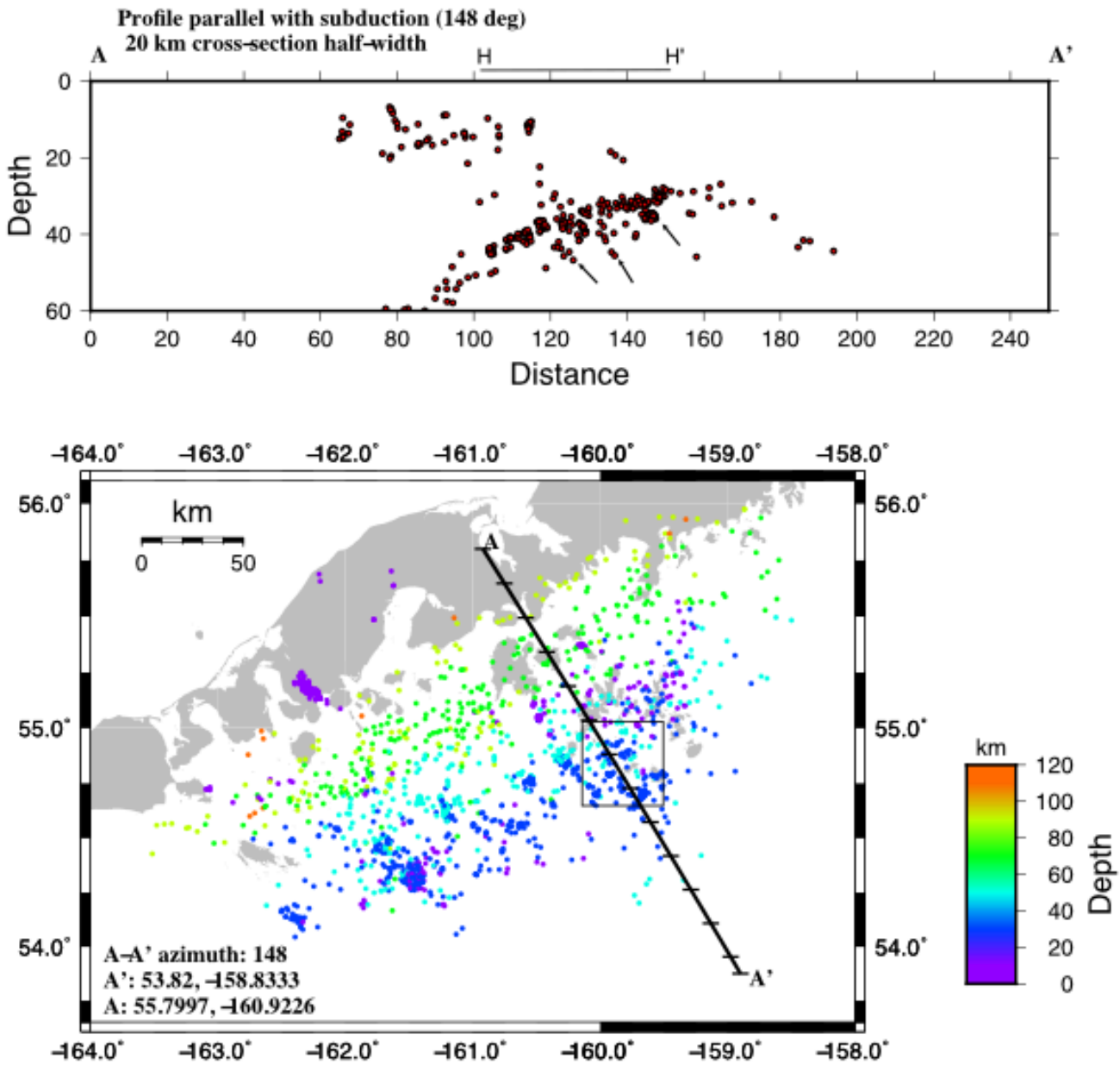

Figure 6: Profile A – A'. Box outlines the area of Subset 3, Profile H – H' (Figure 14). Black line above cross-section indicates the area covered by Profile H – H'. Black arrows in cross-section indicate linear features that extend trenchward down from the plate interface. Earthquakes are colored by depth. Tick marks on cross-section and profile line in map view are 20 km.

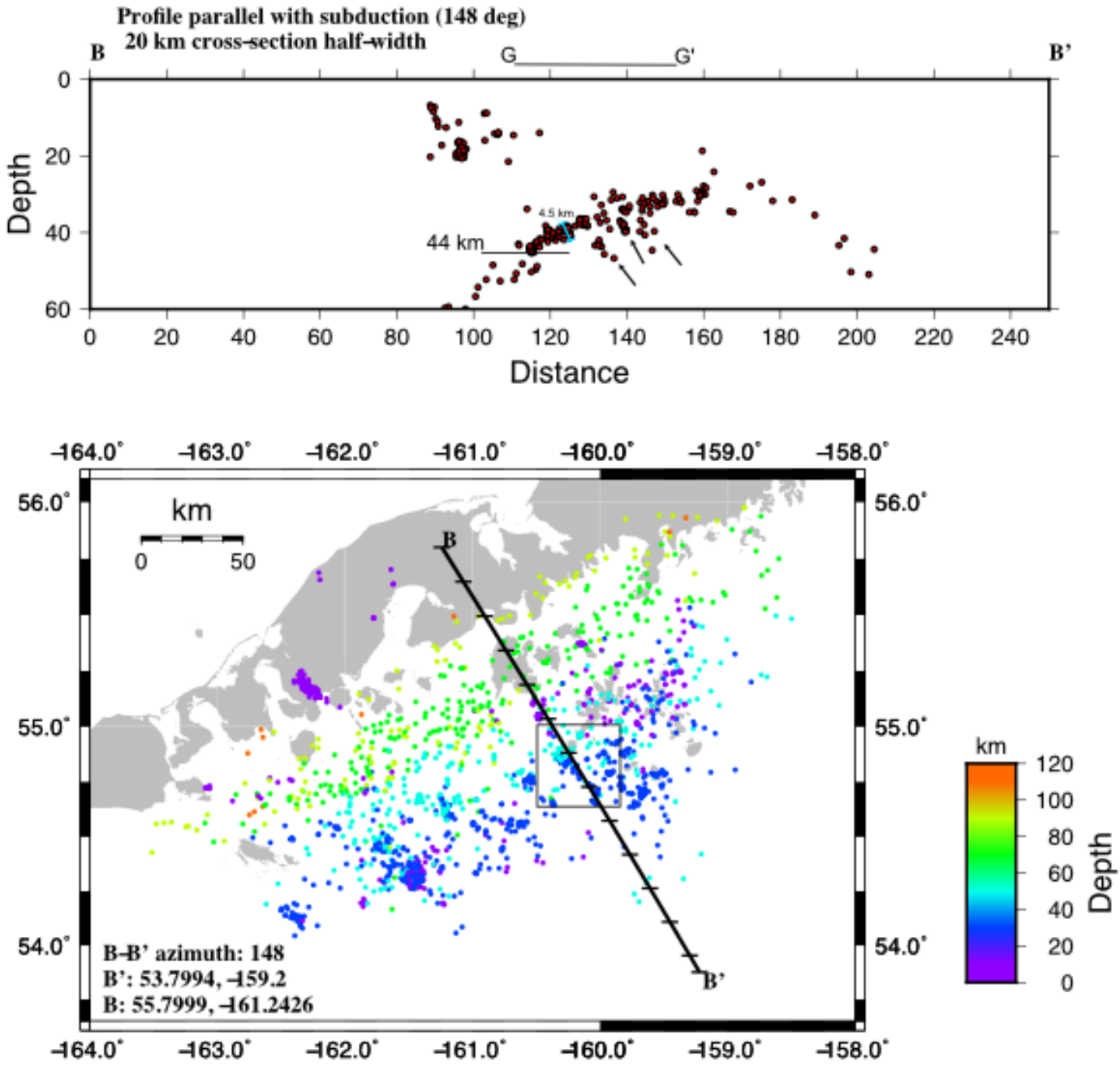

Figure 7: Profile B – B'. Box outlines the area of Subset 2, Profile G – G' (Figure 13). Black line above cross-section indicates the area covered by Profile G – G'. Black arrows in cross-section indicate linear features that extend trenchward down from the plate interface. Horizontal line at 44 km depth marks the abrupt transition in seismicity character downdip. Cyan bar shows a thickness of 4.5 km for the plate interface. Colors and tick marks as in Figure 6.

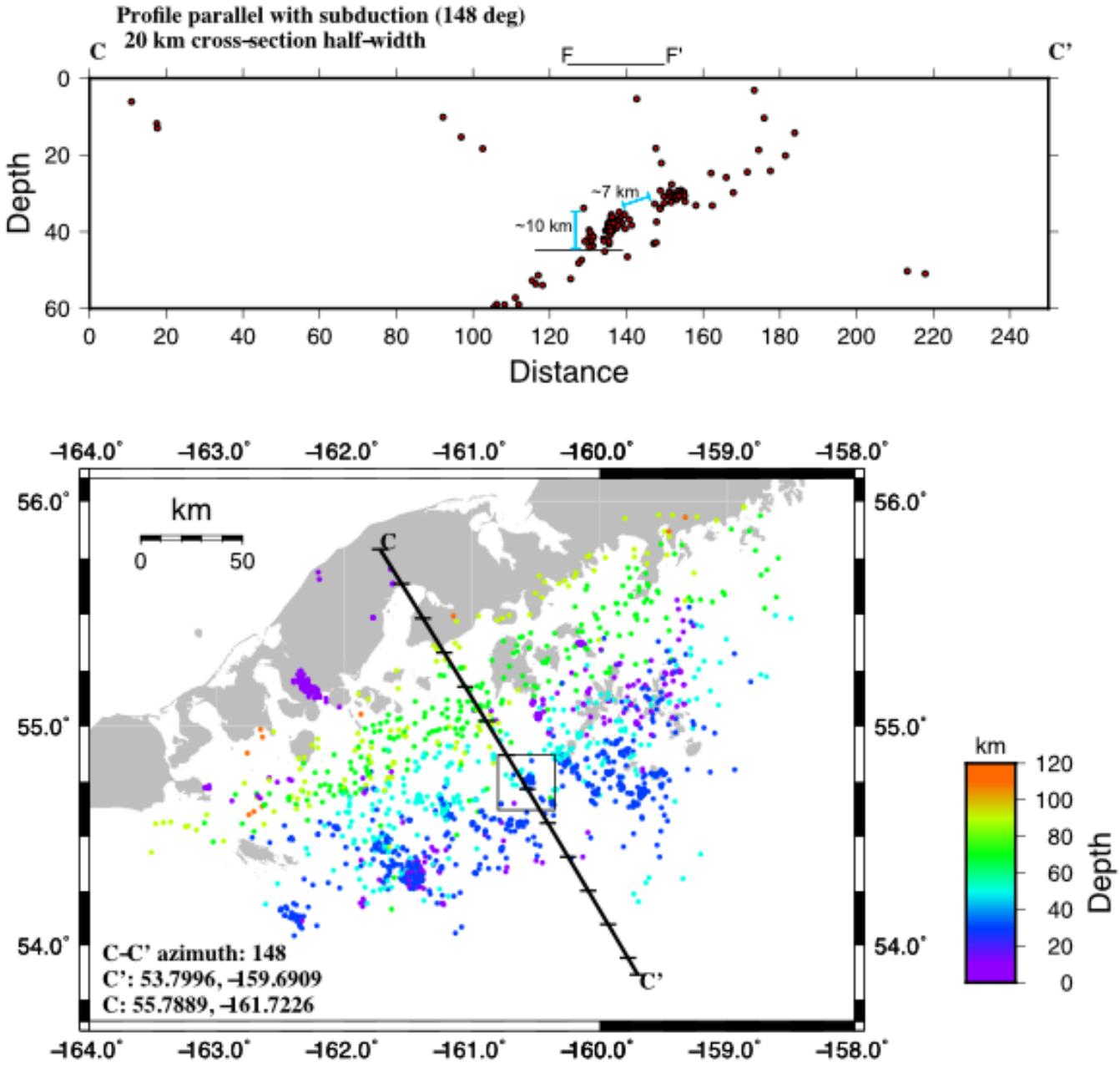

Figure 8: Profile C – C'. Box outlines the area of Subset 1, Profile F – F' (Figure 12). Black line above cross-section indicates the area covered by Profile F – F'. Horizontal line at 44 km depth marks the abrupt transition in seismicity character downdip. Cyan bars show the width of the lower clusters and the break in seismicity along the discontinuous interface. Colors and tick marks as in Figure 6.

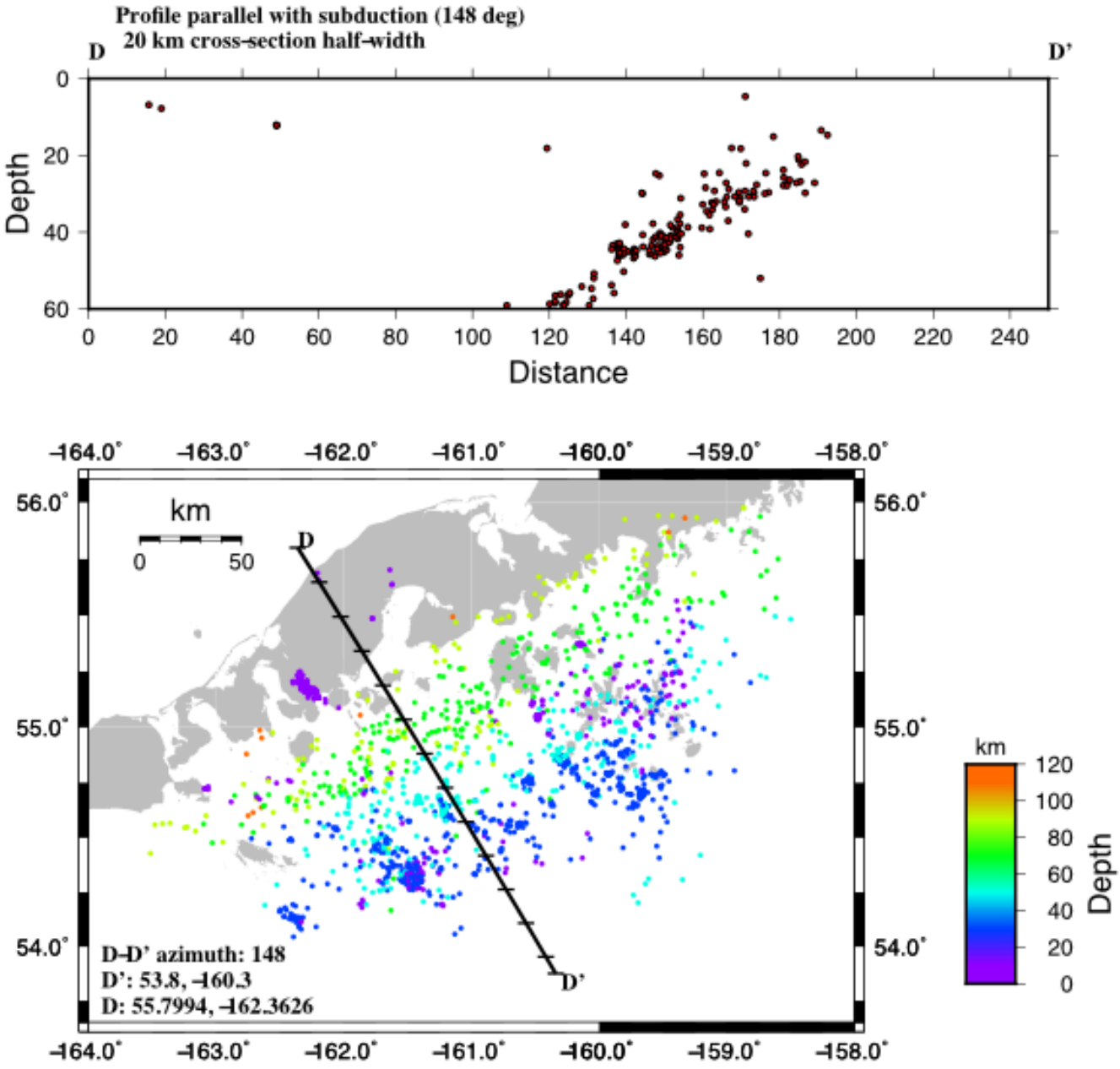

Figure 9: Profile D – D'. Colors and tick marks as in Figure 6.

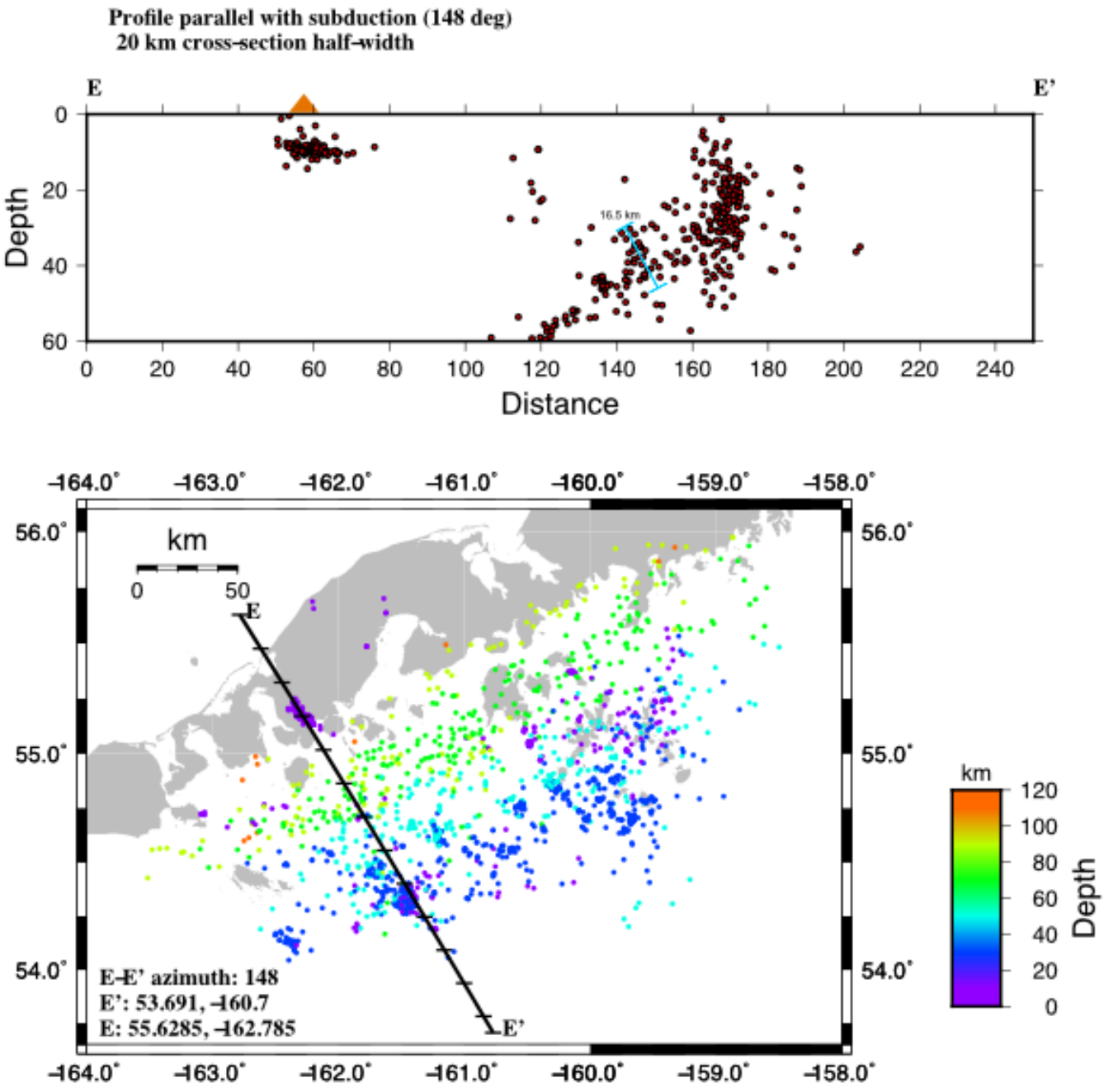

Figure 10: Profile E – E'. Cyan bar show the width of the broadly defined interface. Orange triangle above cross-section indicates the location of Mt. Dutton. Colors and tick marks as in Figure 6.

Seismicity is present in the overriding continental crust throughout the study area, though there are large clusters in the western part of the region. Around 55 latitude, -160.5 longitude (~80 – 100 km along Profile B – B' in Figure 7) there are two clusters of closely spaced earthquakes extending from ~5 – 20 km depth. The upper cluster appears to elongate landward. To the west, the upper crustal seismicity broadens and events are not tightly clustered seaward, toward the updip region of the interface. Around latitude 55.2, longitude -162.3 there is a shallow cluster many tightly spaced events from ~4 – 14.3 km depth, 23 km long and ~10 km wide (Figure 10). Many of these events occurred in mid – late 1988. This cluster lies beneath Mount Dutton, a small (5 km in diameter) volcano that experienced a seismic swarm between July and August 1988, which may have occurred during emplacement of a magmatic dike into the shallow subsurface beneath the volcano (Miller *et al.,* 1998). Figure 10 also shows a thick cluster of earthquakes extending from the seaward end of the profile in a band of seismicity that is near-vertical.

In Profile C – C' (Figure 8), the seismicity is separated into 3 clusters, instead of the relatively continuous band imaged in Figures 6 and 7. The updip cluster is 9.5 km long and 5 km thick, and the next downdip cluster is larger, 12 km long and 7 km thick. The spacing between the two larger clusters is 7 km, comparable to the width of the two clusters. The third cluster, at ~43 km depth extends upward from the interface as a ~3 km thick, 6 km long band of seismicity at an angle ~30° from the interface.

4.1 Subsets on features in hypoDD

The three subsets outlined in Figures 11, 13, and 14 were each run through hypoDD separately to gain more insight in finer scale features of these areas. The earthquakes input into hypoDD for each run are only those within the boundaries of the subsets. The same parameters are used the as with the larger dataset, with an additional final line of iterations added with WDCT=5, so that only the closest neighbors are linked.

4.1.1 Subset 1: Potential Splay Fault

In Figure 11, Profile F – F' focuses in on the lower clusters from Figure 8. Relocation of these events reveal a 1.8 km wide cluster centered at 37.4 km depth. The smaller linear cluster seen at 43 km depth in Figure 8 is not present in this subset. In map view, two linear features are visible, neither of which was present in the larger dataset. One is located ~3 km west of the cluster, trending N-S and is ~1 km long. The second linear feature is ~1.3 km long and intersects Profile F – F' at 11 km. These earthquakes appear to strike within the range of ~ 247° - 254°. Figure 12 shows faults mapped by Bruns and Carlson (1987) in the Eastern Sanak Basin which strike ~254°. In cross-section, the fault extends from approximately 35.5 km to 38.4 km depth, appearing to meet with the plate boundary; if so, that would indicate an active splay fault.

4.1.2 Subset 2: Downdip Seismicity

Subset 2 focuses on the streak of earthquakes in seen in map view (Figure 13) and in Profile B – B' (Figure 7). The events relocated in this subset show a more planar interface than in Figure 7. Where the dip of the interface in Profile B – B' gradually increases in dip, the events relocated

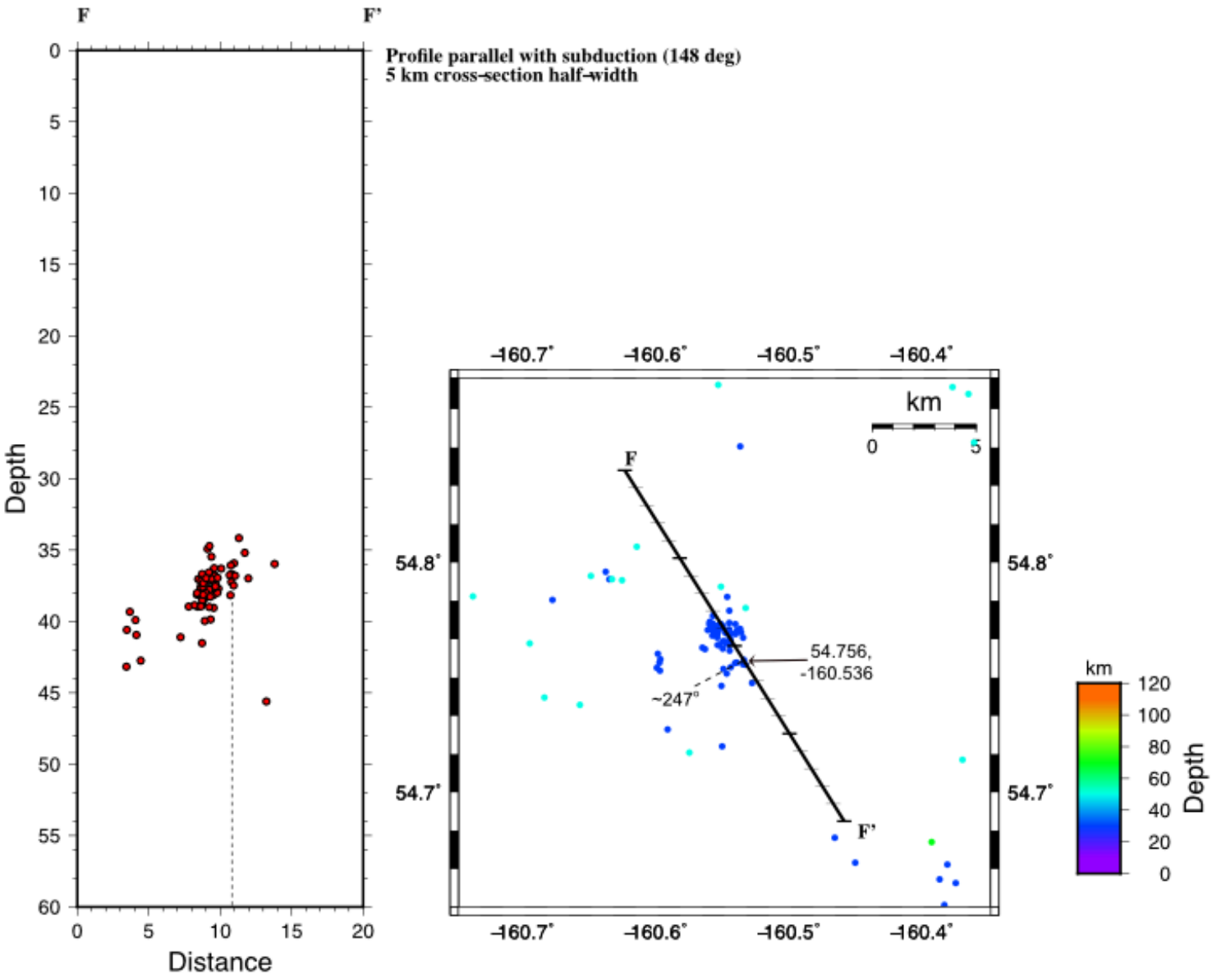

Figure 11: Subset 1, Profile F – F'. Location of this subset is outlined in Figure 8. Thin dotted line in cross-section indicates when the splay fault intersects the Profile F – F'. In map view, dashed line approximates the strike of the fault. Black arrow marks the coordinates of the intersection of the splay fault with Profile F – F'. Earthquakes are colored by depth. Major tick marks on cross-section and profile line in map view are 5 km.

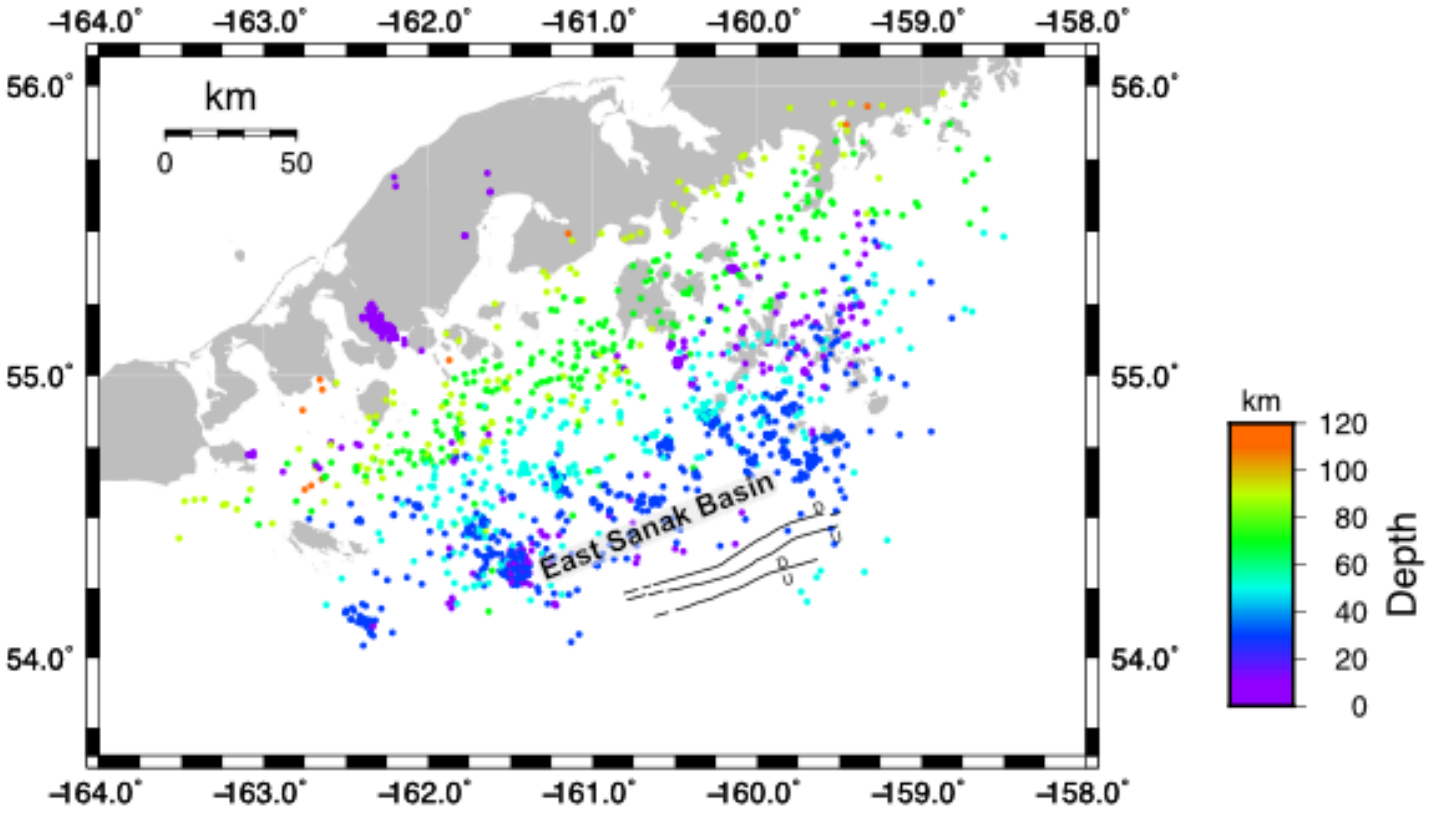

Figure 12: Map of relocations, showing faults (black lines) as mapped by Bruns and Carlson, 1987, with down (D) and up (U) indicators. Earthquakes are colored by depth.

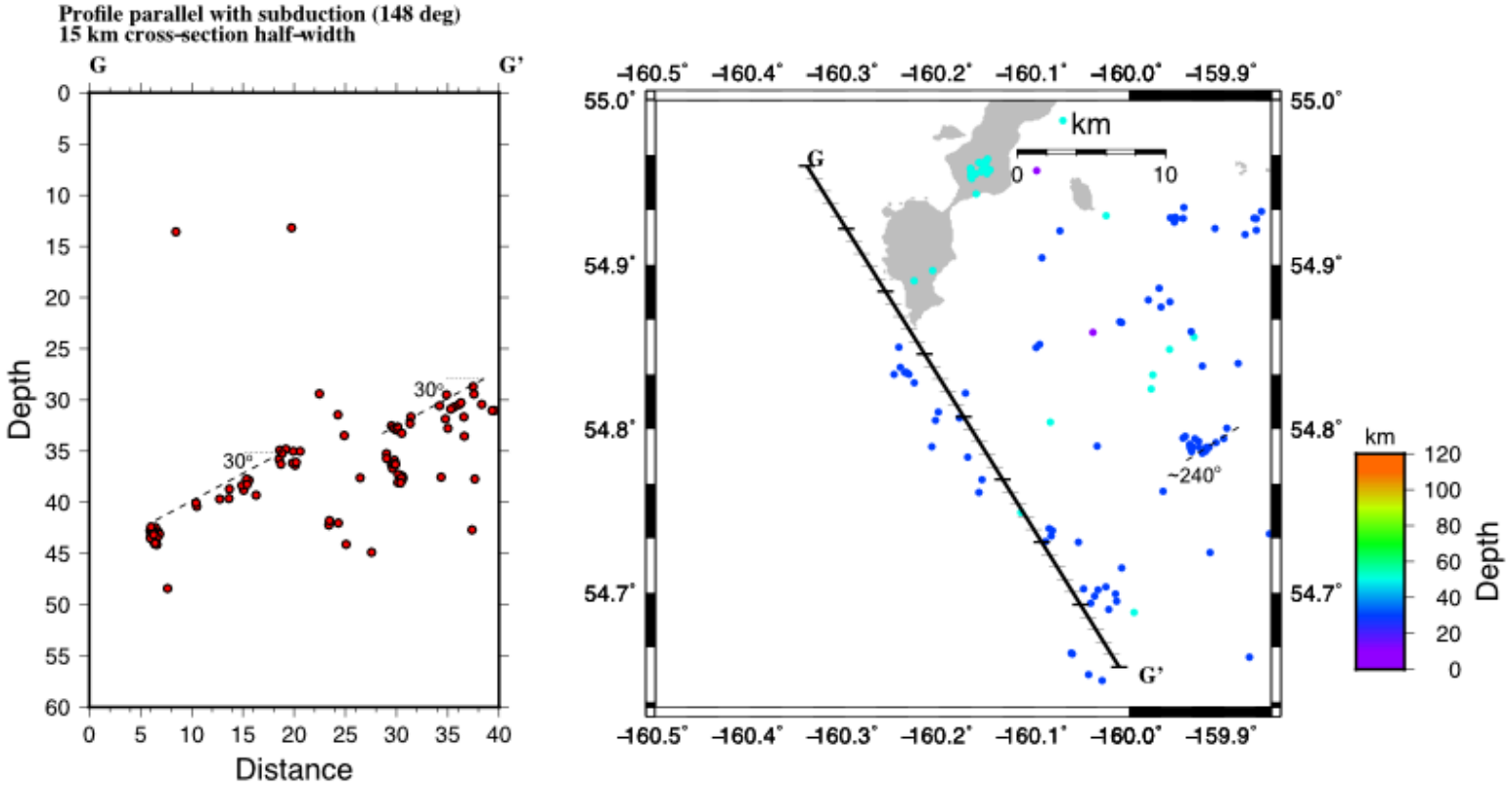

Figure 13: Subset 2, Profile G – G'. Location of this subset is outlined in Figure 8. Dashed lines in cross-section approximate the dip of the interface for two discontinuous traces of the interface, dipping at approximately the same angle of 30°. The earthquake cluster at 44 km depth is shown in Figure 7 to delineate the abrupt change in seismic character from a definitive plane to broad and sparse. Dashed line in map view approximates the strike of a fault east of Profile G – G'. Colors and tick marks as in Figure 11.

on G – G' show a consistent dip of ~30°. However, the interface is not continuous between 21 and 28 km along G – G', and the interface appears to step upward ~2.5 km over this distance. There may actually be a more gradual change in dip over this ~ 7 km that is not resolved in the relocation. The cluster of earthquakes at 44 km depth is the is the same 2 km by 2.5 km cluster in Figure 7 at the abrupt transition to sparse seismicity. As seen in the larger dataset, no earthquakes are located in the area southwest of this streak. To the east, there is a 3 km long fault that strikes ~240°.

4.1.3 Subset 3: Potential Deep-rooted faults

The plate interface in this area is shallow (~28°) until 35 km depth, where the dip increases to 30° (Figure 14). The focus of Subset 3 are the linear features extending downward from the plate interface in Figures 6 and 7. These potential faults range between 5 – 10 km in length and dip trenchward away from convergence direction, over a wide range, ~37° - 64°. Note there is some overlap of Subsets 2 and 3; the fault to the west of H – H' is the same in Figure 13 (east of G – G'). This fault is 3.7 km wide, and dips 64° trenchward.

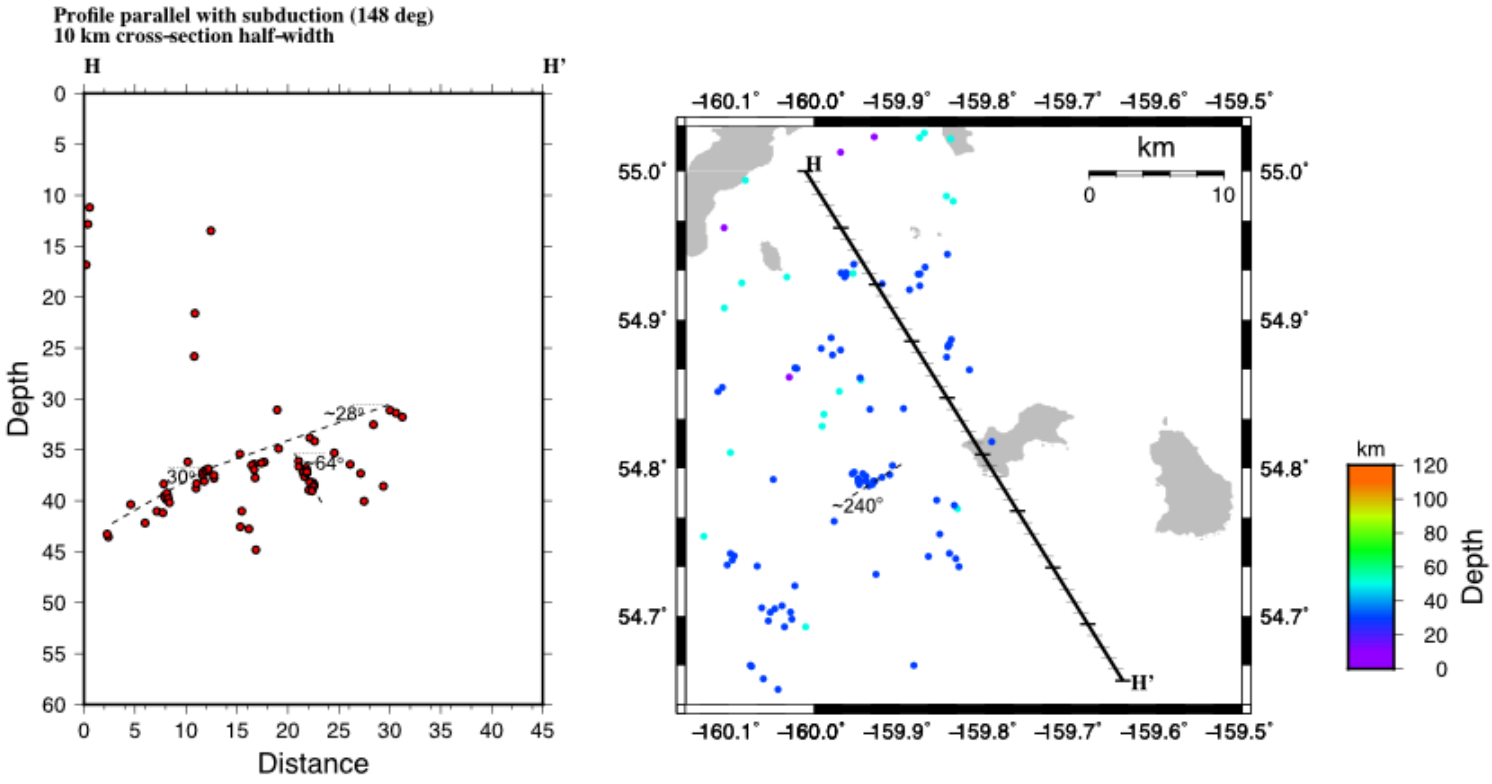

Figure 14: Subset 3, Profile H – H'. Location of this subset is outlined in Figure 7. The Interface remains relatively shallow to ~ 36 km depth, and steepens downdip. Planes of earthquakes extend down from the bottom of the plate interface, dipping steeply trenchward. Colors and tick marks as in Figure 11.

4.2 Uncertainty Analyses

4.2.1 Difference Between Initial and Final hypoDD Locations

The distances between input locations and hypoDD relocations for individual earthquakes range from 0 km to 29.75 km, with a mean of 4.84 km. Seventy-two percent of earthquakes are moved less than 5 km. Figure 15 shows the input locations and output locations for all events. Histograms of total change in km distance show a bias toward a negative shift in depth, with 73% of relocated earthquakes moving downward (Figure 16). Ninety-one percent of depth shifts are less than 5 km. However, it is important to note that a depth uncertainty of 5 km could significantly affect the structure of the thrust zone portrayed by the calculated locations.

The histogram of horizontal location shift is highly skewed, with 85 % of earthquakes moving less than 5 km (Figure 16, middle). Figures 17 and 18 show the change in horizontal and vertical location changes for events within each of the six segments shown in Figure 15 (top). Histograms of total, horizontal and vertical distances for each segment are shown in Figures 19, 20 and 21 respectively. Table 7 gives the percentage of location adjustments greater than 5 km for each of the segments. Fewer earthquakes in Segments 4 and 5, the area beneath the Shumagin Islands, are moved greater than 5 km from their starting location.

Table 8: Percentage of location adjustment in hypoDD for each of the six segments shown in Figure 17.

	Total adjustment > 5 km, %	Horizontal adjustment > 5 km, %	Vertical adjustment > 5 km, %
Segment 1	44.0	24.0	8.8
Segment 2	37.8	6.1	12.3
Segment 3	49.8	6.4	4.8
Segment 4	8.6	1.9	0.28
Segment 5	10.0	2.6	0.29
Segment 6	32.1	7.9	0.71

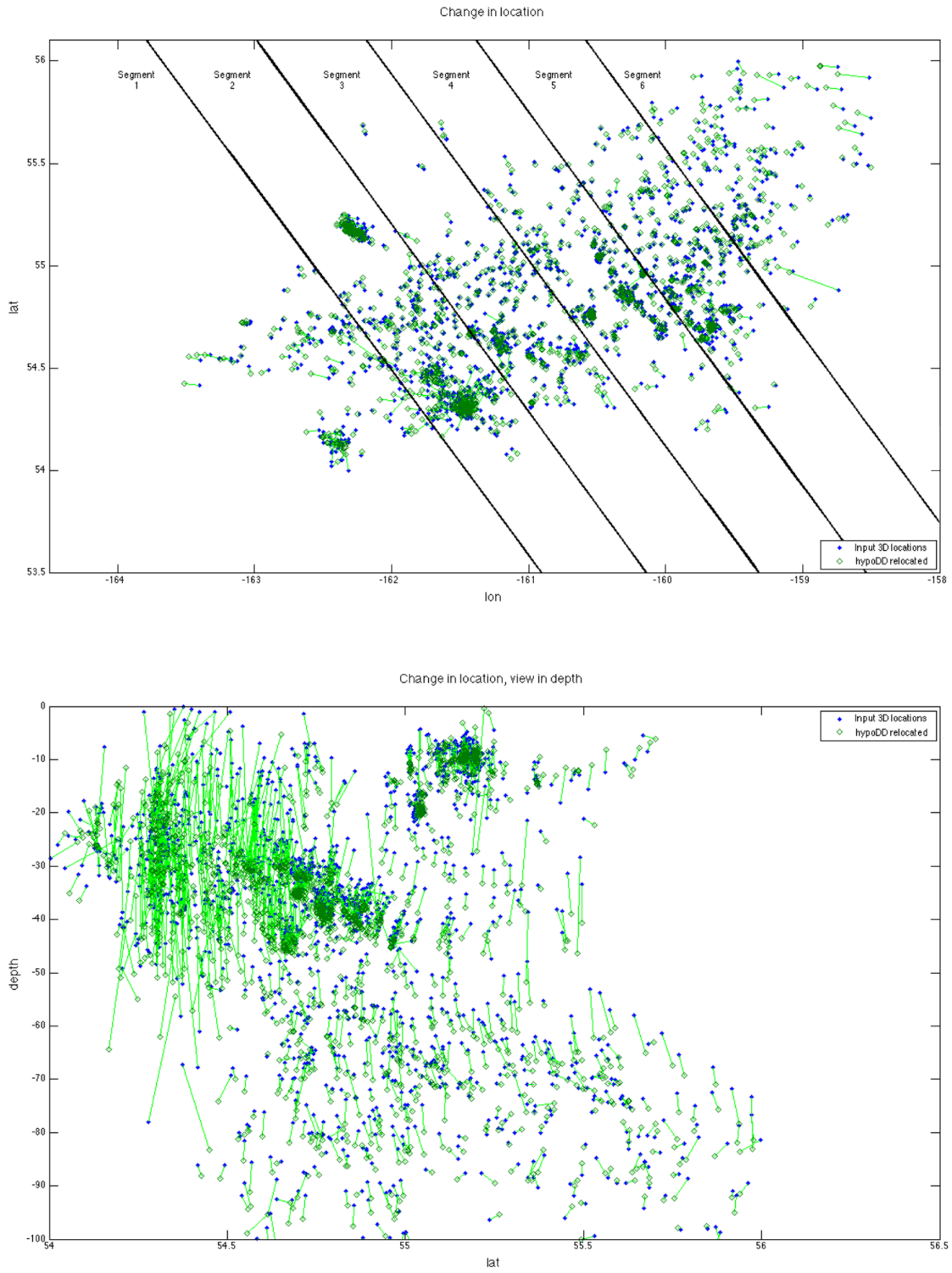

Figure 15: Map view (top) and cross-section view (bottom) showing the change in location for all events. Blue dots are the input locations to hypoDD. Green diamonds show the final locations output from hypoDD. Green bars connect the initial and final location of each individual earthquake.

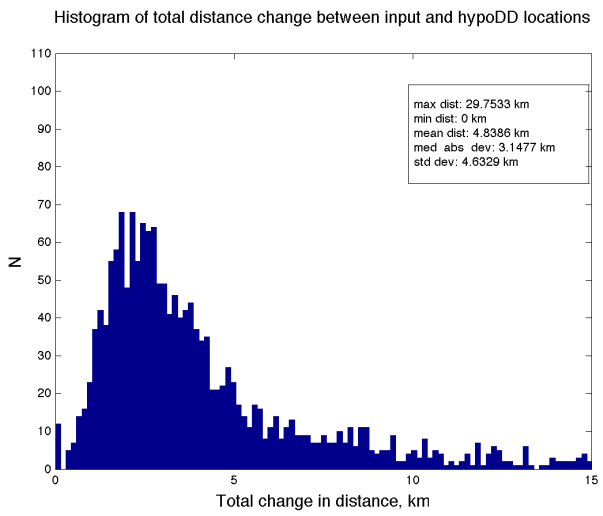

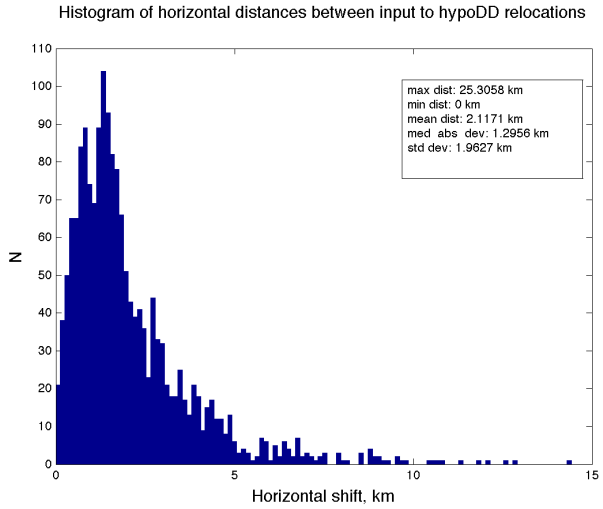

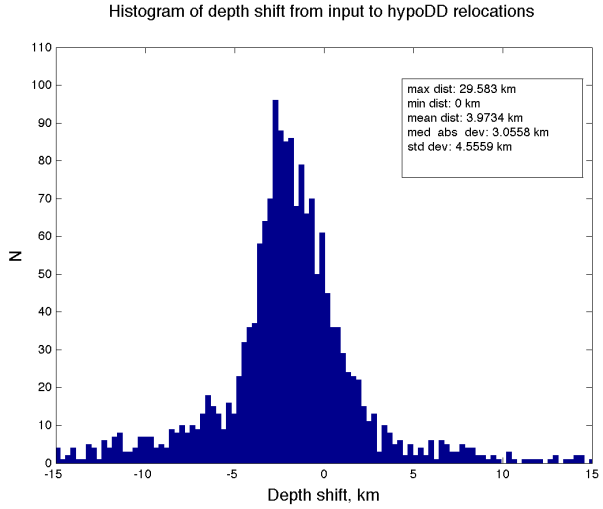

Figure 16. Histograms showing the total (top), horizontal (middle), and vertical (bottom) adjustments from initial to hypoDD final locations for all events.

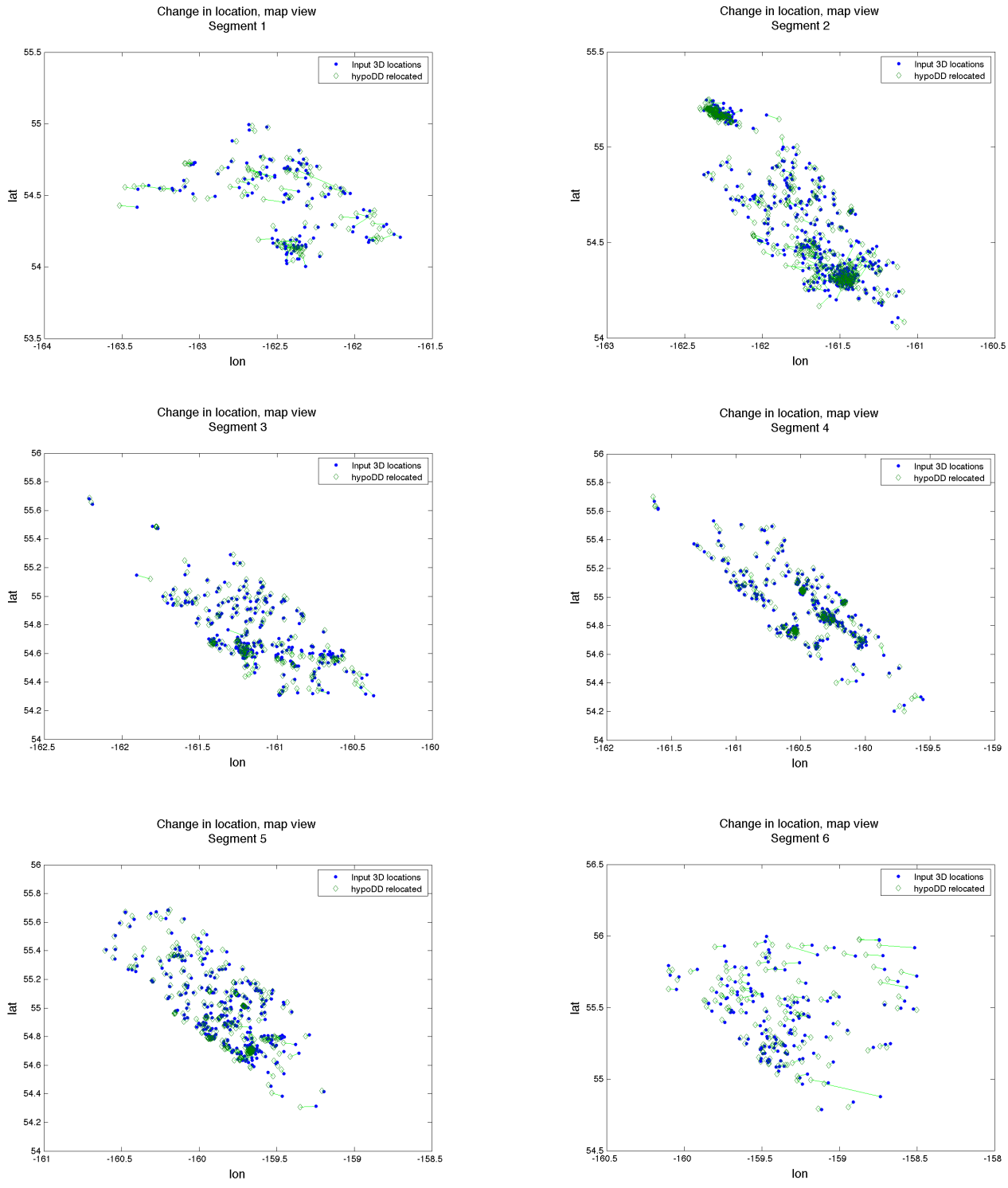

Figure 17: Map view showing the horizontal change from input to hypoDD output locations for the events within each of the six segments shown in Figure 15, top. Markers as in Figure 15.

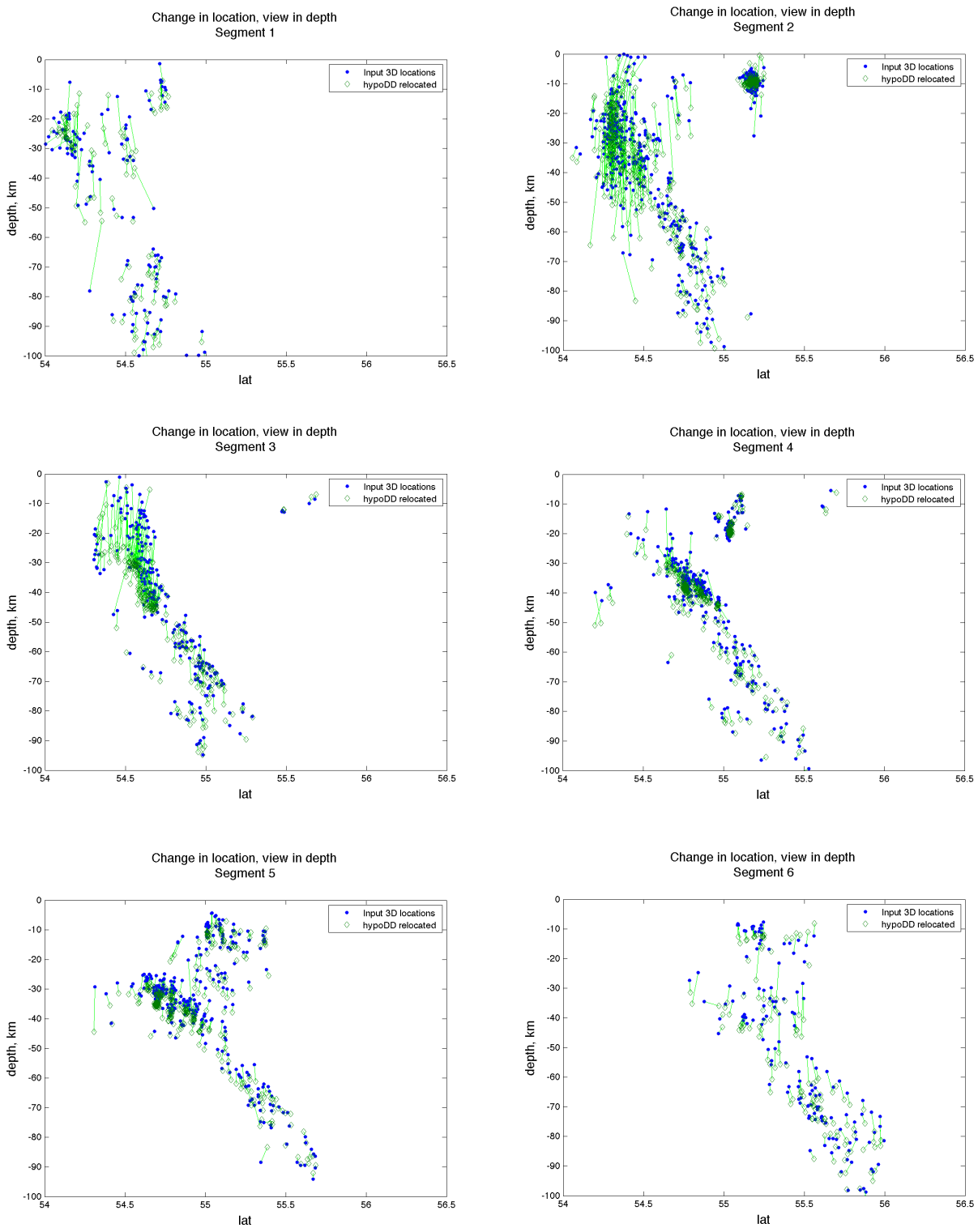

Figure 18: Cross-sections for each of the six segments shown in Figure 15, top, showing the shift in depth between the initial and hypoDD locations. Markers as in Figure 15.

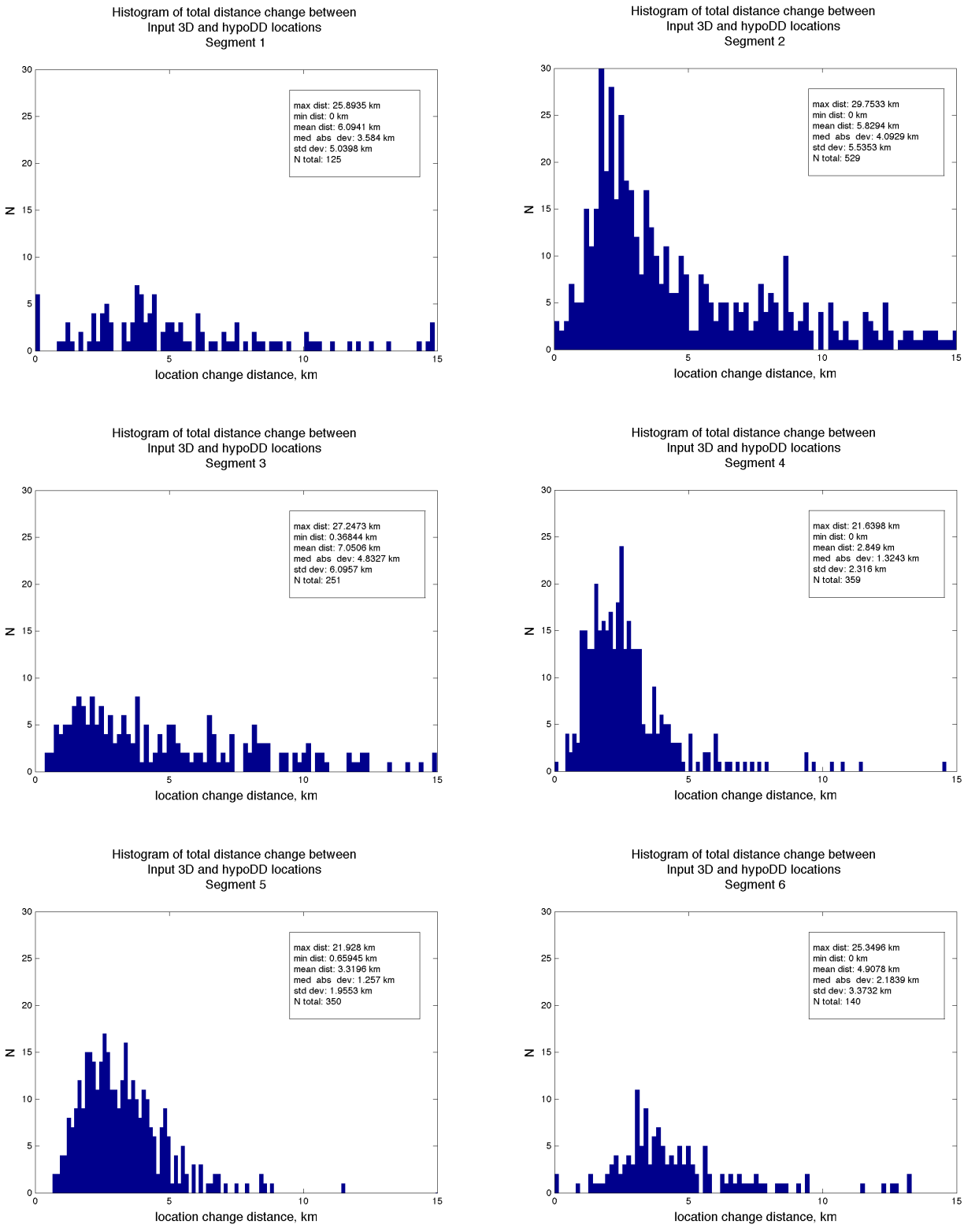

Figure 19: Histograms of the total distances of location change from hypoDD input to hypoDD output for events within each of the six segments from Figure 15.

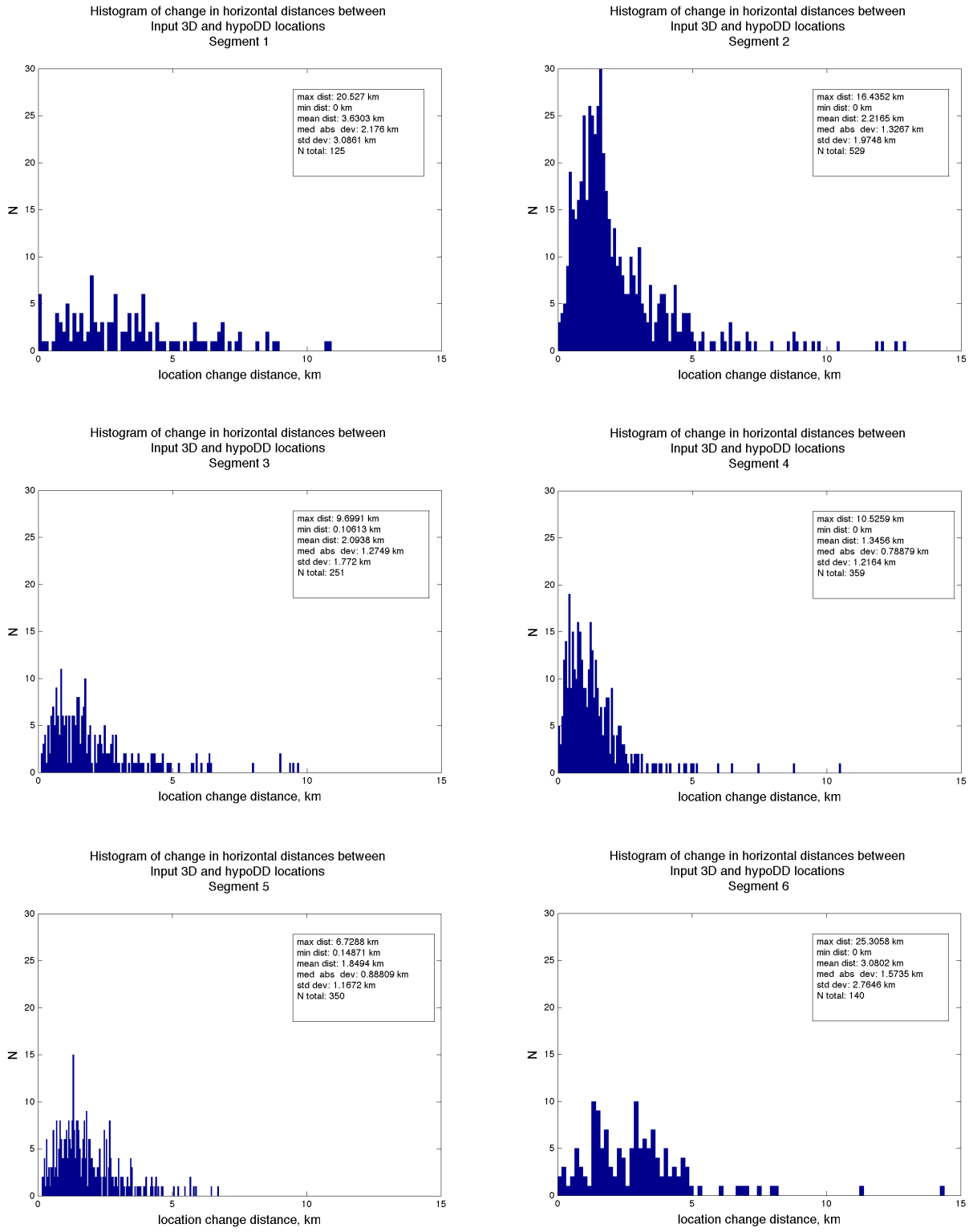

Figure 20: Histograms of the horizontal distances of location change from hypoDD input to hypoDD output for events within each of the six segments from Figure 15.

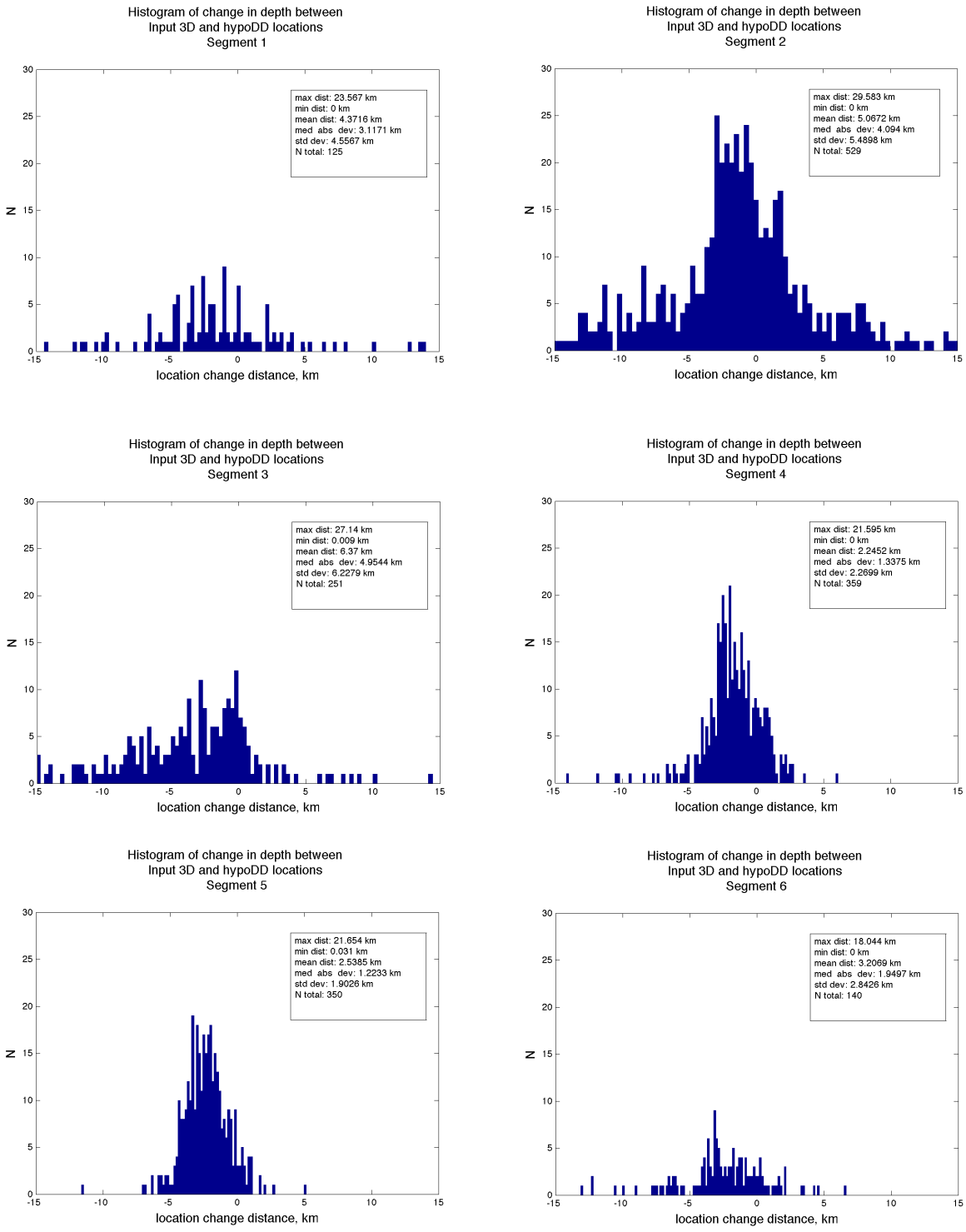

Figure 21: Histograms of the vertical distances of location change from hypoDD input to hypoDD output for events within each of the six segments from Figure 15.

4.2.2 Velocity model perturbation ± 10%

To test the effect on earthquake relocation of an incorrect velocity model, final locations from hypoDD are compared to locations calculated with a velocity model 10% faster and locations calculated with a velocity model 10% slower. The earthquake locations resulting from the faster velocity model are predominantly moved upward in depth (93%) and outward horizontally from the center of the data compared to the locations calculated using the velocity model of Abers, 1994 (Figure 22). Conversely, the slower velocity model results in an overall shift of events deeper than the locations using the unaltered velocity model, as well as an overall adjustment inward toward the center of the data (Figure 24). Plots and histograms of total, horizontal and vertical shifts from both the faster and slower velocity model results for the six segments in Figures 22 and 24 are presented in Appendices C and D, respectively.

The different velocity models have a large effect on the absolute locations, as the events move up or down with the velocity perturbation, but there is less of an effect on the location of the events relative to one another. The standard deviations for the faster model locations and slower model locations are nearly the same, ~3.9, and smaller than the standard deviation of 4.6 for the locations calculated using the unaltered velocity model. Although hypoDD can accurately calculate earthquake locations relative to one another, the program does not have good control on absolute location (Waldhauser and Ellsworth, 2000). Thus, using an appropriate velocity model is an important factor in calculating accurate locations. The use of the 3D velocity model of Abers (1994) on the data prior to relocation in hypoDD increase confidence in the absolute locations that were relocated in the double-difference algorithm for this study.

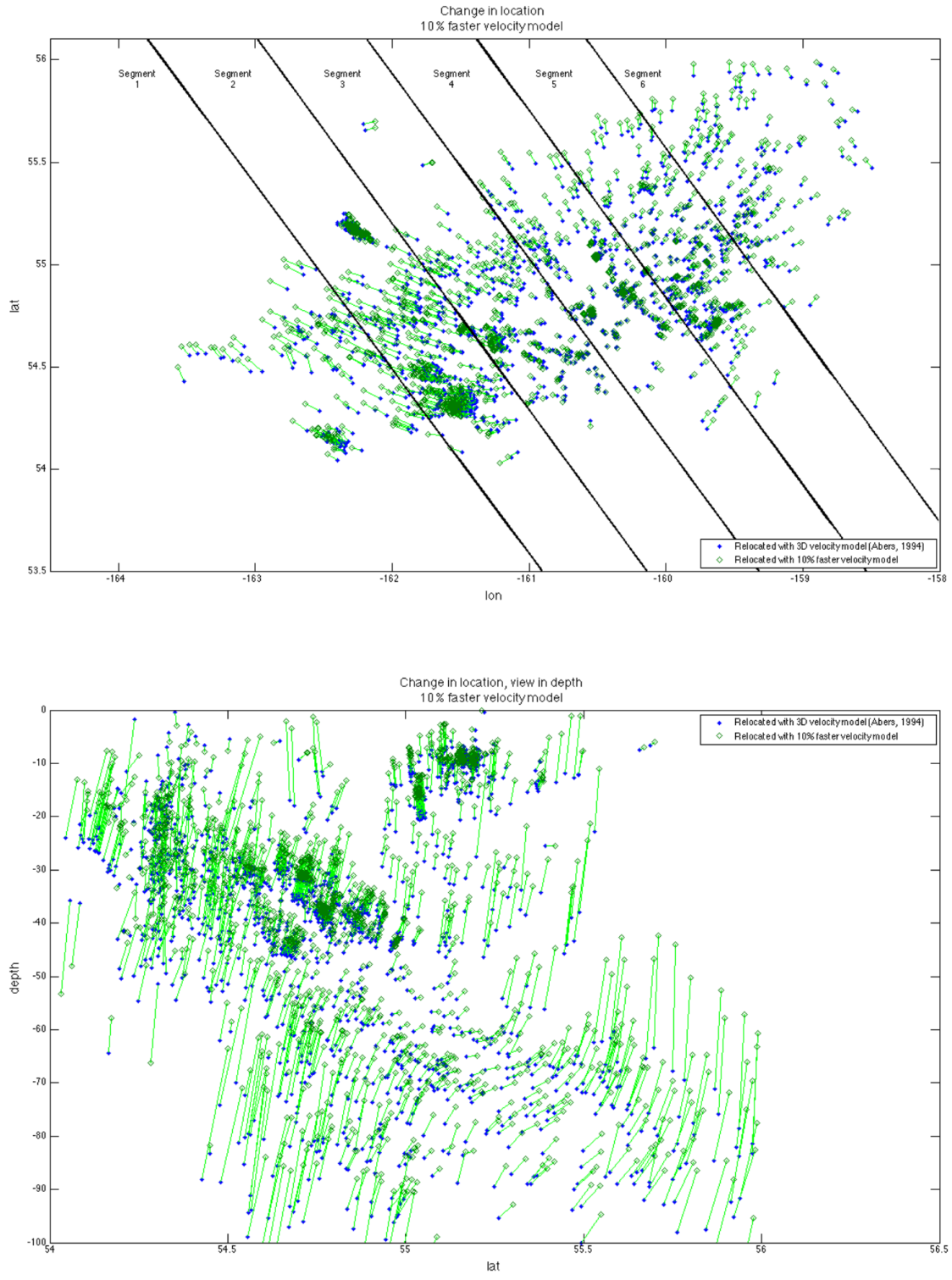

Figure 22: Map view (top) and cross-section (bottom) of changes in locations to hypoDD output from using a velocity model that is 10% faster, for all events passed through hypoDD.

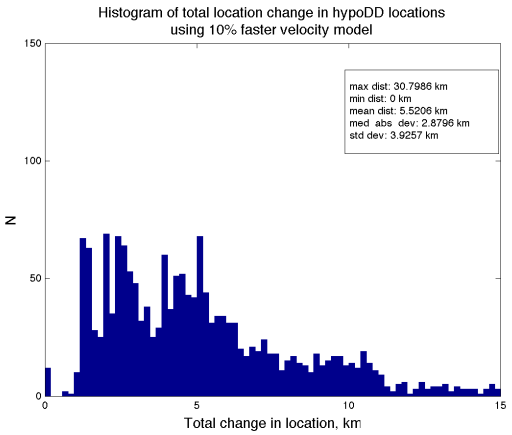

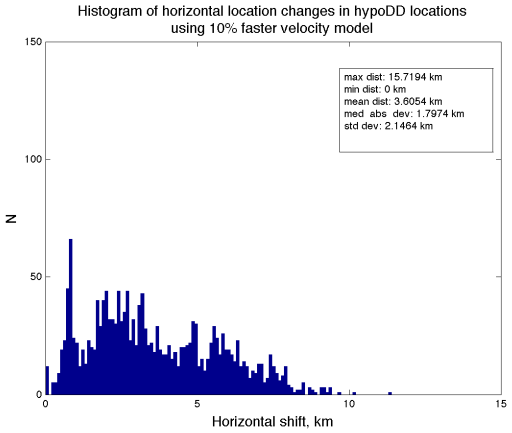

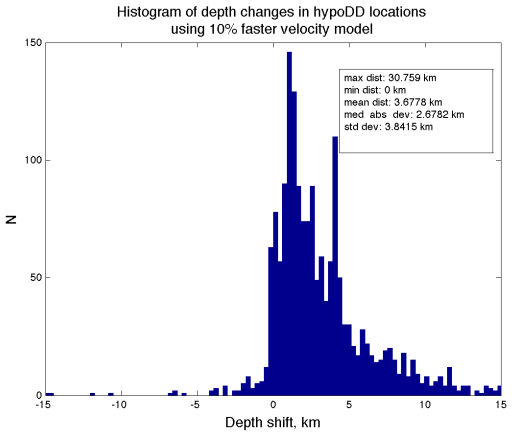

Figure 23: Histograms of the total (top), horizontal (middle), and vertical (bottom) distances of location change to hypoDD output from using a velocity model that is 10% faster, for all events.

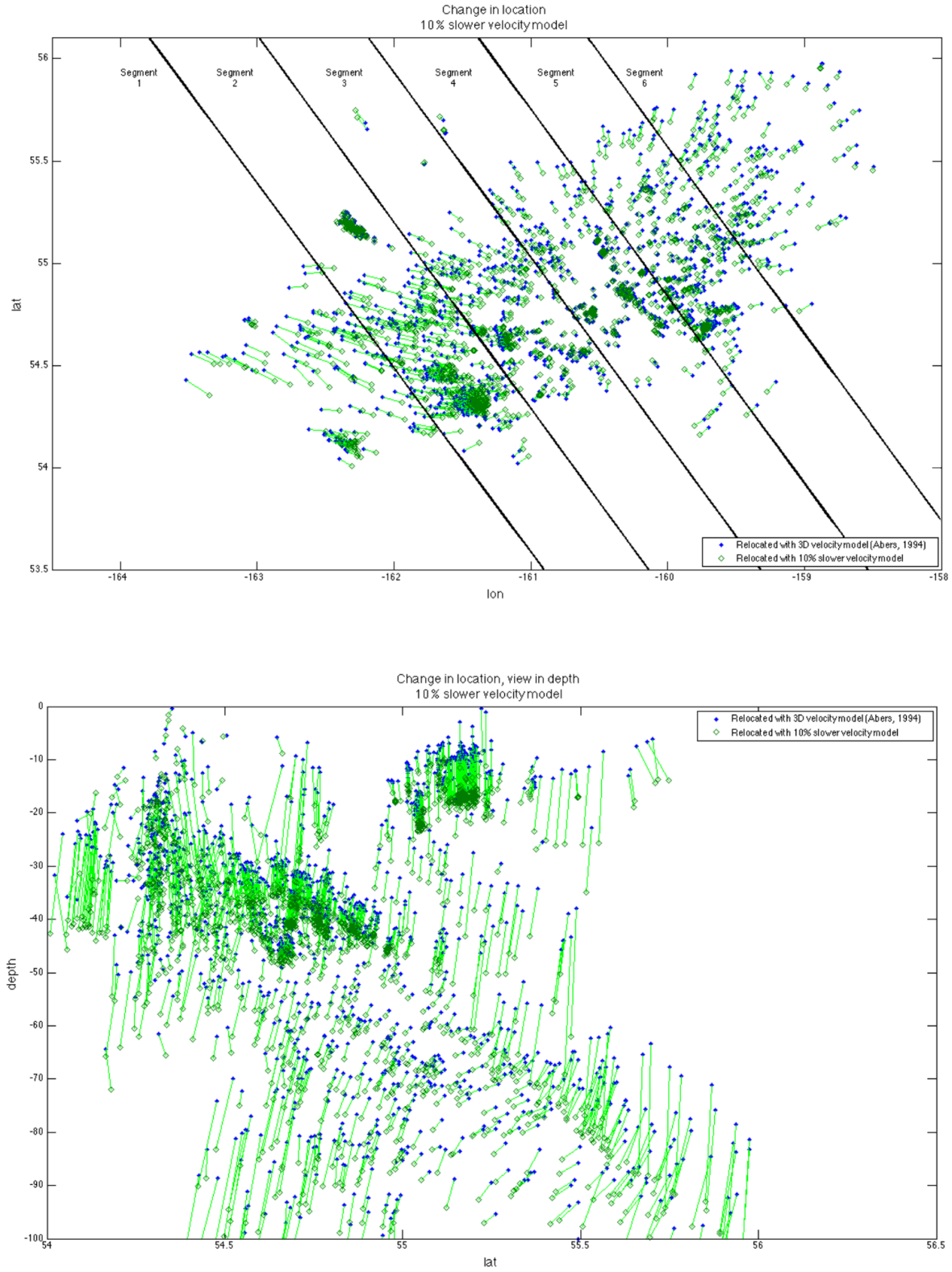

Figure 24: Map view (top) and cross-section (bottom) of changes in locations to hypoDD output from using a velocity model that is 10% slower, for all events passed through hypoDD.

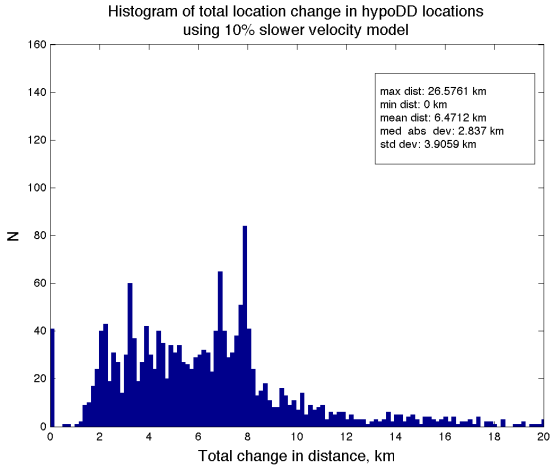

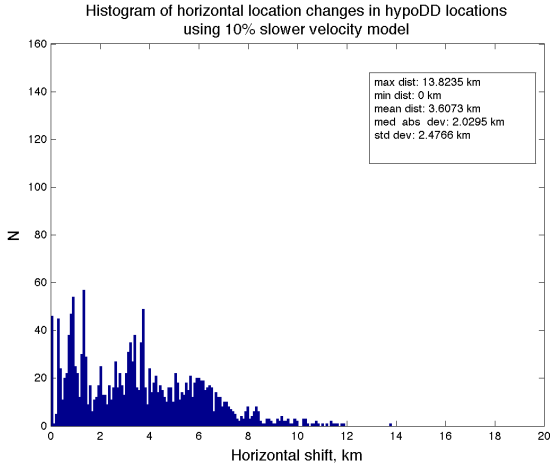

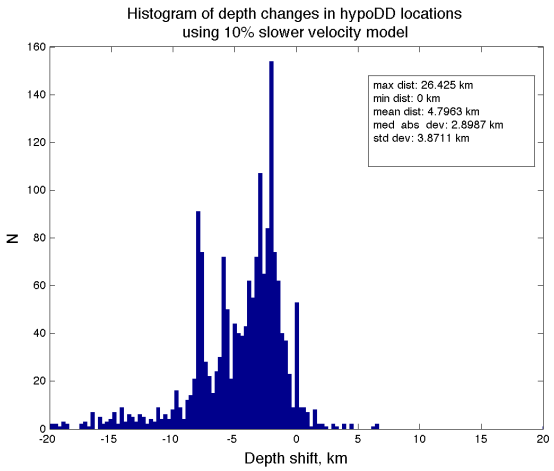

Figure 25: Histograms of the total (top), horizontal (middle), and vertical (bottom) distances of location change to hypoDD output from using a velocity model that is 10% slower, for all events.

Chapter 5

Discussion

The results of this study are similar to previous studies of Shumagin Gap seismicity (e.g. Hudnut and Taber, 1987; Abers, 1992; Abers, 1994, Li *et al*., 2013). However, the relocated seismicity presented here does provide some interesting observations of the active seismicity along the seismogenic zone in the Shumagin Gap. Because the earthquakes in the Shumagin Gap are recorded by stations able to receive direct waves generated within the seismogenic zone, the constraint on depth is greatly improved compared to other subduction zones where on-land seismometers record earthquake data originating from some distance offshore. While few subduction zones globally provide the ability to install on-land seismometers above the seismogenic zone, the findings of this study do indicate an advantage to using direct seismic rays from the megathrust. Ocean bottom seismometers (OBS) provide a better constraint on subduction megathrust seismicity (e.g. Obana *et al*., 2015) where onland seismometers are not an available option.

5.1 Potential Splay faults

Recent findings by Bécel *et al.* (2017) illustrate an active landward dipping splay fault imaged in MCS Line 5 collected during the 2011 ALEUT program. The seismic reflection image shows a normal fault that has offset the youngest sediments at the seafloor, and extends through the crust to intersect the plate boundary at 35 km depth. The southwestward-striking fault in Figure 11 intersects Profile F – F' at 54.756, -160.756. This point is approximately 2 km east of the

ALEUT MCS Line 5 and 140 km from the trench, where the seismic reflection and seismicity data of Bécel *et al.* (2017) image the intersection of the recently active normal fault with the plate interface.

Understanding the locations active splay faults provides important information for hazards assessments of the Shumagin Gap, as these faults can cause tsunami such as the catastrophic 2011 Tohoku-oki event. The potential of rupture along splay faults greatly increases the risk of tsunami. Thus, identifying seismically active faults is of great importance to assessments of hazards in the from the Shumagin Island region. Geodetic data indicate a low strain accumulation rate in the Shumagin Gap (Savage *et al*., 1986). However, there is evidence of past great earthquake ruptures within the Shumagin Gap, and paleoseismic evidence indicates these events produced tsunami (Davies *et al*., 1981; Savage *et al*., 1986; Boyd *et al*., 1988; Nishenko and Jacob, 1990; Estabrook and Boyd, 1992). The 1946 tsunamigenic earthquake illustrates the significant impact of rupture in the shallow portion of the plate megathrust around the Shumagin Gap region.

Occurrences of splay faults rupturing coseismically during megathrust earthquakes have been described in Chile and Sumatra. During the 2011 Araucania earthquake (M 7.1) in Chile, a large upper plate normal fault was dynamically triggered by the main thrust earthquake, 30 km away (Hicks and Reitbrock, 2015). Reactivated splay faults west of the Aceh basin may have ruptured coseismically with the December 2004 Mw 9.2 Sumatra-Andaman megathrust earthquake and contributed to the devastating tsunami that inundated coastlines surrounding the Indian Ocean (Waldhauser *et al*., 2012).

5.2 Downdip transition in thrust zone seismicity

The abrupt transition in seismicity at ~44 km depth is visible in the five profiles presented in this study, particularly in Figures 6 and 7. For older, colder subducting plates, like the Pacific plate in Alaska, the downdip limit to seismicity occurs beneath the intersection of the subducting slab with the forearc mantle (Oleskevich *et al*., 1999). Seismic reflection data collected offshore of the Alaska Peninsula indicate that the oceanic plate intersects the continental Moho at 40 km depth (Janiszewski *et al*., 2013; Li *et al*., 2015). The abrupt transition in of seismic character at 44 km depth is interpreted here as the downdip limit to seismicity on the main thrust zone in the Shumagin Gap.

5.3 Deeply rooted faults cutting the subducting plate

The planes of seismicity extending down from the interface in Figures 6 and 7 may indicate faults formed from lithospheric flexure during subduction are active along the subducting slab in this region. Abers (1992) concluded that bending was not likely occurring in the Shumagin Gap as there was not a correlation seen between curvature along the interface and the locations of earthquakes. In MCS reflection profiles gathered near the Shumagin Gap, bending faults are imaged within the seafloor and the igneous basement (Shillington *et al*., 2015). These bending faults correspond with changes in hydration and seismicity of the subducting Pacific plate, and are aligned with preexisting structures within 10-25° of the orientation of the trench (Shillington *et al*., 2015). While the structures seen in the seismicity presented in this study are much deeper than those imaged by Shillington *et al*. (2015), they may be the deeper expression of bending-related stresses in the subducting Pacific Plate. In the Middle America trench at Nicaragua bending faults cut > 20 km depth from the seafloor (Ranero *et al*., 2003). The depth uncertainty

in Segments 5 and 6 (Figures 15, 21), where these features are most prominent (along Profiles B – B' and A – A') are 2.54 km with a standard deviation of 1.22m and 3.2 km with a standard deviation of 1.95 km, respectively. The addition of focal mechanism analysis for the earthquakes that compose these potential faults would provide a more objective constraint on the processes and stress conditions at work here.

5.4 Downdip and lateral variations in slab dip

The change in slab dip beneath the seismicity cutoff seen in Figure 6 and 7 may have an impact on rupture models of the Shumagin Gap, where dip is a key input to the models. In the rupture models of Slab 1.0 (Hayes *et al*., 2012) the estimates of the potential rupture width are dependent in part on the dip of the interface. An inaccurate dip, which does not accurately present the geometry of the subducting slab, will introduce considerable error into the modeled width of the rupture interface (Hayes *et al*., 2012)

5.5 Undefined updip limit to seismicity

The updip limit of seismicity is not defined in this study. Although earthquakes are present seaward and southeast of ~154° latitude (Figure 5, top), these events did not have enough strongly linked neighboring events in these tests and were removed during the process of double-difference relocation in hypoDD. The area seaward, to the south and southwest, is lacking station coverage compared to the north and northeast, which may account for some reduction in data quality and travel-time information. However, the events are still within good range of the network and are expected to have reliable recorded arrivals. The addition of waveform cross-correlation for P and S arrivals would better constrain the locations of the hypocenters, and

perhaps provide better resolution of the shallow updip seismicity. Cross-correlation of waveforms ensures that arrivals are determined identically for all events (Deichman and Garcia-Fernandez, 1992) and greatly increases the resolution of relative hypocenter locations (Poupinet *et al*., 1984; Frechet, 1985; Fremont and Malone, 1987; Deichmann and Garcia-Fernandez, 1992; Got *et al.,* 1994; Dodge *et al*., 1995; Nadeau *et al*., 1995; Shearer, 1997; Lees, 1998; Menke, 1999; Phillips, 2000; Waldhauser and Ellsworth, 2000; Morya *et al*., 2003; Schaff *et al*., 2004; Schaff and Waldhauser, 2005; Hauksson and Shearer, 2005). Additionally, focal mechanisms are needed to clearly define the downdip limit to seismicity on the main thrust interface, as well as differentiate between upper plate, interface, and downgoing plate seismicity.

Chapter 6

Conclusions

Double-difference relative relocation using hypoDD delineate a clearly defined subduction thrust interface beneath the Shumagin Islands in Alaska. Streaks of earthquakes trend northwest at a small angle to subduction orientation. At depth in the eastern portion of the study area, these features form a clear, defined interface between ~30 – 45 km depth. Deeply rooted faults are interpreted to be cutting through the subducting Pacific Plate, dipping steeply trenchward from about 30 – 40 km depth in the eastern section of the Shumagin Islands. The relocated seismicity provides a good constraint on the downdip limit to seismicity in the Shumagin Gap, where the interface stops abruptly. More analyses of these data are required to improve understanding of the seismicity updip and confidently identify and characterize the finer scale structure of the plate interface. In particular, waveform cross-correlation in combination with double-difference relative relocation can drastically improvise the accuracy of relocations. The addition of focal mechanisms will also provide the information needed to assess the sources of these earthquakes and differentiate between upper plate, lower plate, and plate boundary seismicity along the shallow subduction interface.

APPENDIX A

hypoDD Input and Output

I: Input Parameters and hypoDD Output for Main Results Presented in this Study

Table 9: Input parameters and Output for hypoDD relocations presented

--- DATA SELECTION:

IDAT	IPHA	DIST
2	3	400

--- EVENT CLUSTERING:

OBSCC	OBSCT	MINDS	MAXDS	MAXGAP
0	12	0	150	-999

--- SOLUTION CONTROL:

ISTART	ISOLV	IAQ	NSET
2	2	1	4

DATA WEIGHTING AND REWEIGHTING:

NITER	WTCCP	WTCCS	WRCC	WDCC	WTCTP	WTCTS	WRCT	WDCT	DAMP
3	-999	-999	-999	-999	1.00	0.80	-999	-999	55
5	-999	-999	-999	-999	1.00	0.80	-999	-999	65
3	-999	-999	-999	-999	1.00	0.80	6	50	90
5	-999	-999	-999	-999	1.00	0.80	6	20	100

Output:

```
starting hypoDD (v2.1beta - 09/30/2011)...
Input parameters: ./hypoDD_3d_ct.inp (hypoDD2.0 format)
INPUT FILES:
 cross dtime data: empty.cc
 catalog dtime data: dt.ct
 events: event.sel
 stations: station.sel
OUTPUT FILES:
 initial locations: hypoDD_3d_ct_27.loc
 relocated events: hypoDD_3d_ct_27.reloc
 event pair residuals: hypoDD_3d_ct_27.res
 station residuals: hypoDD_3d_ct_27.sta
 source parameters: hypoDD_3d_ct_27.src
Use local 3D model vel3d.dat
Relocate all clusters
```

```
Relocate all events
Remove air quakes.
Reading data ...   Mon Jul 10 04:29:59 201761
# events =  3395
# stations < maxdist =     21
# stations w/ neg. elevation (set to 0) =    0
# catalog P dtimes =  630340
# catalog S dtimes =  524488
# dtimes total =  1154828
    after gap/distance check:   987143 ( 85%)
    nccp,nccs,nctp,ncts:            0           0      528167      458976
# events after dtime match =       3383
# stations =     21
clustering ...
Clustered events:  1798
Isolated events:  1585
# clusters:    3
Cluster   1:  1794 events
Cluster   2:     2 events
Cluster   3:     2 events

RELOCATION OF CLUSTER: 1     Mon Jul 10 04:30:13 201761
----------------------
Reading data ...   Mon Jul 10 04:30:13 201761
# events =  1794
# stations < maxdist =     21
# stations w/ neg. elevation (set to 0) =    0
# catalog P dtimes =  340050
# catalog S dtimes =  288842
# dtimes total =   628892
    after gap/distance check:   567994 ( 90%)
    nccp,nccs,nctp,ncts:            0           0      303690      264304
# events after dtime match =       1794
# stations =     21
Initial trial sources =  1794
3D ray tracing.
```

IT	EV	CT	RMSCT		RMSST	DX	DY	DZ	DT	OS	AQ	CND
		%	%	ms	%	ms	m	m	m	ms	m		
1		100	100	224	-50.8	0	1096	1289	2815	182	0	12	396
2		99	99	220	-2.0	0	1065	1287	2518	176	0	2	396
3	1	99	99	219	-0.1	528	1063	1287	2511	176	794	0	396
4		99	99	208	-5.0	528	400	293	982	59	794	2	368
5	2	99	99	201	-3.6	522	277	296	1026	56	1084	0	365
6		99	99	192	-4.6	522	145	178	680	30	1084	1	362
7	3	99	99	192	-0.0	519	144	177	680	30	1314	0	358
8		99	99	190	-0.6	519	86	94	389	14	1314	1	279
9	4	99	99	190	-0.0	516	91	97	397	15	1504	0	279
10	5	99	99	190	-0.1	516	80	73	351	10	1652	0	267
11	6	99	99	190	-0.1	515	65	53	291	8	1730	0	264
12		99	99	190	-0.1	515	66	49	331	8	1730	2	264
13	7	99	99	186	-1.9	516	72	56	319	7	1859	0	268
14	8	99	99	186	-0.0	515	65	45	274	7	1909	0	265
15	9	99	95	125	-33.1	334	144	204	514	22	1961	0	206

```
16 10  99  94  116  -6.7   310   78  114  305   15 2057   0  196
17 11  99  93  112  -3.3   302   57   77  240   11 2133   0  193
18 12  98  71  106  -5.4   292   86  112  250   12 2172   0  190
19 13  98  69  101  -5.2   276   50   69  179    8 2227   0  183
20 14  98  69   98  -2.4   270   38   55  144    7 2252   0  181
21 15  98  68   97  -1.4   266   32   43  141    5 2298   0  178
22 16  98  68   96  -1.0   264   28   38  108    4 2328   0  173

writing out results ...

RELOCATION OF CLUSTER: 2
----------------------
Reading data ...   Mon Jul 10 05:05:04 201762
# events =     2
# stations < maxdist =     21
# stations w/ neg. elevation (set to 0) =    0
# catalog P dtimes =       6
# catalog S dtimes =       6
# dtimes total =       12
    after gap/distance check:       12 (100%)
    nccp,nccs,nctp,ncts:            0           0           6           6
# events after dtime match =          2
# stations =      6
Initial trial sources =     2
3D ray tracing.

  IT   EV  CT    RMSCT   RMSST   DX   DY   DZ   DT   OS  AQ  CND
        %   %    ms      %    ms    m    m    m   ms    m
 1  1 100 100  239  -0.3   395    1    3   12    3    4   0    2
 2  2 100 100  239  -0.3   393    1    3   11    2    7   0    2
 3  3 100 100  238  -0.3   392    1    3   11    1   11   0    2
 4  4 100 100  238  -0.2   391    1    2    8    1   13   0    2
 5  5 100 100  237  -0.2   389    1    2    8    1   16   0    2
 6  6 100 100  237  -0.2   388    1    2    8    0   18   0    2
 7  7 100 100  236  -0.2   387    1    2    7    0   20   0    2
 8  8 100 100  236  -0.2   386    1    2    7    0   22   0    2
 9  9 100 100  208 -11.9   386    0    1    3    0   23   0    2
10 10 100 100  208  -0.1   385    0    1    3    0   24   0    2
11 11 100 100  207  -0.1   385    0    1    3    0   25   0    2
12 12 100 100  207  -0.1   385    0    1    2    0   26   0    2
13 13 100 100  207  -0.1   384    0    1    2    0   26   0    2
14 14 100 100  207  -0.1   384    0    1    2    0   27   0    2
15 15 100 100  207  -0.1   384    0    1    2    0   28   0    2
16 16 100 100  207  -0.1   383    0    1    2    0   28   0    2

writing out results ...

RELOCATION OF CLUSTER: 3
----------------------
Reading data ...   Mon Jul 10 05:05:07 201762
# events =     2
# stations < maxdist =     21
# stations w/ neg. elevation (set to 0) =    0
# catalog P dtimes =       8
```

```
# catalog S dtimes =       7
# dtimes total =       15
    after gap/distance check:       13 ( 87%)
    nccp,nccs,nctp,ncts:            0           0           7           6
# events after dtime match =          2
# stations =      7
Initial trial sources =     2
3D ray tracing.

  IT   EV  CT    RMSCT   RMSST   DX   DY   DZ   DT   OS  AQ  CND
        %   %   ms     %    ms    m    m    m   ms    m
 1  1 100 100   630  -0.8  1427   11   10   30    1   30   0    3
 2  2 100 100   625  -0.8  1418   11    9   29    2   59   0    3
 3  3 100 100   619  -0.8  1409   10    9   29    2   88   0    3
 4  4 100 100   616  -0.6  1402    7    7   20    2  108   0    2
 5  5 100 100   612  -0.6  1396    7    7   20    2  128   0    2
 6  6 100 100   609  -0.6  1391    7    7   20    1  147   0    2
 7  7 100 100   605  -0.5  1385    7    6   19    1  167   0    2
 8  8 100 100   602  -0.5  1379    7    6   19    1  186   0    2
 9  9 100 100   504 -16.2  1377    3    4    7    1  193   0    2
10 10 100 100   503  -0.2  1375    3    4    7    1  201   0    2
11 11 100 100   502  -0.2  1372    3    4    7    1  208   0    2
  Cluster has less than 2 events.
   Program hypoDD finished.
```

II: OBSCT Tests

OBSCT=8

Table 10: Input parameters and Output for hypoDD OBSCT Test 1

```
--- DATA SELECTION:
 IDAT   IPHA   DIST
 2      3      400
--- EVENT CLUSTERING:
 OBSCC  OBSCT  MINDS  MAXDS  MAXGAP
 0      8      0      150    -999
--- SOLUTION CONTROL:
 ISTART  ISOLV  IAQ  NSET
 2       2      1    4

 DATA WEIGHTING AND REWEIGHTING:
 NITER  WTCCP  WTCCS  WRCC  WDCC  WTCTP  WTCTS  WRCT  WDCT  DAMP
```

3	-999	-999	-999	-999	1.00	0.80	-999	-999	55
5	-999	-999	-999	-999	1.00	0.80	-999	-999	65
3	-999	-999	-999	-999	1.00	0.80	6	50	90
5	-999	-999	-999	-999	1.00	0.80	6	20	100

Output:

```
starting hypoDD (v2.1beta - 09/30/2011)...
Input parameters: ./hypoDD_3d_ct.inp (hypoDD2.0 format)
INPUT FILES:
 cross dtime data: empty.cc
 catalog dtime data: dt.ct
 events: event.sel
 stations: station.sel
OUTPUT FILES:
 initial locations: hypoDD_3d_ct_12.loc
 relocated events: hypoDD_3d_ct_12.reloc
 event pair residuals: hypoDD_3d_ct_12.res
 station residuals: hypoDD_3d_ct_12.sta
 source parameters: hypoDD_3d_ct_12.src
Use local 3D model vel3d.dat
Relocate all clusters
Relocate all events
Remove air quakes.
Reading data ...
# events =  3395
# stations < maxdist =     21
# stations w/ neg. elevation (set to 0) =    0
# catalog P dtimes =  630340
# catalog S dtimes =  524488
# dtimes total =  1154828
    after gap/distance check:   987143 ( 85%)
    nccp,nccs,nctp,ncts:            0           0      528167      458976
# events after dtime match =       3383
# stations =     21
clustering ...
Clustered events:  2606
Isolated events:   777
# clusters:    2
Cluster   1:  2604 events
Cluster   2:     2 events

RELOCATION OF CLUSTER: 1
----------------------
Reading data ...
# events =  2604
# stations < maxdist =     21
# stations w/ neg. elevation (set to 0) =    0
# catalog P dtimes =  502990
# catalog S dtimes =  428407
# dtimes total =   931397
    after gap/distance check:   831375 ( 89%)
    nccp,nccs,nctp,ncts:            0           0      442586      388789
# events after dtime match =       2604
```

```
# stations =     21
Initial trial sources =  2604
3D ray tracing.

  IT   EV  CT    RMSCT   RMSST   DX   DY   DZ   DT   OS  AQ  CND
         %   %    ms      %     ms    m    m    m   ms    m
 1     100 100   252 -62.5      0 1599 1854 3991  266     0  33  568
 2      99  99   231  -8.3      0 1512 1750 3486  248     0   1  553
 3   1  99  99   231  -0.1    537 1510 1750 3484  248   974   0  553
 4      99  99   221  -4.2    537  659  547 1574   83   974   7  523
 5   2  98  98   221  -0.2    525  650  535 1529   82 1496   0  519
 6      98  98   209  -5.1    525  380  362  995   43 1496   7  495
 7   3  98  98   200  -4.3    521  403  316  995   42 1511   0  497
 8      98  98   199  -0.5    521  241  178  638   21 1511   1  395
 9   4  98  98   199   0.0    519  242  177  637   21 1645   0  395
10      98  98   198  -0.7    519  179  140  647   17 1645   2  398
11   5  98  98   198  -0.0    516  178  145  635   17 1880   0  398
12      98  98   200   0.9    516  214  149  570   16 1880   1  393
13   6  98  98   200  -0.0    514  214  149  571   16 1873   0  393
14   7  98  98   198  -0.7    513  178  118  423   13 1900   0  385
15      98  98   198   0.1    513  138  120  420   12 1900   1  379
16   8  98  98   198  -0.0    515  138  120  420   12 2016   0  379
17   9  98  93   122 -38.5    345  216  289  618   30 1967   0  323
18      98  91   112  -8.2    345  120  167  382   21 1967   1  320
19  10  98  91   110  -1.4    302  122  170  387   21 2052   0  316
20      98  90   107  -3.5    302   85  118  298   15 2052   1  308
21  11  98  90   106  -0.7    292   86  119  299   16 2144   0  311
22  12  96  67    99  -6.5    288  117  146  301   15 2001   0  265
23  13  96  65    93  -6.1    267   70   87  206   10 2069   0  253
24  14  96  64    90  -3.0    258   56   64  168    8 2125   0  249
25  15  96  64    88  -1.9    253   46   53  157    7 2154   0  241
26      96  63    87  -1.2    253   40   46  152    6 2154   1  238
27  16  96  63    87  -0.3    256   40   47  153    6 2212   0  238

writing out results ...
 WARNING: org time diff > 5s for         4772

RELOCATION OF CLUSTER: 2
-----------------------
Reading data ...
# events =     2
# stations < maxdist =     21
# stations w/ neg. elevation (set to 0) =    0
# catalog P dtimes =       6
# catalog S dtimes =       4
# dtimes total =       10
    after gap/distance check:        9 ( 90%)
    nccp,nccs,nctp,ncts:           0           0           5           4
# events after dtime match =          2
# stations =      6
Initial trial sources =     2
3D ray tracing.

  IT   EV  CT    RMSCT   RMSST   DX   DY   DZ   DT   OS  AQ  CND
```

```
         %   %   ms      %    ms     m    m    m   ms    m
 1   1 100 100  406  -0.2  1746    2    1   21    3   11    0    2
 2   2 100 100  405  -0.2  1740    2    1   21    2   23    0    2
 3   3 100 100  404  -0.2  1734    2    1   21    1   34    0    2
 4   4 100 100  404  -0.1  1730    2    0   15    1   42    0    2
 5   5 100 100  403  -0.1  1726    2    0   15    0   50    0    2
 6   6 100 100  403  -0.1  1722    2    0   15    0   58    0    2
 7   7 100 100  402  -0.1  1718    2    0   15    0   66    0    2
 8   8 100 100  401  -0.1  1714    2    0   15    0   73    0    2
 9   9 100 100  324 -19.3  1712    1    0    6    0   76    0    2
10  10 100 100  324  -0.0  1711    1    0    6    0   80    0    2
11  11 100 100  324  -0.0  1709    1    0    6    0   83    0    2
  Cluster has less than 2 events.
   Program hypoDD finished.
```

OBSCT=16

Table 11: Input parameters and Output for hypoDD OBSCT Test 2

--- DATA SELECTION:

IDAT	IPHA	DIST
2	3	400

--- EVENT CLUSTERING:

OBSCC	OBSCT	MINDS	MAXDS	MAXGAP
0	16	0	150	-999

--- SOLUTION CONTROL:

ISTART	ISOLV	IAQ	NSET
2	2	1	4

DATA WEIGHTING AND REWEIGHTING:

NITER	WTCCP	WTCCS	WRCC	WDCC	WTCTP	WTCTS	WRCT	WDCT	DAMP
3	-999	-999	-999	-999	1.00	0.80	-999	-999	55
5	-999	-999	-999	-999	1.00	0.80	-999	-999	65
3	-999	-999	-999	-999	1.00	0.80	6	50	90
5	-999	-999	-999	-999	1.00	0.80	6	20	100

Output:

```
starting hypoDD (v2.1beta - 09/30/2011)...
Input parameters: ./hypoDD_3d_ct.inp (hypoDD2.0 format)
INPUT FILES:
 cross dtime data: empty.cc
 catalog dtime data: dt.ct
 events: event.sel
 stations: station.sel
OUTPUT FILES:
 initial locations: hypoDD_3d_ct_28.loc
```

```
 relocated events: hypoDD_3d_ct_28.reloc
 event pair residuals: hypoDD_3d_ct_28.res
 station residuals: hypoDD_3d_ct_28.sta
 source parameters: hypoDD_3d_ct_28.src
Use local 3D model vel3d.dat
Relocate all clusters
Relocate all events
Remove air quakes.
Reading data ...
# events =  3395
# stations < maxdist =     21
# stations w/ neg. elevation (set to 0) =    0
# catalog P dtimes =  630340
# catalog S dtimes =  524488
# dtimes total =  1154828
    after gap/distance check:   987143 ( 85%)
    nccp,nccs,nctp,ncts:            0           0      528167      458976
# events after dtime match =       3383
# stations =     21
clustering ...
Clustered events:  1102
Isolated events:  2281
# clusters:    5
Cluster   1:  1089 events
Cluster   2:     5 events
Cluster   3:     4 events
Cluster   4:     2 events
Cluster   5:     2 events

RELOCATION OF CLUSTER: 1
----------------------
Reading data ...
# events =  1089
# stations < maxdist =     21
# stations w/ neg. elevation (set to 0) =    0
# catalog P dtimes =  183450
# catalog S dtimes =  157944
# dtimes total =   341394
    after gap/distance check:   319182 ( 93%)
    nccp,nccs,nctp,ncts:            0           0      169981      149201
# events after dtime match =       1089
# stations =     21
Initial trial sources =  1089
3D ray tracing.

  IT   EV  CT    RMSCT   RMSST   DX   DY   DZ   DT   OS  AQ  CND
        %   %   ms     %    ms    m    m    m   ms    m
 1    100 100  219 -43.6     0  672 1001 2040  125    0   8  292
 2     99  99  214  -2.2     0  674 1005 1955  124    0   2  287
 3  1  99  99  214  -0.0   553  669 1006 1935  124  506   0  287
 4     99  99  198  -7.5   553  176  203  768   43  506   1  273
 5  2  99  99  198  -0.1   524  173  202  759   43  920   0  273
 6  3  99  99  187  -5.7   498   85  140  432   31 1170   0  270
 7  4  99  99  184  -1.3   499   44   77  288   14 1253   0  210
```

```
 8      99  99  183  -0.4   499   35   55  216     9 1253   1  202
 9   5  99  99  183  -0.0   502   35   54  215     9 1416   0  202
10   6  99  99  183  -0.2   504   32   47  180     7 1503   0  195
11      99  99  183  -0.1   504   32   45  218     6 1503   1  190
12   7  99  99  183  -0.0   505   33   43  181     6 1620   0  190
13   8  99  99  183  -0.0   503   28   34  162     5 1632   0  190
14   9  99  95  126 -30.8   336  106  166  359    15 1615   0  145
15  10  99  94  119  -6.1   308   54   92  223    11 1699   0  141
16  11  99  94  116  -2.6   296   36   60  164     8 1774   0  135
17  12  97  71  111  -3.8   281   59   82  183     8 1789   0  117
18  13  97  70  106  -4.6   267   31   47  120     6 1840   0  113
19  14  97  70  104  -2.0   261   22   34   94     4 1879   0  112
20  15  97  70  103  -1.0   260   19   27   90     4 1926   0  107
21  16  97  69  102  -0.6   259   16   23   85     3 1957   0  105

writing out results ...

RELOCATION OF CLUSTER: 2
----------------------
Reading data ...
# events =     5
# stations < maxdist =     21
# stations w/ neg. elevation (set to 0) =    0
# catalog P dtimes =     117
# catalog S dtimes =      85
# dtimes total =      202
    after gap/distance check:      157 ( 78%)
    nccp,nccs,nctp,ncts:            0           0          93          64
# events after dtime match =          5
# stations =     10
Initial trial sources =     5
3D ray tracing.

  IT   EV  CT    RMSCT   RMSST   DX   DY   DZ   DT   OS  AQ  CND
         %   %    ms      %     ms    m    m    m   ms    m
 1   1 100 100   348   -4.5  2214   34   23   81    5   21   0    4
 2   2 100 100   335   -3.7  2180   30   20   72    5   39   0    4
 3   3 100 100   324   -3.2  2150   25   19   64    4   56   0    4
 4   4 100 100   318   -2.0  2132   16   13   42    3   68   0    4
 5   5 100 100   312   -1.8  2114   15   13   39    3   80   0    4
 6   6 100 100   307   -1.5  2099   13   13   36    2   90   0    4
 7   7 100 100   304   -1.2  2085   12   13   34    2  100   0    4
 8   8 100 100   300   -1.2  2072   11   12   31    2  110   0    4
 9   9 100  99   225  -25.0   584    3    7    6    1  110   0    3
10  10 100  98   221   -1.6   505    3    7    6    1  110   0    3
11  11 100  98   221   -0.2   507    3    7    5    1  110   0    3
12  12  80  59   169  -23.7   363    1    3    1    0  327   0    3
13  13  80  59   167   -0.9   362    1    3    1    0  327   0    3
14  14  80  59   167   -0.2   362    1    3    1    0  327   0    3
15  15  80  59   166   -0.2   362    1    3    1    0  327   0    3
16  16  80  59   166   -0.2   361    1    3    1    0  327   0    3

writing out results ...
```

```
RELOCATION OF CLUSTER: 3
----------------------
Reading data ...
# events =     4
# stations < maxdist =     21
# stations w/ neg. elevation (set to 0) =    0
# catalog P dtimes =      50
# catalog S dtimes =      35
# dtimes total =       85
    after gap/distance check:       79 ( 93%)
    nccp,nccs,nctp,ncts:            0           0          45          34
# events after dtime match =          4
# stations =     10
Initial trial sources =     4
3D ray tracing.

  IT   EV  CT    RMSCT   RMSST   DX   DY   DZ   DT   OS  AQ  CND
        %   %   ms     %    ms    m    m    m   ms    m
 1  1 100 100  207  -1.5   532   16    7   92    1   79   0    4
 2  2 100 100  204  -1.4   528   15    7   88    1  155   0    4
 3  3 100 100  202  -1.2   524   14    6   82    1  226   0    4
 4  4 100 100  200  -0.9   522   10    4   58    1  275   0    3
 5  5 100 100  198  -0.8   519   10    4   56    1  322   0    3
 6  6 100 100  197  -0.8   517    9    4   53    1  367   0    3
 7  7 100 100  195  -0.7   514    9    4   49    1  407   0    3
 8  8 100 100  194  -0.7   512    9    4   46    1  444   0    3
 9  9 100 100  168 -13.3   512    3    2   18    0  461   0    3
10 10 100 100  168  -0.4   511    3    2   18    0  478   0    3
11 11 100 100  167  -0.5   510    3    2   18    0  495   0    3
12 12 100 100  157  -5.7   511    2    2   18    0  513   0    3
13 13 100 100  157  -0.5   511    2    2   18    0  531   0    3
14 14 100 100  156  -0.6   510    2    2   18    0  548   0    3
15 15 100 100  155  -0.5   510    2    2   17    0  565   0    3
16 16 100 100  154  -0.6   510    2    2   17    0  581   0    3

writing out results ...

RELOCATION OF CLUSTER: 4
----------------------
Reading data ...
# events =     2
# stations < maxdist =     21
# stations w/ neg. elevation (set to 0) =    0
# catalog P dtimes =      10
# catalog S dtimes =       7
# dtimes total =       17
    after gap/distance check:       16 ( 94%)
    nccp,nccs,nctp,ncts:            0           0           9           7
# events after dtime match =          2
# stations =      9
Initial trial sources =     2
3D ray tracing.

  IT   EV  CT    RMSCT   RMSST   DX   DY   DZ   DT   OS  AQ  CND
```

```
         %   %   ms      %    ms     m    m    m   ms    m
 1   1 100 100  496  -0.1  1813    6    0   44    0    3   0    3
 2   2 100 100  495  -0.1  1810    5    0   44    0    6   0    3
 3   3 100 100  495  -0.1  1807    5    0   42    0    8   0    3
 4   4 100 100  494  -0.1  1805    4    0   30    0   10   0    2
 5   5 100 100  494  -0.1  1803    4    0   30    0   11   0    2
 6   6 100 100  493  -0.1  1801    4    0   29    0   12   0    2
 7   7 100 100  493  -0.1  1799    4    0   29    0   13   0    2
 8   8 100 100  492  -0.1  1797    4    0   29    0   13   0    2
 9   9 100  94  212 -56.8   467    1    1   12    0   25   0    2
10  10 100  94  209  -1.8   466    1    1   12    0   37   0    2
11  11 100  94  208  -0.2   465    1    1   12    0   49   0    2
12  12 100  94  208  -0.1   464    1    1    9    0   58   0    2
13  13 100  94  208  -0.2   463    1    1    9    0   67   0    2
14  14 100  94  207  -0.2   463    1    1    9    0   77   0    2
15  15 100  94  207  -0.2   462    1    1    9    0   86   0    2
16  16 100  94  206  -0.2   461    1    0    9    0   95   0    2

writing out results ...

RELOCATION OF CLUSTER: 5
------------------------
Reading data ...
# events =     2
# stations < maxdist =     21
# stations w/ neg. elevation (set to 0) =    0
# catalog P dtimes =      10
# catalog S dtimes =       9
# dtimes total =       19
    after gap/distance check:       17 ( 89%)
    nccp,nccs,nctp,ncts:            0           0           9           8
# events after dtime match =          2
# stations =      9
Initial trial sources =     2
3D ray tracing.

  IT   EV  CT    RMSCT   RMSST   DX   DY   DZ   DT   OS  AQ  CND
         %   %   ms      %    ms     m    m    m   ms    m
 1   1 100 100  349  -0.3   695    5    5    2    1    2   0    3
 2   2 100 100  349  -0.2   695    5    5    2    1    3   0    3
 3   3 100 100  348  -0.2   695    5    5    2    1    5   0    3
 4   4 100 100  347  -0.1   695    4    3    1    1    6   0    3
 5   5 100 100  347  -0.1   695    3    3    1    1    8   0    3
 6   6 100 100  346  -0.1   695    3    3    1    1    9   0    3
 7   7 100 100  346  -0.2   695    3    3    1    1   10   0    3
 8   8 100 100  345  -0.2   695    3    3    1    1   11   0    3
 9   9 100 100  299 -13.4   696    2    1    1    1   12   0    2
10  10 100 100  299  -0.1   697    2    1    1    0   12   0    2
11  11 100 100  291  -2.6   697    2    0    1    0   12   0    2
12  12 100 100  290  -0.1   698    2    0    1    0   12   0    2
13  13 100 100  290  -0.1   699    2    0    1    0   12   0    2
14  14 100 100  297   2.4   699    1    0    1    0   13   0    2
15  15 100 100  297  -0.1   699    1    0    1    0   13   0    2
16  16 100 100  296  -0.1   700    1    0    1    0   13   0    2
```

```
writing out results ...

   Program hypoDD finished.
```

III: P vs. S Weighting Tests

P=1.0, S=0.5

Table 12: Input parameters and Output for hypoDD P to S weighting Test 1

DATA WEIGHTING AND REWEIGHTING:

NITER	WTCCP	WTCCS	WRCC	WDCC	WTCTP	WTCTS	WRCT	WDCT	DAMP
3	-999	-999	-999	-999	1.00	0.50	-999	-999	55
5	-999	-999	-999	-999	1.00	0.50	-999	-999	65
3	-999	-999	-999	-999	1.00	0.50	6	50	90
5	-999	-999	-999	-999	1.00	0.50	6	20	100

Output:

```
starting hypoDD (v2.1beta - 09/30/2011)...
Input parameters: ./hypoDD_3d_ct.inp (hypoDD2.0 format)
INPUT FILES:
 cross dtime data: empty.cc
 catalog dtime data: dt.ct
 events: event.sel
 stations: station.sel
OUTPUT FILES:
 initial locations: hypoDD_3d_ct_30.loc
 relocated events: hypoDD_3d_ct_30.reloc
 event pair residuals: hypoDD_3d_ct_30.res
 station residuals: hypoDD_3d_ct_30.sta
 source parameters: hypoDD_3d_ct_30.src
Use local 3D model vel3d.dat
Relocate all clusters
Relocate all events
Remove air quakes.
Reading data ...
# events =  3395
# stations < maxdist =     21
# stations w/ neg. elevation (set to 0) =    0
# catalog P dtimes =  630340
# catalog S dtimes =  524488
```

```
# dtimes total =  1154828
    after gap/distance check:   987143 ( 85%)
    nccp,nccs,nctp,ncts:            0           0      528167      458976
# events after dtime match =       3383
# stations =     21
clustering ...
Clustered events:  1798
Isolated events:  1585
# clusters:    3
Cluster   1:  1794 events
Cluster   2:     2 events
Cluster   3:     2 events

RELOCATION OF CLUSTER: 1
----------------------
Reading data ...
# events =  1794
# stations < maxdist =     21
# stations w/ neg. elevation (set to 0) =    0
# catalog P dtimes =  340050
# catalog S dtimes =  288842
# dtimes total =   628892
    after gap/distance check:   567994 ( 90%)
    nccp,nccs,nctp,ncts:            0           0      303690      264304
# events after dtime match =       1794
# stations =     21
Initial trial sources =  1794
3D ray tracing.

  IT   EV  CT    RMSCT   RMSST   DX   DY   DZ   DT   OS  AQ  CND
         %   %   ms     %    ms    m    m    m   ms    m
 1    100 100  201 -56.4     0 1091 1279 2865  178    0  11  399
 2  1  99  99  198  -1.6   573 1064 1270 2583  174  843   0  399
 3     99  99  184  -7.0   573  367  355 1051   68  843   2  377
 4  2  99  99  178  -3.4   574  265  329  960   62 1079   0  379
 5  3  99  99  175  -1.4   573  121  146  568   28 1312   0  361
 6     99  99  175  -0.4   573   70   78  385   15 1312   1  279
 7  4  99  99  175  -0.0   575   69   77  384   15 1485   0  276
 8  5  99  99  174  -0.2   575   64   62  346   11 1635   0  270
 9     99  99  174  -0.0   575   62   49  302    9 1635   1  270
10  6  99  99  174  -0.1   575   59   48  304    9 1770   0  267
11  7  99  99  174  -0.1   575   52   38  271    8 1887   0  265
12  8  99  99  174  -0.0   575   49   36  276    7 1936   0  264
13  9  99  95  120 -31.0   342  127  177  444   20 2005   0  208
14 10  99  93  112  -6.4   318   69  101  269   14 2097   0  205
15 11  99  93  109  -3.1   308   51   72  222   11 2178   0  200
16 12  98  70  102  -6.6   298   84  111  240   11 2189   0  187
17 13  98  68   96  -5.5   278   49   69  184    8 2247   0  182
18 14  98  68   94  -2.4   271   36   51  142    7 2276   0  177
19 15  98  67   92  -1.4   267   29   42  119    5 2315   0  172
20     98  67   92  -0.9   267   27   36  113    5 2315   1  169
21 16  98  67   91  -0.2   266   27   37  113    5 2350   0  169

writing out results ...
```

```
RELOCATION OF CLUSTER: 2
----------------------
Reading data ...
# events =     2
# stations < maxdist =     21
# stations w/ neg. elevation (set to 0) =    0
# catalog P dtimes =       6
# catalog S dtimes =       6
# dtimes total =       12
    after gap/distance check:       12 (100%)
    nccp,nccs,nctp,ncts:            0           0           6           6
# events after dtime match =          2
# stations =      6
Initial trial sources =     2
3D ray tracing.

  IT   EV  CT    RMSCT   RMSST   DX   DY   DZ   DT   OS  AQ  CND
        %   %    ms     %    ms    m    m    m   ms    m
 1  1 100 100  253  -0.6   394    2    4   17    3    8   0    2
 2  2 100 100  252  -0.5   391    2    4   17    2   15   0    2
 3  3 100 100  251  -0.5   389    2    4   16    1   22   0    2
 4  4 100 100  250  -0.3   387    2    3   11    1   27   0    2
 5  5 100 100  249  -0.4   386    2    3   11    1   32   0    2
 6  6 100 100  248  -0.3   384    1    3   11    1   37   0    2
 7  7 100 100  247  -0.3   382    1    3   11    1   42   0    2
 8  8 100 100  246  -0.3   381    1    3    9    1   45   0    2
 9  9 100 100  213 -13.6   380    0    1    4    0   46   0    2
10 10 100 100  213  -0.1   379    0    1    4    0   47   0    2
11 11 100 100  212  -0.1   379    0    1    3    0   48   0    2
12 12 100 100  212  -0.1   378    0    1    2    0   48   0    2
13 13 100 100  212  -0.1   378    0    1    2    0   48   0    2
14 14 100 100  211  -0.2   377    0    1    2    0   48   0    2
15 15 100 100  211  -0.1   377    0    1    2    0   49   0    2
16 16 100 100  211  -0.1   376    0    1    2    0   49   0    2

writing out results ...

RELOCATION OF CLUSTER: 3
----------------------
Reading data ...
# events =     2
# stations < maxdist =     21
# stations w/ neg. elevation (set to 0) =    0
# catalog P dtimes =       8
# catalog S dtimes =       7
# dtimes total =       15
    after gap/distance check:       13 ( 87%)
    nccp,nccs,nctp,ncts:            0           0           7           6
# events after dtime match =          2
# stations =      7
Initial trial sources =     2
3D ray tracing.
```

```
  IT   EV  CT    RMSCT   RMSST   DX   DY   DZ   DT   OS  AQ  CND
       %   %    ms      %    ms    m    m    m   ms    m
 1   1 100 100  531  -0.6  1429    8    9   22    1   22   0    3
 2   2 100 100  528  -0.7  1423    8    9   21    1   43   0    3
 3   3 100 100  524  -0.6  1416    8    8   21    1   64   0    3
 4   4 100 100  522  -0.5  1412    5    6   15    1   79   0    2
 5   5 100 100  520  -0.4  1407    5    6   15    1   94   0    2
 6   6 100 100  518  -0.4  1403    5    6   14    1  108   0    2
 7   7 100 100  515  -0.4  1399    5    6   14    1  122   0    2
 8   8 100 100  513  -0.4  1395    5    6   14    1  136   0    2
 9   9 100 100  458 -10.9  1393    2    3    6    1  142   0    2
10  10 100 100  457  -0.2  1391    2    3    6    1  148   0    2
11  11 100 100  456  -0.2  1390    2    3    6    0  153   0    2
  Cluster has less than 2 events.
   Program hypoDD finished.
```

P=1.0, S=0.3

Table 13: Input parameters and Output for hypoDD P to S weighting Test 2

DATA WEIGHTING AND REWEIGHTING:

NITER	WTCCP	WTCCS	WRCC	WDCC	WTCTP	WTCTS	WRCT	WDCT	DAMP
3	-999	-999	-999	-999	1.00	0.30	-999	-999	55
5	-999	-999	-999	-999	1.00	0.30	-999	-999	65
3	-999	-999	-999	-999	1.00	0.30	6	50	90
5	-999	-999	-999	-999	1.00	0.30	6	20	100

Output:

```
starting hypoDD (v2.1beta - 09/30/2011)...
Input parameters: ./hypoDD_3d_ct.inp (hypoDD2.0 format)
INPUT FILES:
 cross dtime data: empty.cc
 catalog dtime data: dt.ct
 events: event.sel
 stations: station.sel
OUTPUT FILES:
 initial locations: hypoDD_3d_ct_31.loc
 relocated events: hypoDD_3d_ct_31.reloc
 event pair residuals: hypoDD_3d_ct_31.res
 station residuals: hypoDD_3d_ct_31.sta
 source parameters: hypoDD_3d_ct_31.src
Use local 3D model vel3d.dat
Relocate all clusters
Relocate all events
```

```
Remove air quakes.
Reading data ...
# events =  3395
# stations < maxdist =     21
# stations w/ neg. elevation (set to 0) =    0
# catalog P dtimes =  630340
# catalog S dtimes =  524488
# dtimes total =  1154828
    after gap/distance check:   987143 ( 85%)
    nccp,nccs,nctp,ncts:            0           0      528167      458976
# events after dtime match =       3383
# stations =     21
clustering ...
Clustered events:  1798
Isolated events:  1585
# clusters:    3
Cluster   1:  1794 events
Cluster   2:     2 events
Cluster   3:     2 events

RELOCATION OF CLUSTER: 1
----------------------
Reading data ...
# events =  1794
# stations < maxdist =     21
# stations w/ neg. elevation (set to 0) =    0
# catalog P dtimes =  340050
# catalog S dtimes =  288842
# dtimes total =   628892
    after gap/distance check:   567994 ( 90%)
    nccp,nccs,nctp,ncts:            0           0      303690      264304
# events after dtime match =       1794
# stations =     21
Initial trial sources =  1794
3D ray tracing.
```

IT	EV	CT	RMSCT		RMSST	DX	DY	DZ	DT	OS	AQ	CND
	%	%	ms	%	ms	m	m	m	ms	m		
1		100	100	185	-60.7	0	1093	1294	2956	179	0	11	412
2	1	99	99	183	-1.4	608	1069	1279	2678	175	864	0	412
3		99	99	171	-6.6	608	287	393	1075	73	864	1	394
4	2	99	99	166	-2.6	603	266	339	972	71	1139	0	395
5		99	99	164	-1.1	603	122	167	596	32	1139	1	372
6	3	99	99	164	-0.0	608	122	177	598	32	1427	0	372
7	4	99	99	164	-0.4	608	78	96	406	17	1624	0	290
8	5	99	99	163	-0.2	610	82	75	351	13	1801	0	284
9	6	99	99	163	-0.1	610	76	63	303	11	1967	0	278
10	7	99	99	163	-0.1	610	68	52	265	9	2084	0	274
11		99	99	163	-0.1	610	60	48	250	8	2084	1	277
12	8	99	99	163	-0.0	611	60	48	256	8	2164	0	277
13	9	99	94	119	-27.1	350	107	153	360	17	2164	0	209
14	10	99	93	111	-6.2	322	61	92	248	13	2228	0	205
15	11	99	92	108	-2.9	312	44	67	195	10	2271	0	198
16	12	98	68	100	-7.5	306	84	113	234	11	2320	0	190

```
17 13  98  67   95  -5.3   308   48   66  163    8 2368   0  182
18 14  98  66   92  -2.7   309   38   50  145    6 2407   0  177
19 15  98  66   91  -1.5   310   31   38  123    5 2459   0  172
20 16  98  66   90  -0.9   311   27   35  109    4 2471   0  172

writing out results ...

RELOCATION OF CLUSTER: 2
----------------------
Reading data ...
# events =     2
# stations < maxdist =     21
# stations w/ neg. elevation (set to 0) =    0
# catalog P dtimes =       6
# catalog S dtimes =       6
# dtimes total =       12
    after gap/distance check:       12 (100%)
    nccp,nccs,nctp,ncts:            0           0           6           6
# events after dtime match =          2
# stations =      6
Initial trial sources =     2
3D ray tracing.

  IT   EV  CT    RMSCT   RMSST   DX   DY   DZ   DT   OS  AQ  CND
        %   %   ms     %    ms    m    m    m   ms    m
 1  1 100 100  270  -0.8   393    3    5   28    3   18   0    2
 2  2 100 100  268  -0.7   390    3    5   28    2   36   0    2
 3  3 100 100  266  -0.6   387    3    5   27    1   53   0    2
 4  4 100 100  265  -0.5   385    2    4   19    1   65   0    2
 5  5 100 100  264  -0.4   383    2    3   19    1   78   0    2
 6  6 100 100  263  -0.4   381    2    3   19    1   90   0    2
 7  7 100 100  262  -0.4   379    2    3   12    1   96   0    2
 8  8 100 100  260  -0.4   377    2    3   12    1  102   0    2
 9  9 100 100  222 -14.7   376    1    1    3    0  102   0    2
10 10 100 100  222  -0.1   376    1    1    3    0  103   0    2
11 11 100 100  222  -0.1   375    1    1    3    0  103   0    2
12 12 100 100  221  -0.1   374    1    1    2    0  103   0    2
13 13 100 100  221  -0.1   373    1    1    2    0  104   0    2
14 14 100 100  221  -0.1   373    1    1    2    0  104   0    2
15 15 100 100  221  -0.1   372    1    1    2    0  104   0    2
16 16 100 100  221  -0.1   372    1    1    2    0  105   0    2

writing out results ...

RELOCATION OF CLUSTER: 3
----------------------
Reading data ...
# events =     2
# stations < maxdist =     21
# stations w/ neg. elevation (set to 0) =    0
# catalog P dtimes =       8
# catalog S dtimes =       7
# dtimes total =       15
    after gap/distance check:       13 ( 87%)
```

```
    nccp,nccs,nctp,ncts:            0           0           7           6
# events after dtime match =          2
# stations =      7
Initial trial sources =     2
3D ray tracing.

  IT   EV  CT    RMSCT   RMSST   DX   DY   DZ   DT   OS  AQ  CND
       %   %    ms     %    ms    m    m    m    ms    m
 1   1 100 100   478  -0.5  1430    6    8   17    1   17   0    3
 2   2 100 100   476  -0.6  1425    6    8   17    1   33   0    3
 3   3 100 100   473  -0.5  1421    6    8   16    1   50   0    3
 4   4 100 100   471  -0.4  1417    4    6   11    1   61   0    2
 5   5 100 100   470  -0.4  1414    4    6   11    1   72   0    2
 6   6 100 100   468  -0.4  1410    4    6   11    1   83   0    2
 7   7 100 100   466  -0.3  1407    4    6   11    1   94   0    2
 8   8 100 100   465  -0.3  1404    4    5   11    1  105   0    2
 9   9 100 100   440  -5.4  1403    2    3    5    1  110   0    2
10  10 100 100   439  -0.1  1401    2    3    5    0  114   0    2
11  11 100 100   438  -0.2  1400    2    3    5    0  119   0    2
  Cluster has less than 2 events.

   Program hypoDD finished.
```

IV: WRCT Tests

WRCT 3rd and 4th Iteration sets=20

Table 14: Input parameters and Output for hypoDD WRCT Test 1

DATA WEIGHTING AND REWEIGHTING:									
NITER	WTCCP	WTCCS	WRCC	WDCC	WTCTP	WTCTS	WRCT	WDCT	DAMP
3	-999	-999	-999	-999	1.00	0.80	-999	-999	55
5	-999	-999	-999	-999	1.00	0.80	-999	-999	65
3	-999	-999	-999	-999	1.00	0.80	20	50	90
5	-999	-999	-999	-999	1.00	0.80	20	20	100

Output:

```
starting hypoDD (v2.1beta - 09/30/2011)...
Input parameters: ./hypoDD_3d_ct.inp (hypoDD2.0 format)
INPUT FILES:
 cross dtime data: empty.cc
 catalog dtime data: dt.ct
 events: event.sel
 stations: station.sel
```

```
OUTPUT FILES:
 initial locations: hypoDD_3d_ct_32.loc
 relocated events: hypoDD_3d_ct_32.reloc
 event pair residuals: hypoDD_3d_ct_32.res
 station residuals: hypoDD_3d_ct_32.sta
 source parameters: hypoDD_3d_ct_32.src
Use local 3D model vel3d.dat
Relocate all clusters
Relocate all events
Remove air quakes.
Reading data ...
# events =  3395
# stations < maxdist =     21
# stations w/ neg. elevation (set to 0) =    0
# catalog P dtimes =  630340
# catalog S dtimes =  524488
# dtimes total =  1154828
    after gap/distance check:   987143 ( 85%)
    nccp,nccs,nctp,ncts:            0           0      528167      458976
# events after dtime match =       3383
# stations =     21
clustering ...
Clustered events:  1798
Isolated events:  1585
# clusters:    3
Cluster   1:  1794 events
Cluster   2:     2 events
Cluster   3:     2 events

RELOCATION OF CLUSTER: 1
----------------------
Reading data ...
# events =  1794
# stations < maxdist =     21
# stations w/ neg. elevation (set to 0) =    0
# catalog P dtimes =  340050
# catalog S dtimes =  288842
# dtimes total =   628892
    after gap/distance check:   567994 ( 90%)
    nccp,nccs,nctp,ncts:            0           0      303690      264304
# events after dtime match =       1794
# stations =     21
Initial trial sources =  1794
3D ray tracing.

  IT   EV  CT    RMSCT   RMSST   DX   DY   DZ   DT   OS  AQ  CND
        %   %   ms     %    ms    m    m    m   ms    m
 1    100 100  224 -50.8     0 1096 1289 2815  182    0  12  396
 2     99  99  220  -2.0     0 1065 1287 2518  176    0   2  396
 3  1  99  99  219  -0.1   528 1063 1287 2511  176  794   0  396
 4     99  99  208  -5.0   528  400  293  982   59  794   2  368
 5  2  99  99  201  -3.6   522  277  296 1026   56 1084   0  365
 6     99  99  192  -4.6   522  145  178  680   30 1084   1  362
 7  3  99  99  192  -0.0   519  144  177  680   30 1314   0  358
```

```
 8      99  99  190  -0.6   519   86   94  389   14 1314   1  279
 9   4  99  99  190  -0.0   516   91   97  397   15 1504   0  279
10   5  99  99  190  -0.1   516   80   73  351   10 1652   0  267
11   6  99  99  190  -0.1   515   65   53  291    8 1730   0  264
12      99  99  190  -0.1   515   66   49  331    8 1730   2  264
13   7  99  99  186  -1.9   516   72   56  319    7 1859   0  268
14   8  99  99  186  -0.0   515   65   45  274    7 1909   0  265
15   9  99  98  164 -11.8   513   96  107  393   12 1954   0  200
16 10  99  98  163  -0.9   516   52   56  250    7 2025   0  191
17 11  99  98  162  -0.3   522   43   41  213    6 2101   0  183
18 12  98  74  155  -4.3   515  111  144  345   14 2164   0  192
19 13  98  74  153  -1.3   521   57   76  234    9 2253   0  183
20 14  98  74  153  -0.3   523   48   56  186    7 2308   0  176
21 15  98  73  153  -0.1   530   41   44  167    5 2386   0  175
22 16  98  73  153  -0.1   531   34   37  150    4 2414   0  173

writing out results ...

RELOCATION OF CLUSTER: 2
------------------------
Reading data ...
# events =     2
# stations < maxdist =     21
# stations w/ neg. elevation (set to 0) =    0
# catalog P dtimes =       6
# catalog S dtimes =       6
# dtimes total =       12
    after gap/distance check:       12 (100%)
    nccp,nccs,nctp,ncts:            0           0           6           6
# events after dtime match =          2
# stations =      6
Initial trial sources =     2
3D ray tracing.

  IT   EV  CT    RMSCT   RMSST   DX   DY   DZ   DT   OS  AQ  CND
         %   %    ms      %     ms    m    m    m   ms    m
 1  1 100 100  239  -0.3   395    1    3   12    2    4   0    2
 2  2 100 100  239  -0.3   393    1    3   11    1    7   0    2
 3  3 100 100  238  -0.3   392    1    3   11    1   11   0    2
 4  4 100 100  238  -0.2   391    1    2    8    1   13   0    2
 5  5 100 100  237  -0.2   389    1    2    8    1   16   0    2
 6  6 100 100  237  -0.2   388    1    2    8    0   18   0    2
 7  7 100 100  236  -0.2   387    1    2    7    0   20   0    2
 8  8 100 100  236  -0.2   386    1    2    7    0   22   0    2
 9  9 100 100  235  -0.4   386    0    1    4    0   24   0    2
10 10 100 100  235  -0.1   385    0    1    4    0   25   0    2
11 11 100 100  234  -0.1   384    0    1    4    0   26   0    2
12 12 100 100  234  -0.1   384    0    1    3    0   27   0    2
13 13 100 100  234  -0.1   384    0    1    3    0   27   0    2
14 14 100 100  234  -0.1   383    0    1    3    0   28   0    2
15 15 100 100  234  -0.1   383    0    1    3    0   29   0    2
16 16 100 100  234  -0.1   382    0    1    3    0   30   0    2

writing out results ...
```

```
RELOCATION OF CLUSTER: 3
-----------------------
Reading data ...
# events =     2
# stations < maxdist =     21
# stations w/ neg. elevation (set to 0) =    0
# catalog P dtimes =       8
# catalog S dtimes =       7
# dtimes total =       15
    after gap/distance check:       13 ( 87%)
    nccp,nccs,nctp,ncts:            0           0           7           6
# events after dtime match =          2
# stations =      7
Initial trial sources =     2
3D ray tracing.

  IT   EV  CT    RMSCT   RMSST   DX   DY   DZ   DT   OS  AQ  CND
        %   %    ms      %    ms    m    m    m   ms    m
 1  1 100 100   630  -0.8  1427   11   10   30    1   30   0    3
 2  2 100 100   625  -0.8  1418   11    9   29    2   59   0    3
 3  3 100 100   619  -0.8  1409   10    9   29    2   88   0    3
 4  4 100 100   616  -0.6  1402    7    7   20    2  108   0    2
 5  5 100 100   612  -0.6  1396    7    7   20    2  128   0    2
 6  6 100 100   609  -0.6  1391    7    7   20    1  147   0    2
 7  7 100 100   605  -0.5  1385    7    6   19    1  167   0    2
 8  8 100 100   602  -0.5  1379    7    6   19    1  186   0    2
 9  9 100 100   597  -0.8  1376    4    3   10    1  196   0    2
10 10 100 100  596  -0.3  1373    3    3   10    1  205   0    2
11 11 100 100  594  -0.3  1370    3    3   10    1  215   0    2
  Cluster has less than 2 events.

   Program hypoDD finished.
```

WRCT 3rd and 4th Iteration sets=1

Table 15: Input parameters and Output for hypoDD WRCT Test 2

DATA WEIGHTING AND REWEIGHTING:

NITER	WTCCP	WTCCS	WRCC	WDCC	WTCTP	WTCTS	WRCT	WDCT	DAMP
3	-999	-999	-999	-999	1.00	0.80	-999	-999	55
5	-999	-999	-999	-999	1.00	0.80	-999	-999	65
3	-999	-999	-999	-999	1.00	0.80	1	50	90
5	-999	-999	-999	-999	1.00	0.80	1	20	100

Output:

```
starting hypoDD (v2.1beta - 09/30/2011)...
Input parameters: ./hypoDD_3d_ct.inp (hypoDD2.0 format)
INPUT FILES:
 cross dtime data: empty.cc
 catalog dtime data: dt.ct
 events: event.sel
 stations: station.sel
OUTPUT FILES:
 initial locations: hypoDD_3d_ct_33.loc
 relocated events: hypoDD_3d_ct_33.reloc
 event pair residuals: hypoDD_3d_ct_33.res
 station residuals: hypoDD_3d_ct_33.sta
 source parameters: hypoDD_3d_ct_33.src
Use local 3D model vel3d.dat
Relocate all clusters
Relocate all events
Remove air quakes.
Reading data ...
# events =  3395
# stations < maxdist =     21
# stations w/ neg. elevation (set to 0) =    0
# catalog P dtimes =  630340
# catalog S dtimes =  524488
# dtimes total =  1154828
    after gap/distance check:   987143 ( 85%)
    nccp,nccs,nctp,ncts:            0           0      528167      458976
# events after dtime match =       3383
# stations =     21
clustering ...
Clustered events:  1798
Isolated events:  1585
# clusters:    3
Cluster   1:  1794 events
Cluster   2:     2 events
Cluster   3:     2 events

RELOCATION OF CLUSTER: 1
----------------------
Reading data ...
# events =  1794
# stations < maxdist =     21
# stations w/ neg. elevation (set to 0) =    0
# catalog P dtimes =  340050
# catalog S dtimes =  288842
# dtimes total =   628892
    after gap/distance check:   567994 ( 90%)
    nccp,nccs,nctp,ncts:            0           0      303690      264304
# events after dtime match =       1794
# stations =     21
Initial trial sources =  1794
3D ray tracing.

  IT   EV  CT    RMSCT   RMSST   DX   DY   DZ   DT   OS  AQ  CND
        %   %   ms     %    ms    m    m    m   ms    m
```

```
 1    100 100  224 -50.8     0 1096 1289 2815  182    0  12  396
 2     99  99  220  -2.0     0 1065 1287 2518  176    0   2  396
 3  1  99  99  219  -0.1   528 1063 1287 2511  176  794   0  396
 4     99  99  208  -5.0   528  400  293  982   59  794   2  368
 5  2  99  99  201  -3.6   522  277  296 1026   56 1084   0  365
 6     99  99  192  -4.6   522  145  178  680   30 1084   1  362
 7  3  99  99  192  -0.0   519  144  177  680   30 1314   0  358
 8     99  99  190  -0.6   519   86   94  389   14 1314   1  279
 9  4  99  99  190  -0.0   516   91   97  397   15 1504   0  279
10  5  99  99  190  -0.1   516   80   73  351   10 1652   0  267
11  6  99  99  190  -0.1   515   65   53  291    8 1730   0  264
12     99  99  190  -0.1   515   66   49  331    8 1730   2  264
13  7  99  99  186  -1.9   516   72   56  319    7 1859   0  268
14  8  99  99  186  -0.0   515   65   45  274    7 1909   0  265
15  9  99  60   45 -75.6    93  114  152  289   15 1856   0  166
16 10  99  38   21 -53.9    40   51   56  106    5 1863   0  130
17 11  99  25   10 -53.3    20   24   25   45    2 1863   0  101
18 12  98  13    4 -56.6     9   12   12   17    1 1871   0   77
19 13  98   8    1 -70.5     4    4    4    6    0 1871   0   57
20 14  97   5    0 -83.9     1    1    1    1    0 1884   0   41
21 15  95   3    0 -86.3     0    0    0    0    0 1832   0   29
22 16  91   2    0 -60.0     0    0    0    0    0 1839   0   21

writing out results ...

RELOCATION OF CLUSTER: 2
------------------------
Reading data ...
# events =     2
# stations < maxdist =     21
# stations w/ neg. elevation (set to 0) =    0
# catalog P dtimes =       6
# catalog S dtimes =       6
# dtimes total =       12
    after gap/distance check:       12 (100%)
    nccp,nccs,nctp,ncts:            0           0           6           6
# events after dtime match =          2
# stations =      6
Initial trial sources =     2
3D ray tracing.

  IT   EV  CT    RMSCT   RMSST   DX   DY   DZ   DT   OS  AQ  CND
         %   %    ms      %     ms    m    m    m   ms    m
 1  1 100 100  239  -0.3   395    1    3   12    0    4   0    2
 2  2 100 100  239  -0.3   393    1    3   11    0    7   0    2
 3  3 100 100  238  -0.3   392    1    3   11    1   11   0    2
 4  4 100 100  238  -0.2   391    1    2    8    0   13   0    2
 5  5 100 100  237  -0.2   389    1    2    8    0   16   0    2
 6  6 100 100  237  -0.2   388    1    2    8    0   18   0    2
 7  7 100 100  236  -0.2   387    1    2    7    0   20   0    2
 8  8 100 100  236  -0.2   386    1    2    7    0   22   0    2
 >>> Warning: ndt < 4*nev
 9  9 100  58   73 -69.1   146    0    0    1    0   22   0    2
 >>> Warning: ndt < 4*nev
```

```
10 10 100  50   63 -12.8   116    0    0    4    0   18   0    2
 >>> Warning: ndt < 4*nev
11 11 100  42   58  -8.7   100    0    0    4    0   15   0    2
 >>> Warning: ndt < 4*nev
12 12 100  17   46 -21.3    46    0    0    1    0   14   0    1
  Cluster has less than 2 events.

RELOCATION OF CLUSTER: 3
-----------------------
Reading data ...
# events =     2
# stations < maxdist =     21
# stations w/ neg. elevation (set to 0) =    0
# catalog P dtimes =       8
# catalog S dtimes =       7
# dtimes total =       15
    after gap/distance check:       13 ( 87%)
    nccp,nccs,nctp,ncts:            0           0           7           6
# events after dtime match =          2
# stations =      7
Initial trial sources =     2
3D ray tracing.

  IT   EV  CT    RMSCT   RMSST   DX   DY   DZ   DT   OS  AQ  CND
        %   %   ms     %    ms    m    m    m   ms    m
 1  1 100 100  630  -0.8  1427   11   10   30    1   30   0    3
 2  2 100 100  625  -0.8  1418   11    9   29    2   59   0    3
 3  3 100 100  619  -0.8  1409   10    9   29    2   88   0    3
 4  4 100 100  616  -0.6  1402    7    7   20    2  108   0    2
 5  5 100 100  612  -0.6  1396    7    7   20    2  128   0    2
 6  6 100 100  609  -0.6  1391    7    7   20    1  147   0    2
 7  7 100 100  605  -0.5  1385    7    6   19    1  167   0    2
 8  8 100 100  602  -0.5  1379    7    6   19    1  186   0    2
 >>> Warning: ndt < 4*nev
 9  9 100  62  187 -69.0   554    0    0    1    1  187   0    2
 >>> Warning: ndt < 4*nev
10 10 100  31   46 -75.6   256    0    0    0    0  187   0    2
 >>> Warning: ndt < 4*nev
11 11 100  15   26 -43.0    21    0    0    0    0  187   0    2
  Cluster has less than 2 events.

   Program hypoDD finished.
```

V: WDCT Tests

WDCT 3rd Iteration set=100, WDCT 4th Iteration set=50

Table 16: Input parameters and Output for hypoDD WDCT Test 1

DATA WEIGHTING AND REWEIGHTING:

NITER	WTCCP	WTCCS	WRCC	WDCC	WTCTP	WTCTS	WRCT	WDCT	DAMP
3	-999	-999	-999	-999	1.00	0.80	-999	-999	55
5	-999	-999	-999	-999	1.00	0.80	-999	-999	65
3	-999	-999	-999	-999	1.00	0.80	6	100	90
5	-999	-999	-999	-999	1.00	0.80	6	50	100

Output:

```
starting hypoDD (v2.1beta - 09/30/2011)...
Input parameters: ./hypoDD_3d_ct.inp (hypoDD2.0 format)
INPUT FILES:
 cross dtime data: empty.cc
 catalog dtime data: dt.ct
 events: event.sel
 stations: station.sel
OUTPUT FILES:
 initial locations: hypoDD_3d_ct_34.loc
 relocated events: hypoDD_3d_ct_34.reloc
 event pair residuals: hypoDD_3d_ct_34.res
 station residuals: hypoDD_3d_ct_34.sta
 source parameters: hypoDD_3d_ct_34.src
Use local 3D model vel3d.dat
Relocate all clusters
Relocate all events
Remove air quakes.
Reading data ...
# events =  3395
# stations < maxdist =     21
# stations w/ neg. elevation (set to 0) =    0
# catalog P dtimes =  630340
# catalog S dtimes =  524488
# dtimes total =  1154828
    after gap/distance check:   987143 ( 85%)
    nccp,nccs,nctp,ncts:            0           0      528167      458976
# events after dtime match =       3383
# stations =     21
clustering ...
Clustered events:  1798
Isolated events:  1585
# clusters:    3
Cluster   1:  1794 events
Cluster   2:     2 events
Cluster   3:     2 events

RELOCATION OF CLUSTER: 1
----------------------
Reading data ...
# events =  1794
```

```
# stations < maxdist =     21
# stations w/ neg. elevation (set to 0) =    0
# catalog P dtimes =  340050
# catalog S dtimes =  288842
# dtimes total =   628892
    after gap/distance check:   567994 ( 90%)
    nccp,nccs,nctp,ncts:            0           0      303690      264304
# events after dtime match =       1794
# stations =     21
Initial trial sources =  1794
3D ray tracing.

  IT   EV  CT    RMSCT   RMSST   DX   DY   DZ   DT   OS  AQ  CND
        %   %   ms      %    ms    m    m    m   ms    m
 1    100 100  224 -50.8     0 1096 1289 2815  182    0  12  396
 2     99  99  220  -2.0     0 1065 1287 2518  176    0   2  396
 3  1  99  99  219  -0.1   528 1063 1287 2511  176  794   0  396
 4     99  99  208  -5.0   528  400  293  982   59  794   2  368
 5  2  99  99  201  -3.6   522  277  296 1026   56 1084   0  365
 6     99  99  192  -4.6   522  145  178  680   30 1084   1  362
 7  3  99  99  192  -0.0   519  144  177  680   30 1314   0  358
 8     99  99  190  -0.6   519   86   94  389   14 1314   1  279
 9  4  99  99  190  -0.0   516   91   97  397   15 1504   0  279
10  5  99  99  190  -0.1   516   80   73  351   10 1652   0  267
11  6  99  99  190  -0.1   515   65   53  291    8 1730   0  264
12     99  99  190  -0.1   515   66   49  331    8 1730   2  264
13  7  99  99  186  -1.9   516   72   56  319    7 1859   0  268
14  8  99  99  186  -0.0   515   65   45  274    7 1909   0  265
15  9  99  96  127 -31.7   335  134  196  482   21 1942   0  190
16 10  99  94  119  -6.5   311   74  112  288   15 2025   0  183
17 11  99  93  115  -3.2   304   52   79  228   11 2093   0  180
18 12  99  92  111  -3.8   298   53   65  213    9 2180   0  164
19 13  99  92  109  -1.4   294   37   47  170    7 2230   0  163
20     99  92  108  -0.9   294   31   40  140    6 2230   1  158
21 14  99  92  108  -0.2   292   31   40  140    6 2293   0  158
22 15  99  92  107  -0.5   291   26   37  132    5 2354   0  159
23 16  99  92  107  -0.4   290   26   34  130    5 2379   0  159

writing out results ...
 WARNING: org time diff > 5s for         2012

RELOCATION OF CLUSTER: 2
----------------------
Reading data ...
# events =     2
# stations < maxdist =     21
# stations w/ neg. elevation (set to 0) =    0
# catalog P dtimes =       6
# catalog S dtimes =       6
# dtimes total =       12
    after gap/distance check:       12 (100%)
    nccp,nccs,nctp,ncts:            0           0           6           6
# events after dtime match =          2
# stations =      6
```

```
Initial trial sources =     2
3D ray tracing.

  IT   EV  CT    RMSCT   RMSST   DX   DY   DZ   DT   OS  AQ  CND
         %   %    ms     %    ms    m    m    m   ms    m
 1  1 100 100   239  -0.3   395    1    3   12    3    4   0    2
 2  2 100 100   239  -0.3   393    1    3   11    2    7   0    2
 3  3 100 100   238  -0.3   392    1    3   11    1   11   0    2
 4  4 100 100   238  -0.2   391    1    2    8    1   13   0    2
 5  5 100 100   237  -0.2   389    1    2    8    1   16   0    2
 6  6 100 100   237  -0.2   388    1    2    8    0   18   0    2
 7  7 100 100   236  -0.2   387    1    2    7    0   20   0    2
 8  8 100 100   236  -0.2   386    1    2    7    0   22   0    2
 9  9 100 100   208 -11.9   386    0    1    3    0   23   0    2
10 10 100 100   208  -0.1   385    0    1    3    0   24   0    2
11 11 100 100   207  -0.1   385    0    1    3    0   25   0    2
12 12 100 100   207  -0.1   385    0    1    2    0   26   0    2
13 13 100 100   207  -0.1   384    0    1    2    0   26   0    2
14 14 100 100   207  -0.1   384    0    1    2    0   27   0    2
15 15 100 100   207  -0.1   384    0    1    2    0   28   0    2
16 16 100 100   207  -0.1   383    0    1    2    0   28   0    2

writing out results ...

RELOCATION OF CLUSTER: 3
------------------------
Reading data ...
# events =     2
# stations < maxdist =     21
# stations w/ neg. elevation (set to 0) =    0
# catalog P dtimes =       8
# catalog S dtimes =       7
# dtimes total =       15
    after gap/distance check:       13 ( 87%)
    nccp,nccs,nctp,ncts:            0           0           7           6
# events after dtime match =          2
# stations =      7
Initial trial sources =     2
3D ray tracing.

  IT   EV  CT    RMSCT   RMSST   DX   DY   DZ   DT   OS  AQ  CND
         %   %    ms     %    ms    m    m    m   ms    m
 1  1 100 100   630  -0.8  1427   11   10   30    1   30   0    3
 2  2 100 100   625  -0.8  1418   11    9   29    2   59   0    3
 3  3 100 100   619  -0.8  1409   10    9   29    2   88   0    3
 4  4 100 100   616  -0.6  1402    7    7   20    2  108   0    2
 5  5 100 100   612  -0.6  1396    7    7   20    2  128   0    2
 6  6 100 100   609  -0.6  1391    7    7   20    1  147   0    2
 7  7 100 100   605  -0.5  1385    7    6   19    1  167   0    2
 8  8 100 100   602  -0.5  1379    7    6   19    1  186   0    2
 9  9 100 100   504 -16.2  1377    3    4    7    1  193   0    2
10 10 100 100   503  -0.2  1375    3    4    7    1  201   0    2
11 11 100 100   502  -0.2  1372    3    4    7    1  208   0    2
12 12 100 100   501  -0.2  1371    2    3    6    1  214   0    2
```

```
13 13 100 100  501  -0.2  1369    2    3    6    0  220   0    2
14 14 100 100  500  -0.2  1367    2    3    6    0  226   0    2
15 15 100 100  499  -0.2  1366    2    3    6    0  232   0    2
16 16 100 100  498  -0.2  1364    2    3    6    0  237   0    2

writing out results ...

   Program hypoDD finished.
```

WDCT 3rd Iteration set=10, WDCT 4th Iteration set=5

Table 17: Input parameters and Output for hypoDD WDCT Test2

DATA WEIGHTING AND REWEIGHTING:

NITER	WTCCP	WTCCS	WRCC	WDCC	WTCTP	WTCTS	WRCT	WDCT	DAMP
3	-999	-999	-999	-999	1.00	0.80	-999	-999	55
5	-999	-999	-999	-999	1.00	0.80	-999	-999	65
3	-999	-999	-999	-999	1.00	0.80	6	10	90
5	-999	-999	-999	-999	1.00	0.80	6	5	100

Output:

```
starting hypoDD (v2.1beta - 09/30/2011)...
Input parameters: ./hypoDD_3d_ct.inp (hypoDD2.0 format)
INPUT FILES:
 cross dtime data: empty.cc
 catalog dtime data: dt.ct
 events: event.sel
 stations: station.sel
OUTPUT FILES:
 initial locations: hypoDD_3d_ct_35.loc
 relocated events: hypoDD_3d_ct_35.reloc
 event pair residuals: hypoDD_3d_ct_35.res
 station residuals: hypoDD_3d_ct_35.sta
 source parameters: hypoDD_3d_ct_35.src
Use local 3D model vel3d.dat
Relocate all clusters
Relocate all events
Remove air quakes.
Reading data ...
# events =  3395
# stations < maxdist =     21
# stations w/ neg. elevation (set to 0) =    0
# catalog P dtimes =  630340
# catalog S dtimes =  524488
# dtimes total =  1154828
    after gap/distance check:   987143 ( 85%)
```

```
    nccp,nccs,nctp,ncts:            0           0      528167      458976
# events after dtime match =       3383
# stations =     21
clustering ...
Clustered events:  1798
Isolated events:  1585
# clusters:    3
Cluster   1:  1794 events
Cluster   2:     2 events
Cluster   3:     2 events

RELOCATION OF CLUSTER: 1
----------------------
Reading data ...
# events =  1794
# stations < maxdist =     21
# stations w/ neg. elevation (set to 0) =    0
# catalog P dtimes =  340050
# catalog S dtimes =  288842
# dtimes total =   628892
    after gap/distance check:   567994 ( 90%)
    nccp,nccs,nctp,ncts:            0           0      303690      264304
# events after dtime match =       1794
# stations =     21
Initial trial sources =  1794
3D ray tracing.

  IT   EV  CT    RMSCT   RMSST   DX   DY   DZ   DT   OS  AQ  CND
        %   %   ms      %    ms    m    m    m   ms    m
 1    100 100  224 -50.8     0 1096 1289 2815  182    0  12  396
 2     99  99  220  -2.0     0 1065 1287 2518  176    0   2  396
 3  1  99  99  219  -0.1   528 1063 1287 2511  176  794   0  396
 4     99  99  208  -5.0   528  400  293  982   59  794   2  368
 5  2  99  99  201  -3.6   522  277  296 1026   56 1084   0  365
 6     99  99  192  -4.6   522  145  178  680   30 1084   1  362
 7  3  99  99  192  -0.0   519  144  177  680   30 1314   0  358
 8     99  99  190  -0.6   519   86   94  389   14 1314   1  279
 9  4  99  99  190  -0.0   516   91   97  397   15 1504   0  279
10  5  99  99  190  -0.1   516   80   73  351   10 1652   0  267
11  6  99  99  190  -0.1   515   65   53  291    8 1730   0  264
12     99  99  190  -0.1   515   66   49  331    8 1730   2  264
13  7  99  99  186  -1.9   516   72   56  319    7 1859   0  268
14  8  99  99  186  -0.0   515   65   45  274    7 1909   0  265
15  9  94  41  110 -41.1   337  171  228  471   21 1829   0  171
16 10  93  39   91 -17.0   273   82  119  273   13 1810   0  162
17 11  93  38   84  -8.2   252   53   80  188   10 1810   0  157
18 12  75  23   76  -8.6   248   42   53  147    6 1917   0   93
19 13  74  23   70  -8.3   218   27   39   93    5 1932   0   91
20 14  74  22   67  -4.4   205   21   33   77    4 1944   0   89
21 15  74  22   65  -2.7   198   18   29   63    3 1928   0   89
22 16  74  22   64  -1.8   193   15   24   58    3 1927   0   87

writing out results ...
```

```
RELOCATION OF CLUSTER: 2
----------------------
Reading data ...
# events =     2
# stations < maxdist =     21
# stations w/ neg. elevation (set to 0) =    0
# catalog P dtimes =       6
# catalog S dtimes =       6
# dtimes total =       12
    after gap/distance check:       12 (100%)
    nccp,nccs,nctp,ncts:            0           0           6           6
# events after dtime match =          2
# stations =      6
Initial trial sources =     2
3D ray tracing.

  IT   EV  CT    RMSCT   RMSST   DX   DY   DZ   DT   OS  AQ  CND
        %   %   ms     %    ms    m    m    m   ms    m
 1  1 100 100  239  -0.3   395    1    3   12    2    4   0    2
 2  2 100 100  239  -0.3   393    1    3   11    1    7   0    2
 3  3 100 100  238  -0.3   392    1    3   11    1   11   0    2
 4  4 100 100  238  -0.2   391    1    2    8    1   13   0    2
 5  5 100 100  237  -0.2   389    1    2    8    1   16   0    2
 6  6 100 100  237  -0.2   388    1    2    8    0   18   0    2
 7  7 100 100  236  -0.2   387    1    2    7    0   20   0    2
 8  8 100 100  236  -0.2   386    1    2    7    0   22   0    2
  Cluster has less than 2 events.

RELOCATION OF CLUSTER: 3
----------------------
Reading data ...
# events =     2
# stations < maxdist =     21
# stations w/ neg. elevation (set to 0) =    0
# catalog P dtimes =       8
# catalog S dtimes =       7
# dtimes total =       15
    after gap/distance check:       13 ( 87%)
    nccp,nccs,nctp,ncts:            0           0           7           6
# events after dtime match =          2
# stations =      7
Initial trial sources =     2
3D ray tracing.

  IT   EV  CT    RMSCT   RMSST   DX   DY   DZ   DT   OS  AQ  CND
        %   %   ms     %    ms    m    m    m   ms    m
 1  1 100 100  630  -0.8  1427   11   10   30    1   30   0    3
 2  2 100 100  625  -0.8  1418   11    9   29    2   59   0    3
 3  3 100 100  619  -0.8  1409   10    9   29    2   88   0    3
 4  4 100 100  616  -0.6  1402    7    7   20    2  108   0    2
 5  5 100 100  612  -0.6  1396    7    7   20    2  128   0    2
 6  6 100 100  609  -0.6  1391    7    7   20    1  147   0    2
 7  7 100 100  605  -0.5  1385    7    6   19    1  167   0    2
 8  8 100 100  602  -0.5  1379    7    6   19    1  186   0    2
```

```
  Cluster has less than 2 events.

   Program hypoDD finished.
```

VI: DAMP Tests

DAMP decreasing: 400, 300, 200, 100

Table 18: Input parameters and Output for hypoDD Damping Test 1

DATA WEIGHTING AND REWEIGHTING:									
NITER	WTCCP	WTCCS	WRCC	WDCC	WTCTP	WTCTS	WRCT	WDCT	DAMP
3	-999	-999	-999	-999	1.00	0.80	-999	-999	400
5	-999	-999	-999	-999	1.00	0.80	-999	-999	300
3	-999	-999	-999	-999	1.00	0.80	6	50	200
5	-999	-999	-999	-999	1.00	0.80	6	20	100

Output:

```
starting hypoDD (v2.1beta - 09/30/2011)...
Input parameters: ./hypoDD_3d_ct.inp (hypoDD2.0 format)
INPUT FILES:
 cross dtime data: empty.cc
 catalog dtime data: dt.ct
 events: event.sel
 stations: station.sel
OUTPUT FILES:
 initial locations: hypoDD_3d_ct_36.loc
 relocated events: hypoDD_3d_ct_36.reloc
 event pair residuals: hypoDD_3d_ct_36.res
 station residuals: hypoDD_3d_ct_36.sta
 source parameters: hypoDD_3d_ct_36.src
Use local 3D model vel3d.dat
Relocate all clusters
Relocate all events
Remove air quakes.
Reading data ...
# events =  3395
# stations < maxdist =     21
# stations w/ neg. elevation (set to 0) =    0
# catalog P dtimes =  630340
# catalog S dtimes =  524488
# dtimes total =  1154828
```

```
    after gap/distance check:   987143 ( 85%)
    nccp,nccs,nctp,ncts:            0           0      528167      458976
# events after dtime match =       3383
# stations =     21
clustering ...
Clustered events:  1798
Isolated events:  1585
# clusters:    3
Cluster   1:  1794 events
Cluster   2:     2 events
Cluster   3:     2 events

RELOCATION OF CLUSTER: 1
-----------------------
Reading data ...
# events =  1794
# stations < maxdist =     21
# stations w/ neg. elevation (set to 0) =    0
# catalog P dtimes =  340050
# catalog S dtimes =  288842
# dtimes total =   628892
    after gap/distance check:   567994 ( 90%)
    nccp,nccs,nctp,ncts:            0           0      303690      264304
# events after dtime match =       1794
# stations =     21
Initial trial sources =  1794
3D ray tracing.

  IT   EV  CT    RMSCT   RMSST   DX   DY   DZ   DT   OS  AQ  CND
        %   %   ms     %    ms    m    m    m   ms    m
 1    100 100  259 -43.0     0  439  527 1112   54    0   7   31
 2  1 100 100  234  -9.8   575  395  501  991   51  168   0   31
 3    100 100  221  -5.4   575  162  204  374   22  168   1   30
 4  2 100 100  212  -4.2   558  155  206  363   22  250   0   30
 5  3 100 100  207  -2.3   550   94  129  242   15  320   0   29
 6    100 100  203  -2.1   550  107  147  279   19  320   1   41
 7  4  99 100  203  -0.1   545  107  147  280   19  393   0   41
 8     99 100  200  -1.3   545   79  107  215   15  393   1   39
 9  5  99 100  200  -0.1   542   79  107  215   15  444   0   39
10  6  99 100  198  -0.9   540   62   82  172   12  476   0   38
11  7  99 100  197  -0.6   538   52   65  146   10  512   0   38
12  8  99 100  196  -0.5   536   44   54  128    9  542   0   36
13  9  99  96  129 -34.0   338  123  156  300   14  625   0   73
14 10  99  95  121  -6.2   315   74   98  210   11  689   0   72
15 11  99  94  118  -3.0   307   56   71  168    9  745   0   71
16     98  72  111  -5.7   307  116  150  355   18  745   1  198
17 12  98  72  107  -3.7   288  116  150  352   18  804   0  200
18 13  98  71  103  -3.0   280   68   88  239   12  842   0  194
19 14  98  70  101  -2.1   274   52   64  199   10  896   0  185
20 15  98  70  100  -1.4   271   45   55  177    8  948   0  183
21 16  98  69   99  -1.2   270   39   47  148    7  999   0  181

writing out results ...
```

```
RELOCATION OF CLUSTER: 2
----------------------
Reading data ...
# events =     2
# stations < maxdist =     21
# stations w/ neg. elevation (set to 0) =    0
# catalog P dtimes =       6
# catalog S dtimes =       6
# dtimes total =       12
    after gap/distance check:       12 (100%)
    nccp,nccs,nctp,ncts:            0           0           6           6
# events after dtime match =          2
# stations =      6
Initial trial sources =     2
3D ray tracing.

  IT   EV  CT    RMSCT   RMSST   DX   DY   DZ   DT   OS  AQ  CND
         %   %   ms      %     ms    m    m    m   ms    m
 1  1 100 100  240  -0.0   397    0    0    0    3    0   0    2
 2  2 100 100  240  -0.0   397    0    0    0    2    0   0    2
 3  3 100 100  240  -0.0   397    0    0    0    1    0   0    2
 4  4 100 100  240  -0.0   397    0    0    0    0    0   0    2
 5  5 100 100  240  -0.0   397    0    0    0    0    0   0    2
 6  6 100 100  240  -0.0   397    0    0    0    0    1   0    2
 7  7 100 100  240  -0.0   396    0    0    0    0    1   0    2
 8  8 100 100  240  -0.0   396    0    0    0    0    1   0    2
 9  9 100 100  213 -11.2   396    0    0    1    0    1   0    2
10 10 100 100  213  -0.0   396    0    0    1    0    1   0    2
11 11 100 100  213  -0.0   396    0    0    1    0    2   0    2
12 12 100 100  213  -0.1   396    0    1    3    0    3   0    2
13 13 100 100  213  -0.1   395    0    1    3    0    3   0    2
14 14 100 100  212  -0.1   395    0    1    3    0    4   0    2
15 15 100 100  212  -0.1   394    0    1    3    0    5   0    2
16 16 100 100  212  -0.1   394    0    1    3    0    6   0    2

writing out results ...

RELOCATION OF CLUSTER: 3
----------------------
Reading data ...
# events =     2
# stations < maxdist =     21
# stations w/ neg. elevation (set to 0) =    0
# catalog P dtimes =       8
# catalog S dtimes =       7
# dtimes total =       15
    after gap/distance check:       13 ( 87%)
    nccp,nccs,nctp,ncts:            0           0           7           6
# events after dtime match =          2
# stations =      7
Initial trial sources =     2
3D ray tracing.

  IT   EV  CT    RMSCT   RMSST   DX   DY   DZ   DT   OS  AQ  CND
```

```
         %   %   ms      %    ms     m    m    m   ms    m
 1   1 100 100  635  -0.0  1435    0    0    1    0    1    0    2
 2   2 100 100  635  -0.0  1435    0    0    1    0    1    0    2
 3   3 100 100  635  -0.0  1435    0    0    1    0    2    0    2
 4   4 100 100  635  -0.0  1434    0    0    1    0    3    0    2
 5   5 100 100  634  -0.0  1434    0    0    1    0    4    0    2
 6   6 100 100  634  -0.0  1434    0    0    1    0    5    0    2
 7   7 100 100  634  -0.0  1433    0    0    1    0    6    0    2
 8   8 100 100  634  -0.0  1433    0    0    1    0    7    0    2
 9   9 100 100  530 -16.3  1433    1    1    2    0    9    0    2
10  10 100 100  530  -0.1  1432    1    1    2    0   10    0    2
11  11 100 100  530  -0.1  1431    1    1    2    0   12    0    2
  Cluster has less than 2 events.
   Program hypoDD finished.
```

DAMP Increasing: 100, 200, 300, 400

Table 19: Input parameters and Output for hypoDD Damping Test 2

DATA WEIGHTING AND REWEIGHTING:									
NITER	WTCCP	WTCCS	WRCC	WDCC	WTCTP	WTCTS	WRCT	WDCT	DAMP
3	-999	-999	-999	-999	1.00	0.80	-999	-999	100
5	-999	-999	-999	-999	1.00	0.80	-999	-999	200
3	-999	-999	-999	-999	1.00	0.80	6	50	300
5	-999	-999	-999	-999	1.00	0.80	6	20	400

Output:

```
starting hypoDD (v2.1beta - 09/30/2011)...
Input parameters: ./hypoDD_3d_ct.inp (hypoDD2.0 format)
INPUT FILES:
 cross dtime data: empty.cc
 catalog dtime data: dt.ct
 events: event.sel
 stations: station.sel
OUTPUT FILES:
 initial locations: hypoDD_3d_ct_37.loc
 relocated events: hypoDD_3d_ct_37.reloc
 event pair residuals: hypoDD_3d_ct_37.res
 station residuals: hypoDD_3d_ct_37.sta
 source parameters: hypoDD_3d_ct_37.src
Use local 3D model vel3d.dat
Relocate all clusters
Relocate all events
Remove air quakes.
Reading data ...
```

```
# events =  3395
# stations < maxdist =     21
# stations w/ neg. elevation (set to 0) =    0
# catalog P dtimes =  630340
# catalog S dtimes =  524488
# dtimes total =  1154828
    after gap/distance check:   987143 ( 85%)
    nccp,nccs,nctp,ncts:            0           0      528167      458976
# events after dtime match =       3383
# stations =     21
clustering ...
Clustered events:  1798
Isolated events:  1585
# clusters:    3
Cluster   1:  1794 events
Cluster   2:     2 events
Cluster   3:     2 events

RELOCATION OF CLUSTER: 1
----------------------
Reading data ...
# events =  1794
# stations < maxdist =     21
# stations w/ neg. elevation (set to 0) =    0
# catalog P dtimes =  340050
# catalog S dtimes =  288842
# dtimes total =   628892
    after gap/distance check:   567994 ( 90%)
    nccp,nccs,nctp,ncts:            0           0      303690      264304
# events after dtime match =       1794
# stations =     21
Initial trial sources =  1794
3D ray tracing.
```

IT	EV	CT	RMSCT		RMSST	DX	DY	DZ	DT	OS	AQ	CND
		%	%	ms	%	ms	m	m	m	ms	m		
1		100	100	229	-49.8	0	849	1063	2269	137	0	12	187
2	1	99	99	218	-4.6	540	769	1029	1974	128	470	0	187
3		99	99	204	-6.7	540	245	299	800	48	470	3	175
4	2	99	99	203	-0.4	529	237	298	764	47	712	0	176
5	3	99	99	195	-3.9	523	132	156	432	30	847	0	169
6	4	99	99	194	-0.5	521	32	39	130	7	899	0	64
7	5	99	99	193	-0.4	520	27	32	111	5	941	0	61
8	6	99	99	192	-0.3	519	23	28	97	5	983	0	58
9		99	99	192	-0.2	519	22	26	100	4	983	1	61
10	7	99	99	192	-0.0	519	22	25	101	4	1036	0	61
11	8	99	99	192	-0.2	518	20	23	94	4	1069	0	59
12	9	99	95	127	-33.8	328	77	97	173	6	1019	0	42
13	10	99	94	120	-5.3	314	42	60	115	5	1043	0	40
14	11	99	94	117	-2.5	306	29	43	92	4	1067	0	39
15	12	98	72	111	-5.0	301	33	40	64	3	1052	0	30
16	13	98	71	107	-4.2	286	22	28	53	2	1059	0	28
17	14	98	70	105	-1.6	281	16	22	42	2	1066	0	28
18	15	98	70	104	-0.9	278	13	18	37	2	1069	0	27

```
19 16  98  70  103  -0.7   276   11   16   33    2 1073   0   27

writing out results ...

RELOCATION OF CLUSTER: 2
----------------------
Reading data ...
# events =     2
# stations < maxdist =     21
# stations w/ neg. elevation (set to 0) =    0
# catalog P dtimes =       6
# catalog S dtimes =       6
# dtimes total =       12
    after gap/distance check:       12 (100%)
    nccp,nccs,nctp,ncts:            0           0           6           6
# events after dtime match =          2
# stations =      6
Initial trial sources =     2
3D ray tracing.

  IT   EV  CT    RMSCT   RMSST   DX   DY   DZ   DT   OS  AQ  CND
       %   %   ms     %    ms    m    m    m   ms    m
 1  1 100 100  240  -0.1   396    0    1    4    1    1   0    2
 2  2 100 100  240  -0.1   396    0    1    4    1    2   0    2
 3  3 100 100  239  -0.1   395    0    1    4    0    4   0    2
 4  4 100 100  239  -0.0   395    0    0    1    0    4   0    2
 5  5 100 100  239  -0.0   395    0    0    1    0    4   0    2
 6  6 100 100  239  -0.0   395    0    0    1    0    4   0    2
 7  7 100 100  239  -0.0   395    0    0    1    0    5   0    2
 8  8 100 100  239  -0.0   395    0    0    1    0    5   0    2
 9  9 100 100  212 -11.3   395    0    0    0    0    5   0    2
10 10 100 100  212  -0.0   395    0    0    0    0    5   0    2
11 11 100 100  212  -0.0   394    0    0    0    0    5   0    2
12 12 100 100  212  -0.0   394    0    0    0    0    5   0    2
13 13 100 100  212  -0.0   394    0    0    0    0    5   0    2
14 14 100 100  212  -0.0   394    0    0    0    0    5   0    2
15 15 100 100  212  -0.0   394    0    0    0    0    5   0    2
16 16 100 100  212   0.0   394    0    0    0    0    6   0    2

writing out results ...

RELOCATION OF CLUSTER: 3
----------------------
Reading data ...
# events =     2
# stations < maxdist =     21
# stations w/ neg. elevation (set to 0) =    0
# catalog P dtimes =       8
# catalog S dtimes =       7
# dtimes total =       15
    after gap/distance check:       13 ( 87%)
    nccp,nccs,nctp,ncts:            0           0           7           6
# events after dtime match =          2
# stations =      7
```

```
Initial trial sources =     2
3D ray tracing.

  IT   EV  CT    RMSCT   RMSST   DX   DY   DZ   DT   OS  AQ  CND
         %   %    ms      %     ms    m    m    m   ms    m
 1   1 100 100   633   -0.3  1433    3    3    9    0    9   0    2
 2   2 100 100   632   -0.3  1430    3    3    9    1   18   0    2
 3   3 100 100   630   -0.3  1427    3    3    9    1   27   0    2
 4   4 100 100   630   -0.1  1426    1    1    2    0   30   0    2
 5   5 100 100   629   -0.1  1426    1    1    2    0   32   0    2
 6   6 100 100   629   -0.1  1425    1    1    2    0   34   0    2
 7   7 100 100   628   -0.1  1424    1    1    2    0   36   0    2
 8   8 100 100   628   -0.0  1423    1    1    2    0   39   0    2
 9   9 100 100   526  -16.3  1423    0    0    1    0   39   0    2
10  10 100 100   526   -0.0  1423    0    0    1    0   40   0    2
11  11 100 100   526   -0.0  1423    0    0    1    0   41   0    2
  Cluster has less than 2 events.

   Program hypoDD finished.
```

APPENDIX B

Maps and Cross-Section Profiles

I: 3D catalog locations of all events in study area above 120 km depth

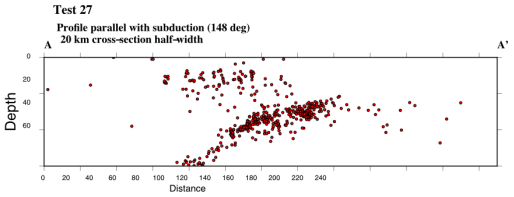
Test 27
Profile parallel with subduction (148 deg)
20 km cross-section half-width
A
A'
Depth
Distance

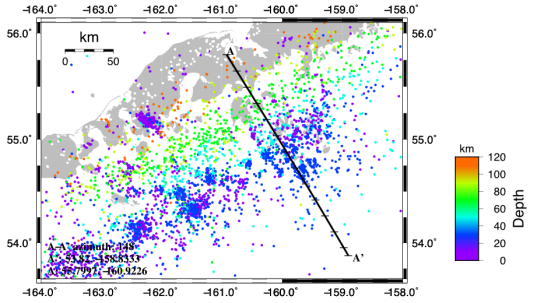
km
0
50
A
A'
A-A' azimuth: 148
Depth

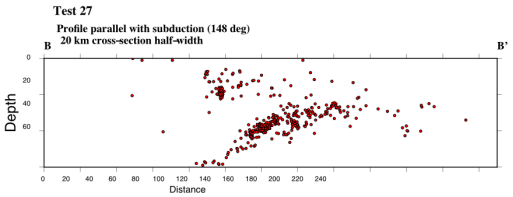
Test 27
Profile parallel with subduction (148 deg)
20 km cross-section half-width
B
B'
Depth
Distance

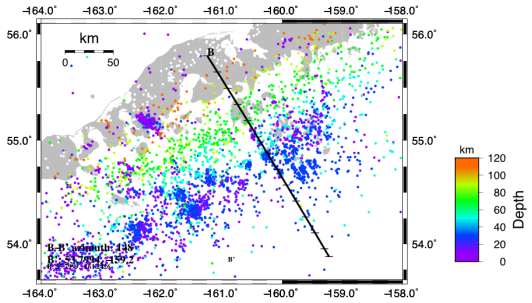
km
0
50
B
B-B' azimuth: 148
Depth

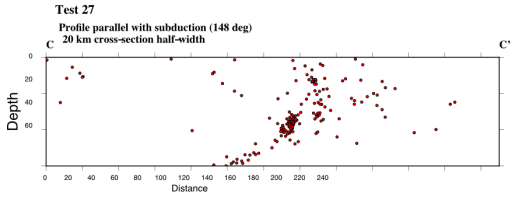
Test 27
Profile parallel with subduction (148 deg)
20 km cross-section half-width
C
C'
Depth
Distance

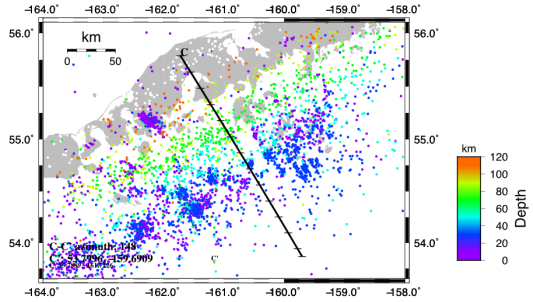
km
0
50
C
C-C' azimuth: 148
Depth

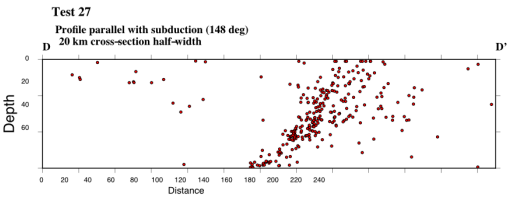
Test 27
Profile parallel with subduction (148 deg)
20 km cross-section half-width
D
D'
Depth
Distance

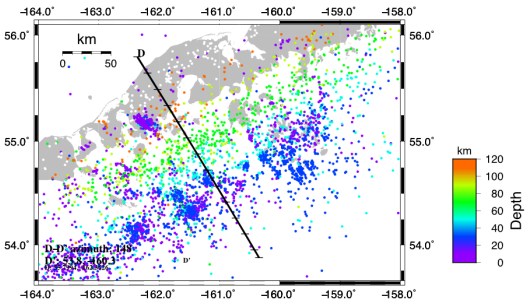
km
0
50
D
D-D' azimuth: 148
Depth

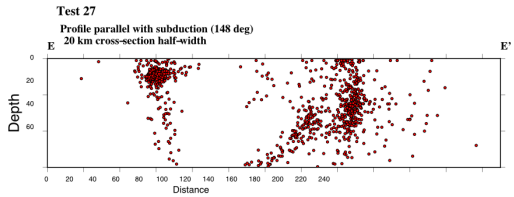
Test 27
Profile parallel with subduction (148 deg)
20 km cross-section half-width
E
E'
Depth
Distance

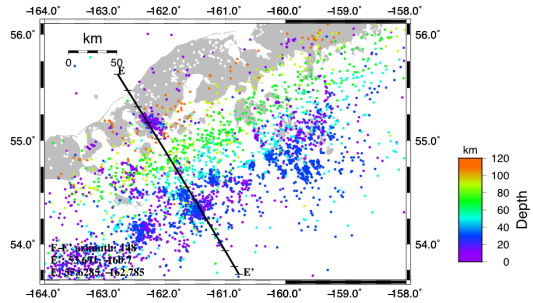
km
0
50
E
E-E' azimuth: 148
Depth

II: Starting Events in hypoDD

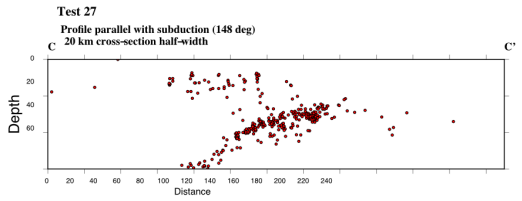
Test 27
Profile parallel with subduction (148 deg)
20 km cross-section half-width
C
C'
Depth
Distance

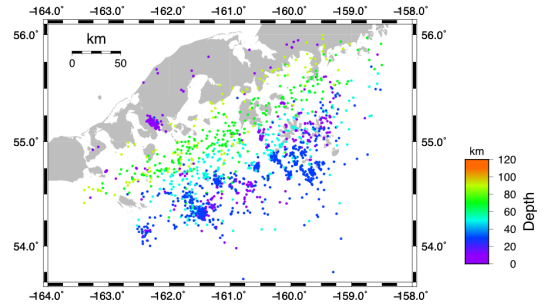
km
0 50
km
120
100
80
60
40
20
0
Depth

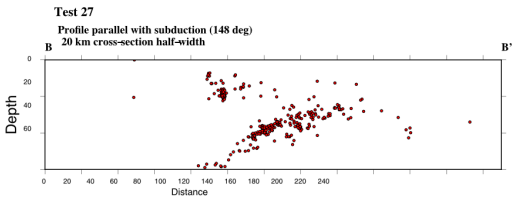
Test 27
Profile parallel with subduction (148 deg)
20 km cross-section half-width
B
B'
Depth
Distance

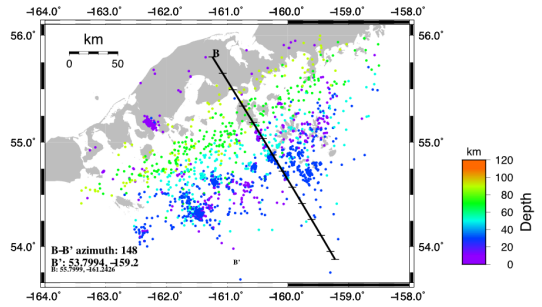
km
0 50
B
B-B' azimuth: 148
B': 53.7994, -159.2
B'
km
120
100
80
60
40
20
0
Depth

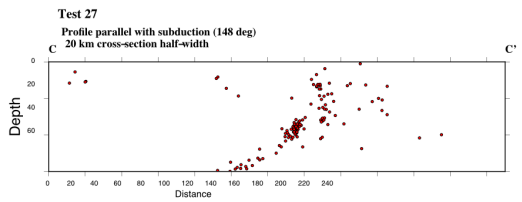
Test 27
Profile parallel with subduction (148 deg)
20 km cross-section half-width
C
C'
Depth
Distance

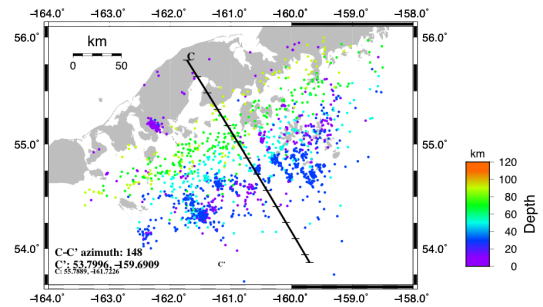
km
0 50
C
C-C' azimuth: 148
C': 53.7996, -159.6909
C'
km
120
100
80
60
40
20
0
Depth

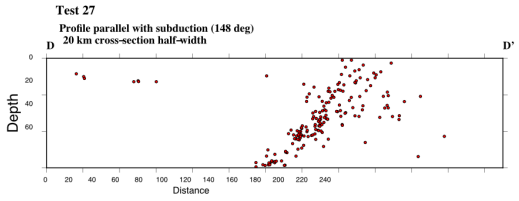
Test 27
Profile parallel with subduction (148 deg)
20 km cross-section half-width
D
D'
Depth
Distance

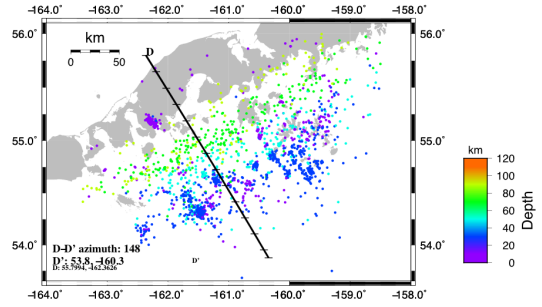
km
0 50
D
D-D' azimuth: 148
D': 53.8, -160.3
D'
km
120
100
80
60
40
20
0
Depth

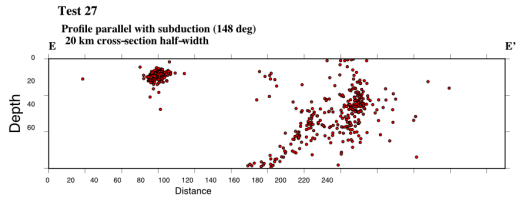
Test 27
Profile parallel with subduction (148 deg)
20 km cross-section half-width
E
E'
Depth
Distance

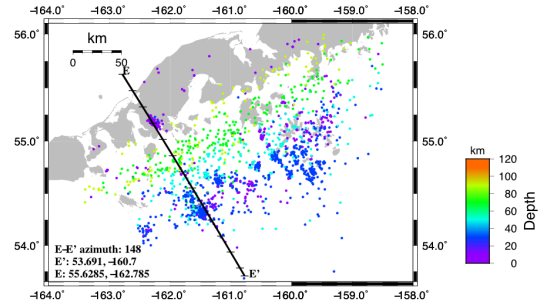
km
0 50
E
E-E' azimuth: 148
E': 53.691, -160.7
E: 55.6285, -162.785
E'
km
120
100
80
60
40
20
0
Depth

III: Final Relocated Events from hypoDD

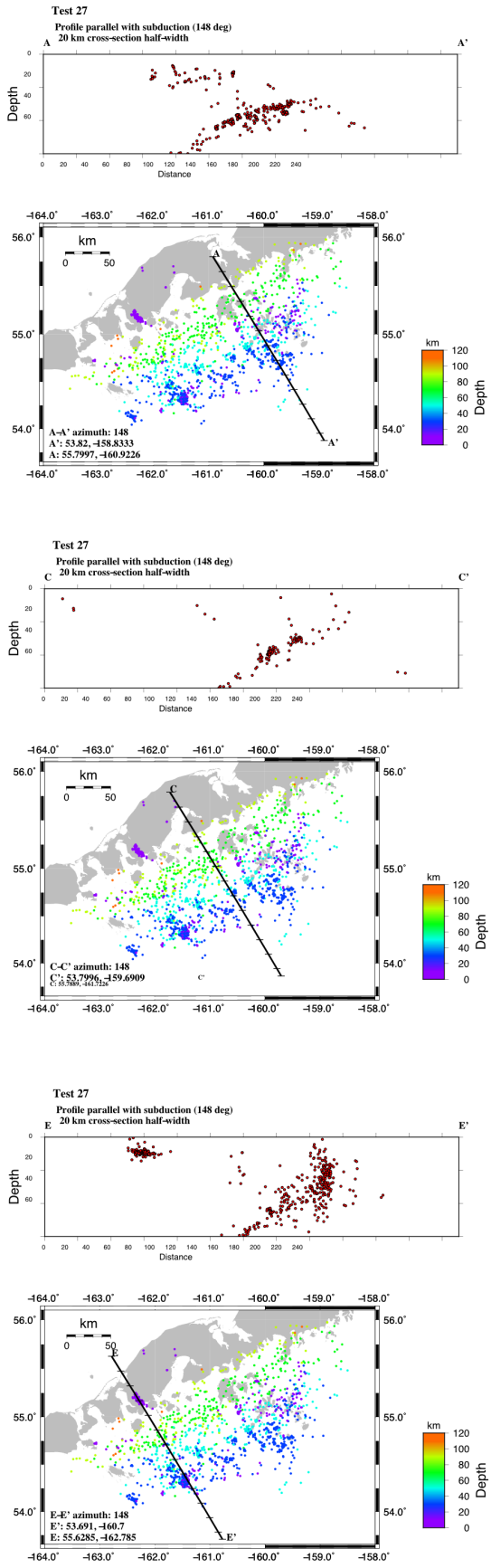
Test 27
Profile parallel with subduction (148 deg)
20 km cross-section half-width
A
A'
Depth
Distance
km
0
50
A–A' azimuth: 148
A': 53.82, -158.8333
A: 55.7997, -160.9226
B
B'
B-B' azimuth: 148
B': 53.7994, -159.2
C
C'
C-C' azimuth: 148
C': 53.7996, -159.6909
D
D'
D-D' azimuth: 148
D': 53.8, -160.3
E
E'
E-E' azimuth: 148
E': 53.691, -160.7
E: 55.6285, -162.785
Depth

IV: OBSCT Tests

IV.1 OBSCT = 8

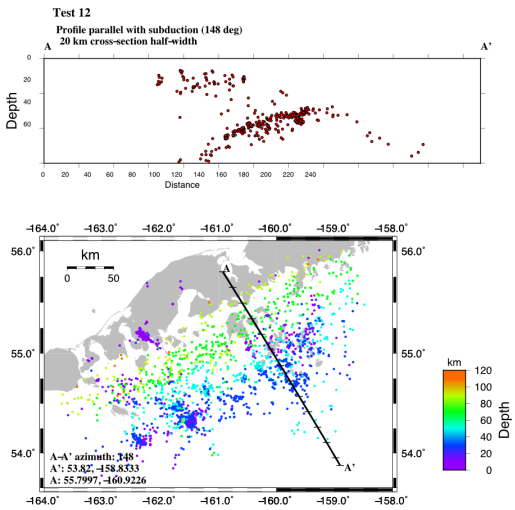
Test 12
Profile parallel with subduction (148 deg)
20 km cross-section half-width
A
A'
Depth
Distance
km
0
50
A-A' azimuth: 148
A': 53.82, -158.8333
A: 55.7997, -160.9226
Depth

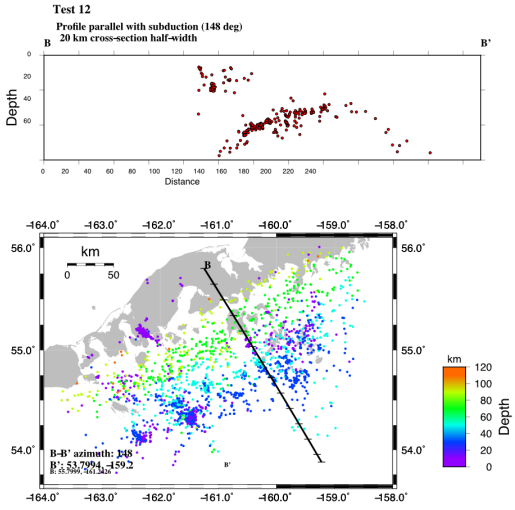
Test 12
Profile parallel with subduction (148 deg)
20 km cross-section half-width
B
B'
Depth
Distance
km
0
50
B-B' azimuth: 148
B': 53.7994, -159.2
Depth

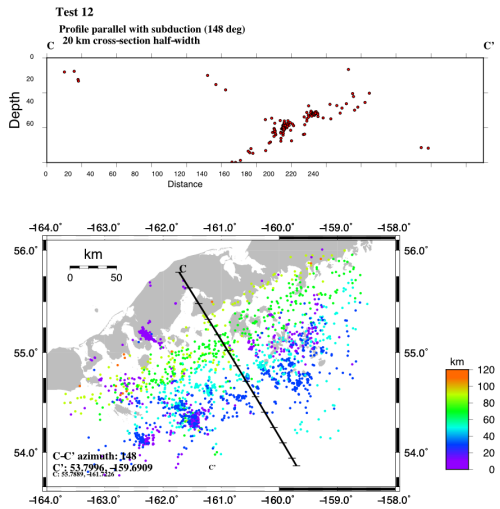
Test 12
Profile parallel with subduction (148 deg)
20 km cross-section half-width
C
C'
Depth
Distance
km
0
50
C-C' azimuth: 148
C': 53.7996, -159.6909
Depth

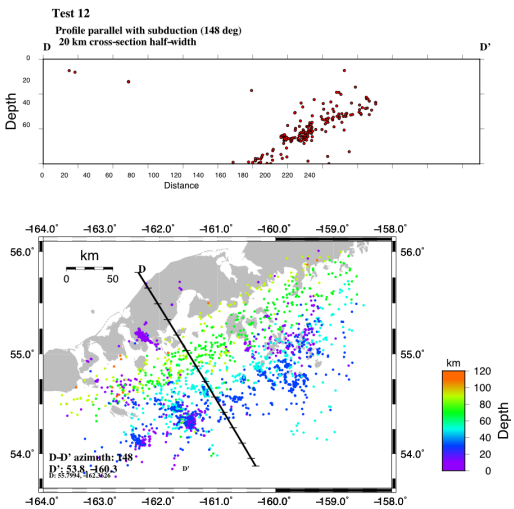
Test 12
Profile parallel with subduction (148 deg)
20 km cross-section half-width
D
D'
Depth
Distance
km
0
50
D-D' azimuth: 148
D': 53.8, -160.3
Depth

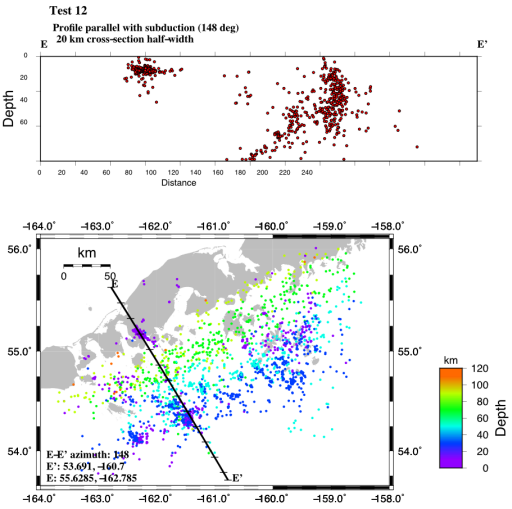
Test 12
Profile parallel with subduction (148 deg)
20 km cross-section half-width
E
E'
Depth
Distance
km
0
50
E-E' azimuth: 148
E': 53.691, -160.7
E: 55.6285, -162.785
Depth

IV.2 OBSCT = 16

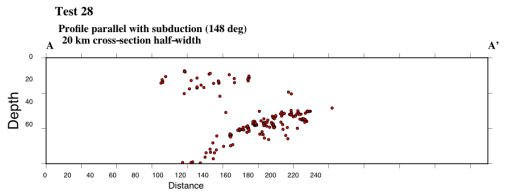
Test 28
Profile parallel with subduction (148 deg)
20 km cross-section half-width
A
A'
Depth
Distance

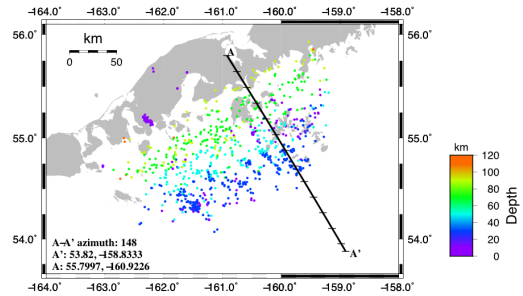
km
0
50
A
A'
A-A' azimuth: 148
A': 53.82, -158.8333
A: 55.7997, -160.9226
km
Depth

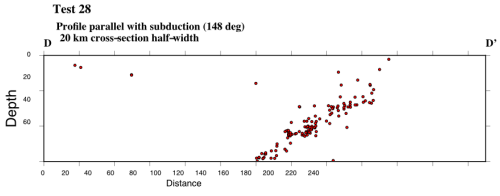
Test 28
Profile parallel with subduction (148 deg)
20 km cross-section half-width
D
D'
Depth
Distance

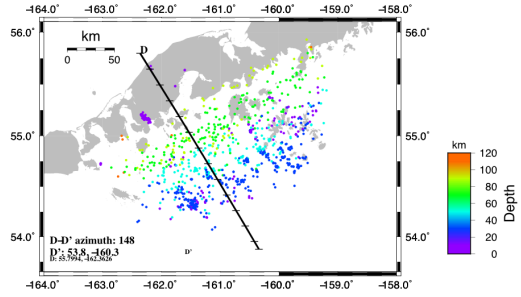
km
0
50
D
D-D' azimuth: 148
D': 53.8, -160.3
km
Depth

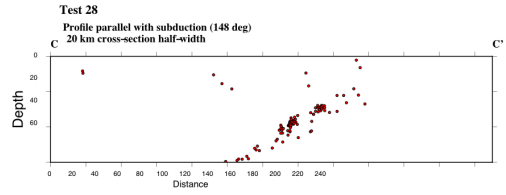
Test 28
Profile parallel with subduction (148 deg)
20 km cross-section half-width
C
C'
Depth
Distance

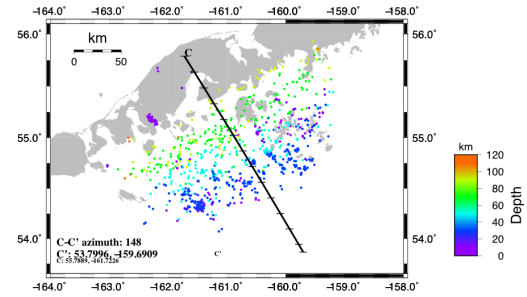
km
0
50
C
C'
C-C' azimuth: 148
C': 53.7996, -159.6909
km
Depth

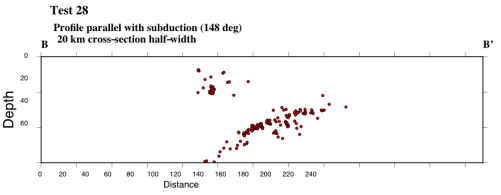
Test 28
Profile parallel with subduction (148 deg)
20 km cross-section half-width
B
B'
Depth
Distance

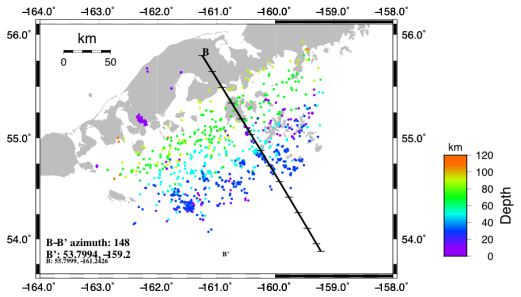
km
0
50
B
B-B' azimuth: 148
B': 53.7994, -159.2
km
Depth

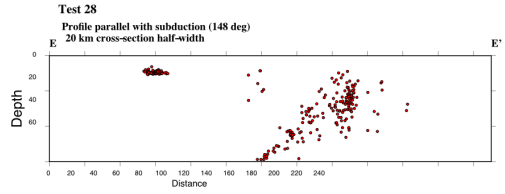
Test 28
Profile parallel with subduction (148 deg)
20 km cross-section half-width
E
E'
Depth
Distance

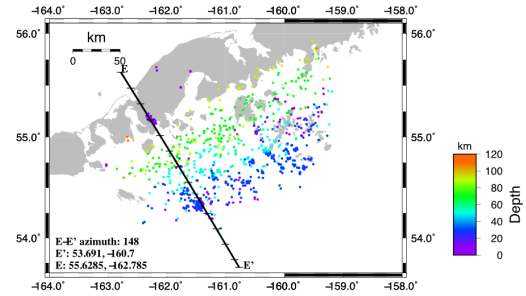
km
0
50
E
E-E' azimuth: 148
E': 53.691, -160.7
E: 55.6285, -162.785
km
Depth

V: P vs. S weighting Tests

V.1 P=1.0, S=0.5

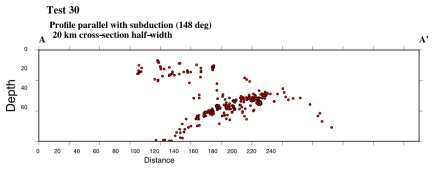
Test 30
Profile parallel with subduction (148 deg)
20 km cross-section half-width
A
A'
Depth
Distance

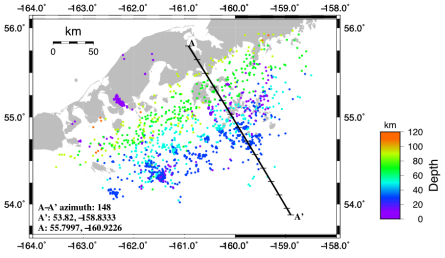
km
0
50
A
A'
A-A' azimuth: 148
A': 53.82, -158.8333
A: 55.7997, -160.9226
km
120
100
80
60
40
20
0
Depth

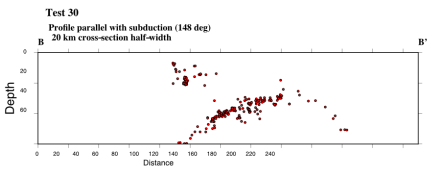
Test 30
Profile parallel with subduction (148 deg)
20 km cross-section half-width
B
B'
Depth
Distance

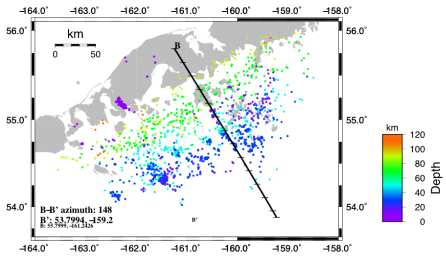
km
0
50
B
B-B' azimuth: 148
B': 53.7994, -159.2
km
120
100
80
60
40
20
0
Depth

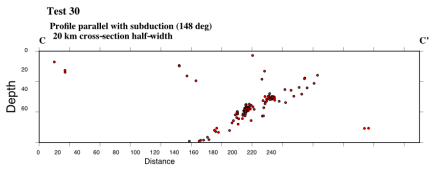
Test 30
Profile parallel with subduction (148 deg)
20 km cross-section half-width
C
C'
Depth
Distance

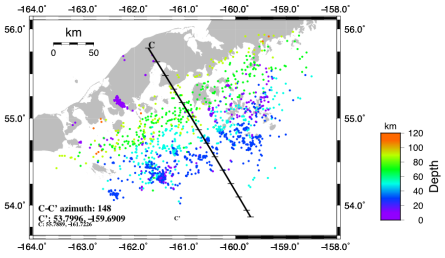
km
0
50
C
C-C' azimuth: 148
C': 53.7996, -159.6909
km
120
100
80
60
40
20
0
Depth

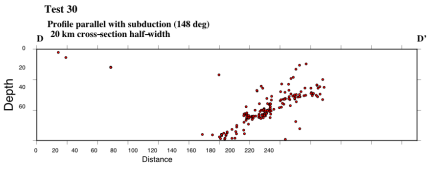
Test 30
Profile parallel with subduction (148 deg)
20 km cross-section half-width
D
D'
Depth
Distance

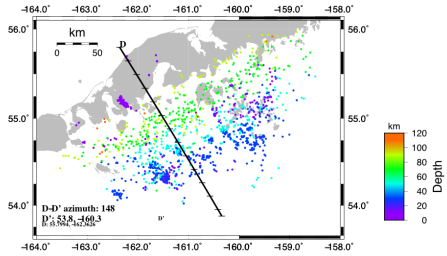
km
0
50
D
D-D' azimuth: 148
D': 53.8, -160.3
km
120
100
80
60
40
20
0
Depth

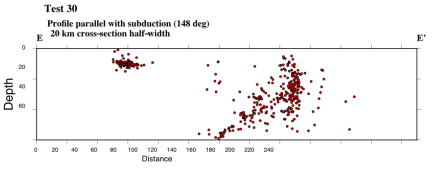
Test 30
Profile parallel with subduction (148 deg)
20 km cross-section half-width
E
E'
Depth
Distance

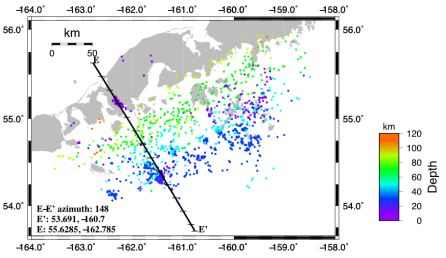
km
0
50
E
E-E' azimuth: 148
E': 53.691, -160.7
E: 55.6285, -162.785
km
120
100
80
60
40
20
0
Depth

V.2 P=1.0, S=0.3

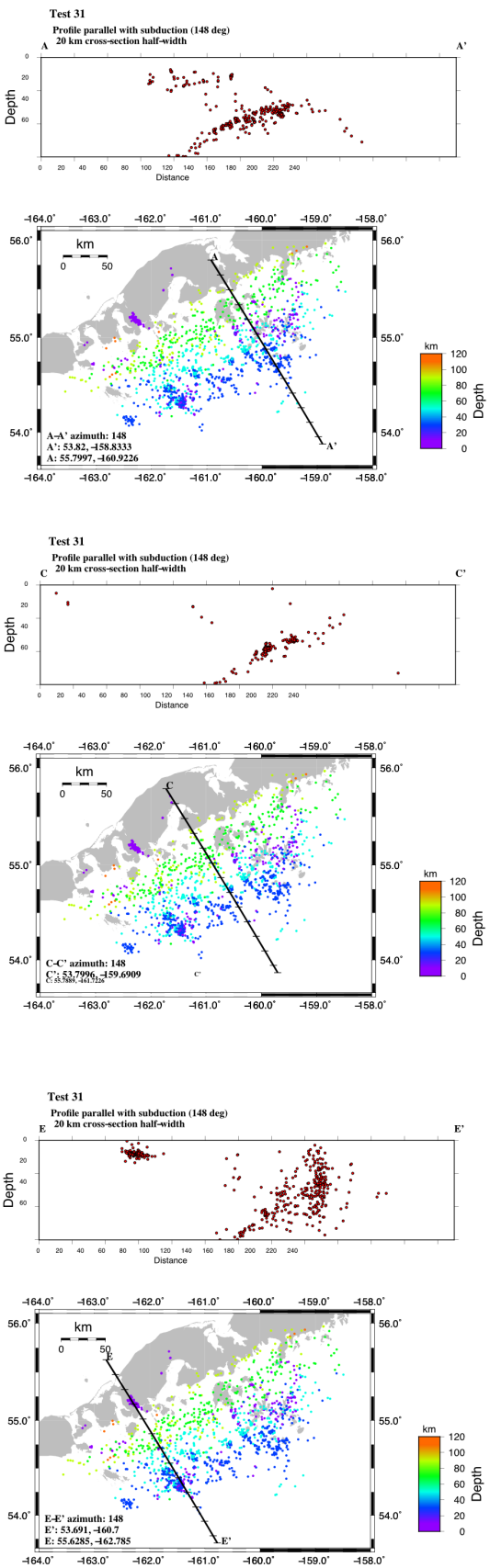
Test 31
Profile parallel with subduction (148 deg)
20 km cross-section half-width
A
A'
Depth
Distance
km
0
50
A-A' azimuth: 148
A': 53.82, -158.8333
A: 55.7997, -160.9226
Depth
Test 31
Profile parallel with subduction (148 deg)
20 km cross-section half-width
B
B'
Depth
Distance
km
0
50
B-B' azimuth: 148
B': 53.7994, -159.2
Depth
Test 31
Profile parallel with subduction (148 deg)
20 km cross-section half-width
C
C'
Depth
Distance
km
0
50
C-C' azimuth: 148
C': 53.7996, -159.6909
Depth
Test 31
Profile parallel with subduction (148 deg)
20 km cross-section half-width
D
D'
Depth
Distance
km
0
50
D-D' azimuth: 148
D': 53.8, -160.3
Depth
Test 31
Profile parallel with subduction (148 deg)
20 km cross-section half-width
E
E'
Depth
Distance
km
0
50
E-E' azimuth: 148
E': 53.691, -160.7
E: 55.6285, -162.785
Depth

VI: WRCT Tests

VI.1 WRCT 3rd Iteration set=20, 4th Iteration set=20

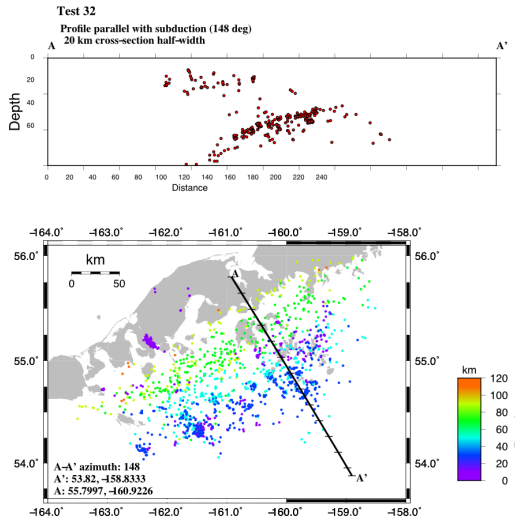
Test 32
Profile parallel with subduction (148 deg)
20 km cross-section half-width
A
A'
Depth
Distance
km
0
50
A-A' azimuth: 148
A': 53.82, -158.8333
A: 55.7997, -160.9226
Depth

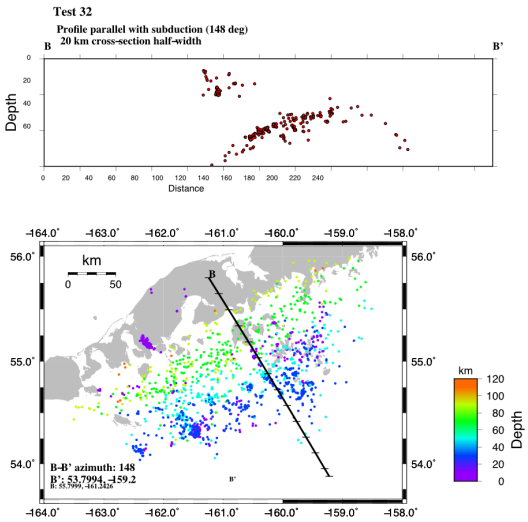
Test 32
Profile parallel with subduction (148 deg)
20 km cross-section half-width
B
B'
Depth
Distance
km
0
50
B-B' azimuth: 148
B': 53.7994, -159.2
Depth

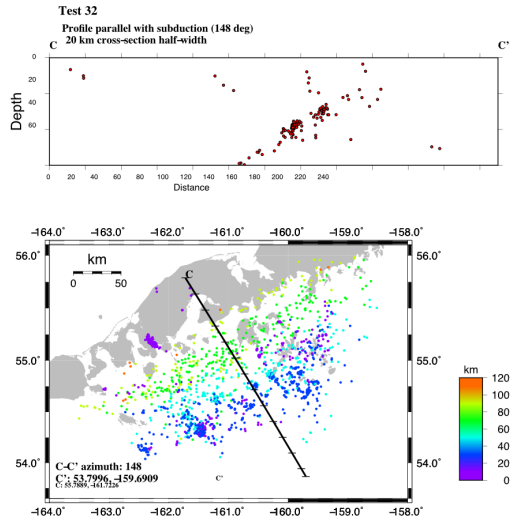
Test 32
Profile parallel with subduction (148 deg)
20 km cross-section half-width
C
C'
Depth
Distance
km
0
50
C-C' azimuth: 148
C': 53.7996, -159.6909
Depth

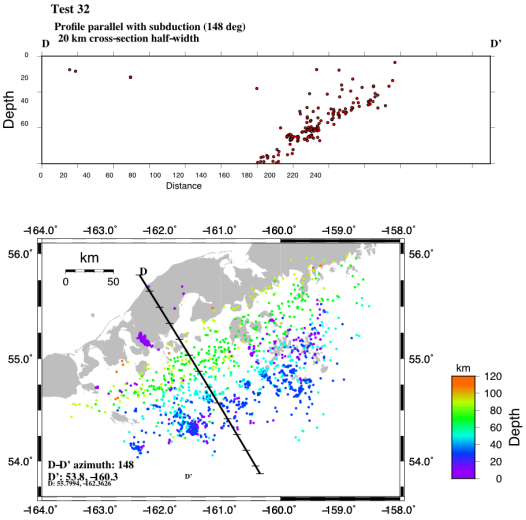
Test 32
Profile parallel with subduction (148 deg)
20 km cross-section half-width
D
D'
Depth
Distance
km
0
50
D-D' azimuth: 148
D': 53.8, -160.3
Depth

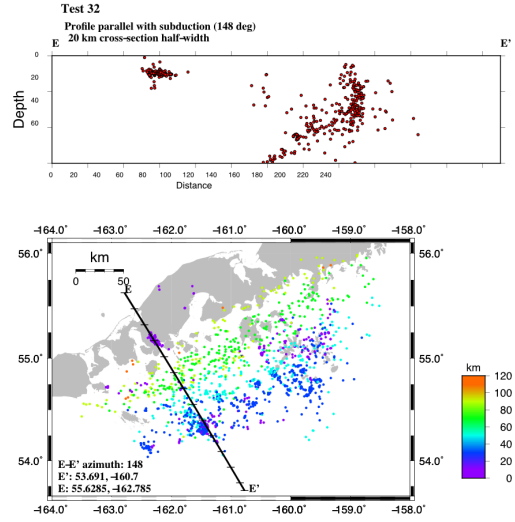
Test 32
Profile parallel with subduction (148 deg)
20 km cross-section half-width
E
E'
Depth
Distance
km
0
50
E-E' azimuth: 148
E': 53.691, -160.7
E: 55.6285, -162.785
Depth

VI.2 WRCT 3rd Iteration set=1, 4th Iteration set=1

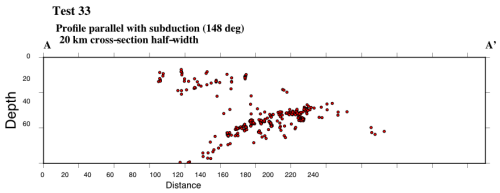
Test 33
Profile parallel with subduction (148 deg)
20 km cross-section half-width
A
A'
Depth
Distance

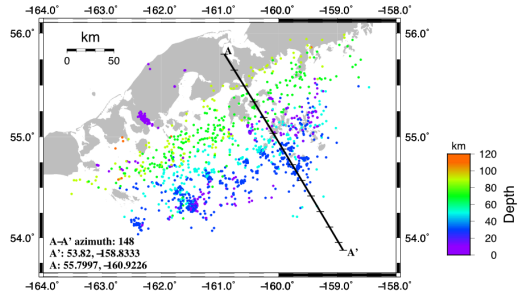
km
0
50
A
A'
km
120
100
80
60
40
20
0
Depth
A-A' azimuth: 148
A': 53.82, -158.8333
A: 55.7997, -160.9226

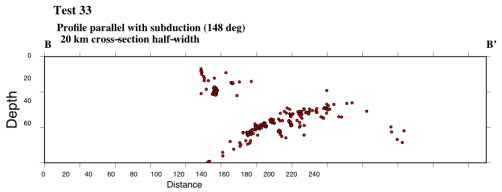
Test 33
Profile parallel with subduction (148 deg)
20 km cross-section half-width
B
B'
Depth
Distance

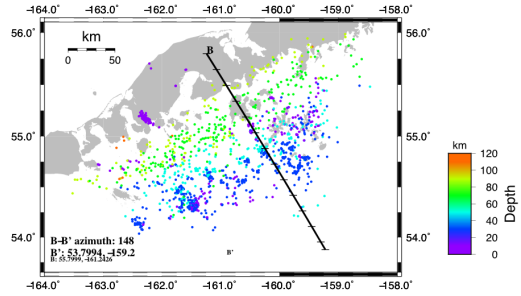
km
0
50
B
km
120
100
80
60
40
20
0
Depth
B-B' azimuth: 148
B': 53.7994, -159.2

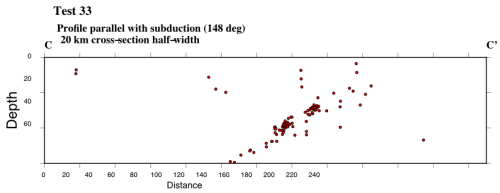
Test 33
Profile parallel with subduction (148 deg)
20 km cross-section half-width
C
C'
Depth
Distance

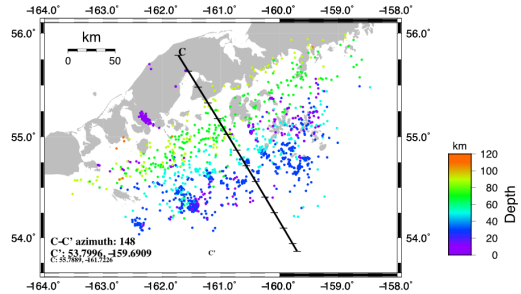
km
0
50
C
km
120
100
80
60
40
20
0
Depth
C-C' azimuth: 148
C': 53.7996, -159.6909

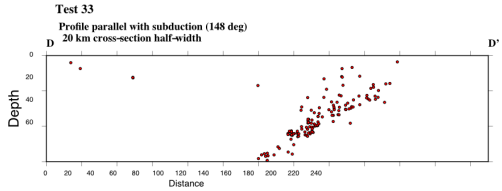
Test 33
Profile parallel with subduction (148 deg)
20 km cross-section half-width
D
D'
Depth
Distance

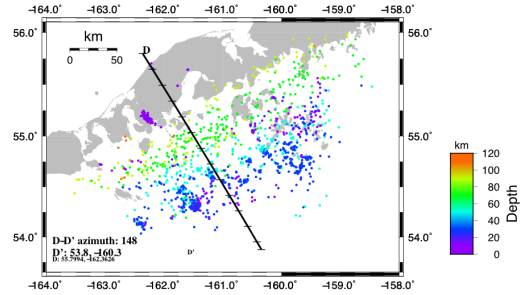
km
0
50
D
km
120
100
80
60
40
20
0
Depth
D-D' azimuth: 148
D': 53.8, -160.3

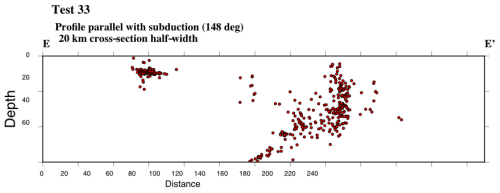
Test 33
Profile parallel with subduction (148 deg)
20 km cross-section half-width
E
E'
Depth
Distance

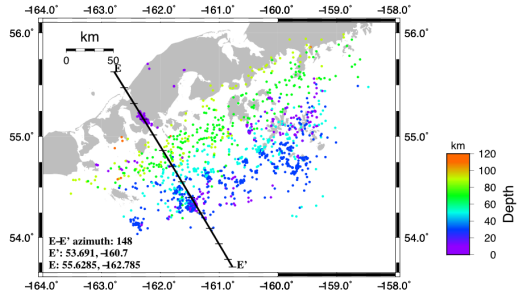
km
0
50
E
E'
km
120
100
80
60
40
20
0
Depth
E-E' azimuth: 148
E': 53.691, -160.7
E: 55.6285, -162.785

VII: WDCT Tests

VII.1 WDCT 3rd Iteration set=100, WDCT 4th Iteration set=50

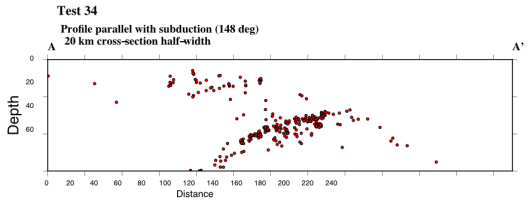
Test 34
Profile parallel with subduction (148 deg)
20 km cross-section half-width
A
A'
Depth
Distance

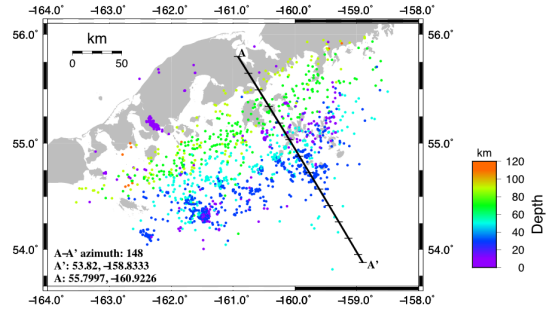
km
0 50
A
A'
A-A' azimuth: 148
A': 53.82, -158.8333
A: 55.7997, -160.9226
km
120
100
80
60
40
20
0
Depth

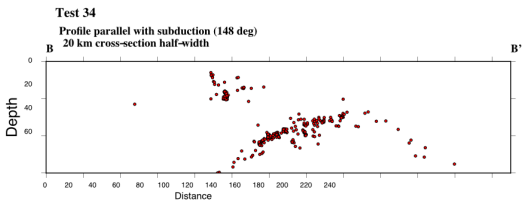
Test 34
Profile parallel with subduction (148 deg)
20 km cross-section half-width
B
B'
Depth
Distance

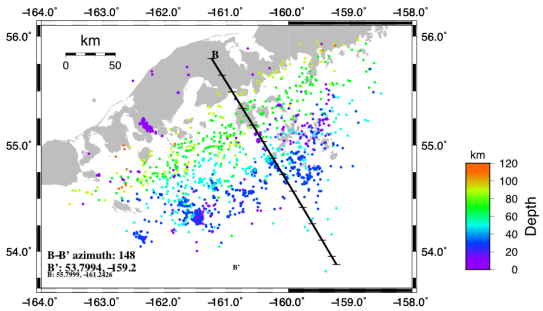
km
0 50
B
B-B' azimuth: 148
B': 53.7994, -159.2
km
120
100
80
60
40
20
0
Depth

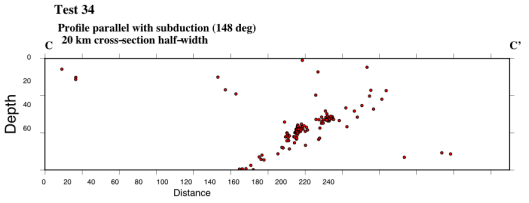
Test 34
Profile parallel with subduction (148 deg)
20 km cross-section half-width
C
C'
Depth
Distance

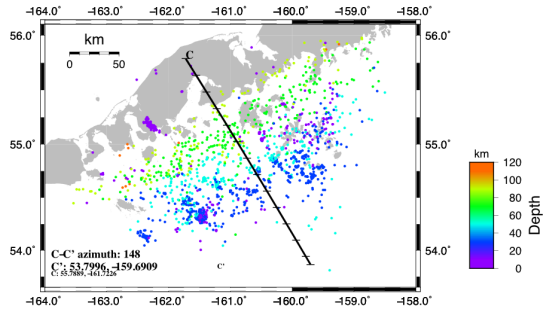
km
0 50
C
C-C' azimuth: 148
C': 53.7996, -159.6909
km
120
100
80
60
40
20
0
Depth

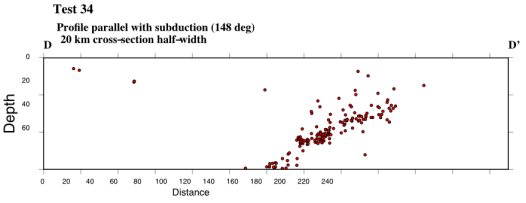
Test 34
Profile parallel with subduction (148 deg)
20 km cross-section half-width
D
D'
Depth
Distance

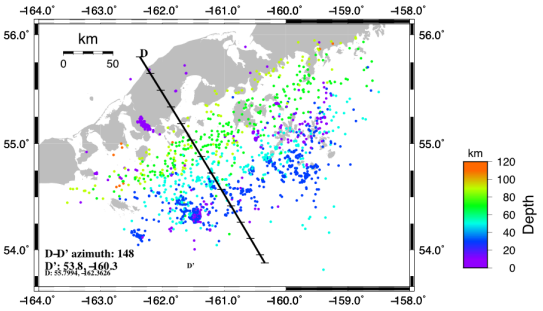
km
0 50
D
D-D' azimuth: 148
D': 53.8, -160.3
km
120
100
80
60
40
20
0
Depth

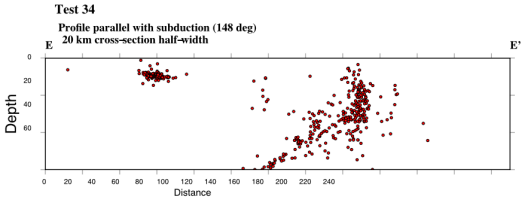
Test 34
Profile parallel with subduction (148 deg)
20 km cross-section half-width
E
E'
Depth
Distance

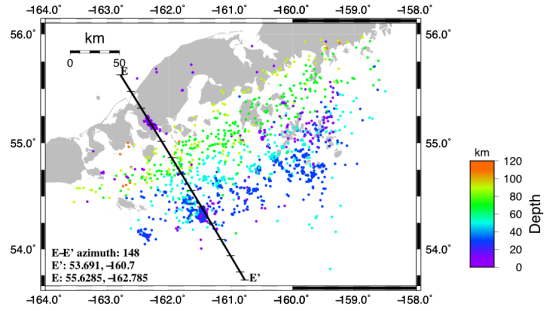
km
0 50
E
E-E' azimuth: 148
E': 53.691, -160.7
E: 55.6285, -162.785
km
120
100
80
60
40
20
0
Depth

VII.1 WDCT 3rd Iteration set=10, WDCT 4th Iteration set=5

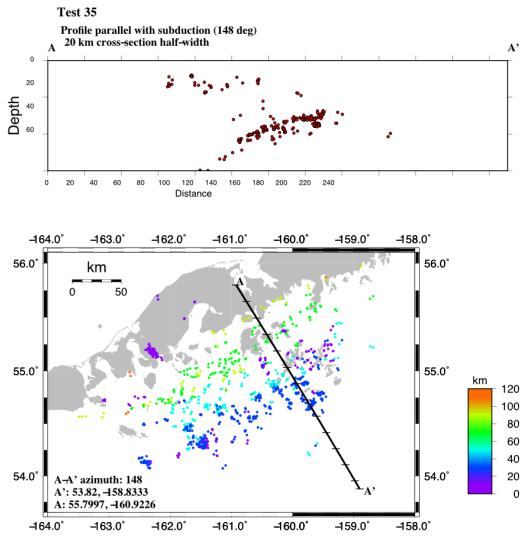
Test 35
Profile parallel with subduction (148 deg)
20 km cross-section half-width
A
A'
Depth
Distance
km
0
50
A-A' azimuth: 148
A': 53.82, -158.8333
A: 55.7997, -160.9226
Depth

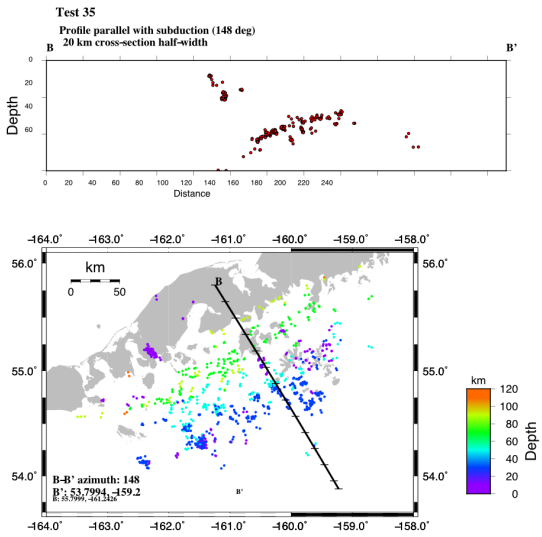
Test 35
Profile parallel with subduction (148 deg)
20 km cross-section half-width
B
B'
Depth
Distance
km
0
50
B-B' azimuth: 148
B': 53.7994, -159.2
Depth

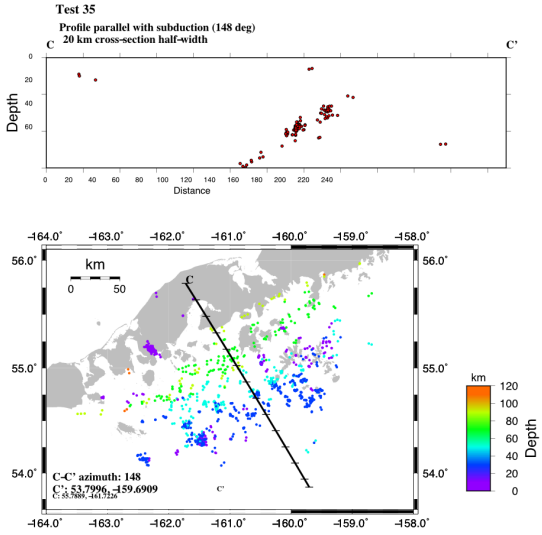
Test 35
Profile parallel with subduction (148 deg)
20 km cross-section half-width
C
C'
Depth
Distance
km
0
50
C-C' azimuth: 148
C': 53.7996, -159.6909
Depth

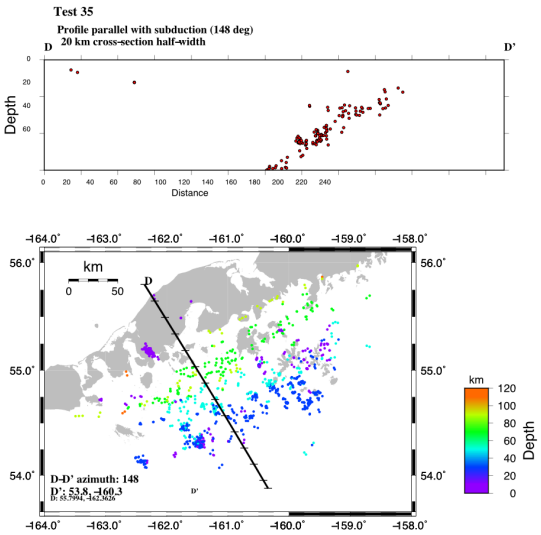
Test 35
Profile parallel with subduction (148 deg)
20 km cross-section half-width
D
D'
Depth
Distance
km
0
50
D-D' azimuth: 148
D': 53.8, -160.3
Depth

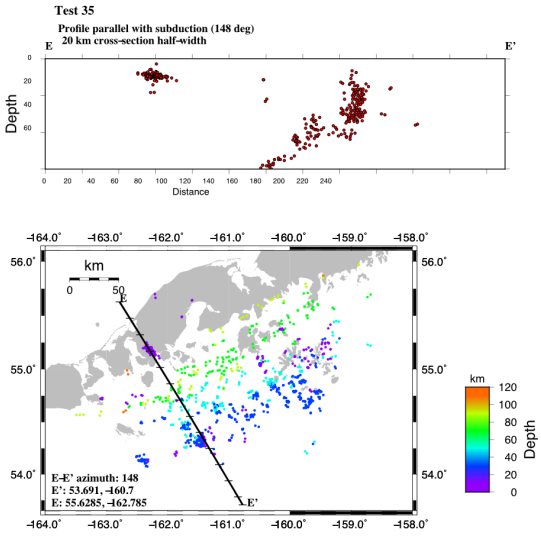
Test 35
Profile parallel with subduction (148 deg)
20 km cross-section half-width
E
E'
Depth
Distance
km
0
50
E-E' azimuth: 148
E': 53.691, -160.7
E: 55.6285, -162.785
Depth

VIII: DAMP Tests

VIII.1 DAMP decreasing: 400, 300, 200, 100

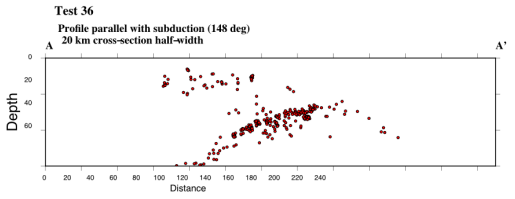
Test 36
Profile parallel with subduction (148 deg)
20 km cross-section half-width
A
A'
Depth
Distance

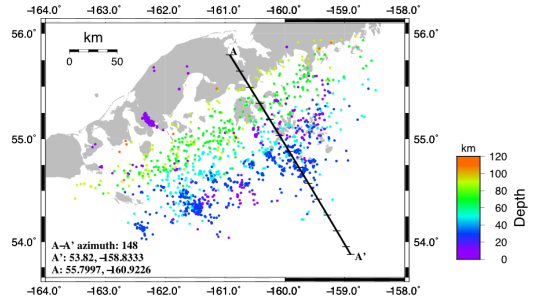
km
0 50
A
A'
A-A' azimuth: 148
A': 53.82, -158.8333
A: 55.7997, -160.9226
km
120
100
80
60
40
20
0
Depth

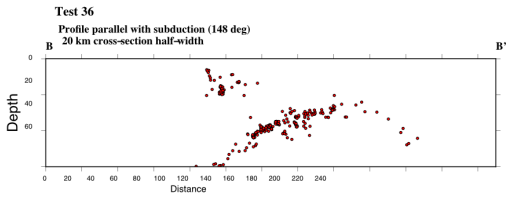
Test 36
Profile parallel with subduction (148 deg)
20 km cross-section half-width
B
B'
Depth
Distance

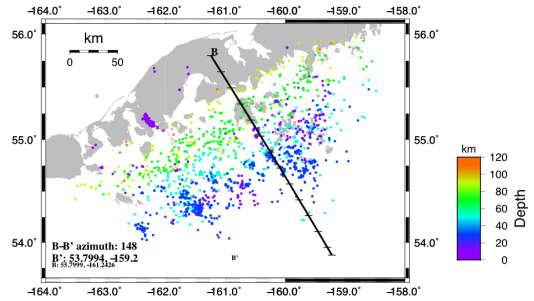
km
0 50
B
B-B' azimuth: 148
B': 53.7994, -159.2
km
120
100
80
60
40
20
0
Depth

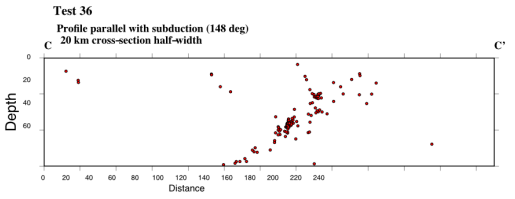
Test 36
Profile parallel with subduction (148 deg)
20 km cross-section half-width
C
C'
Depth
Distance

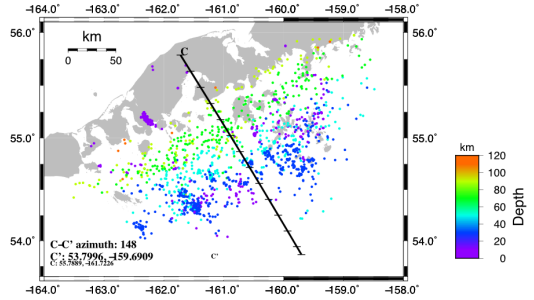
km
0 50
C
C-C' azimuth: 148
C': 53.7996, -159.6909
km
120
100
80
60
40
20
0
Depth

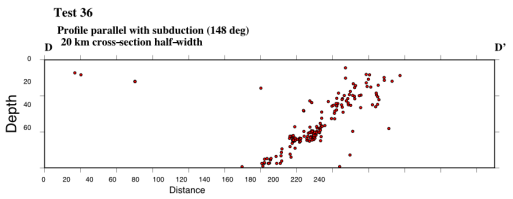
Test 36
Profile parallel with subduction (148 deg)
20 km cross-section half-width
D
D'
Depth
Distance

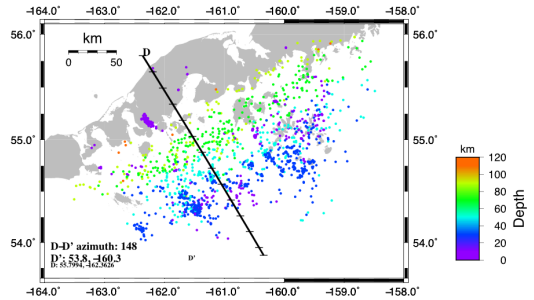
km
0 50
D
D-D' azimuth: 148
D': 53.8, -160.3
km
120
100
80
60
40
20
0
Depth

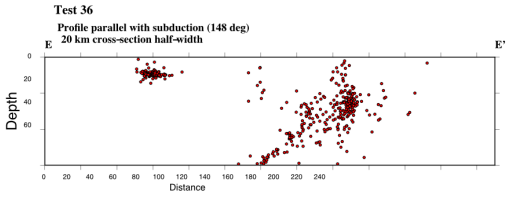
Test 36
Profile parallel with subduction (148 deg)
20 km cross-section half-width
E
E'
Depth
Distance

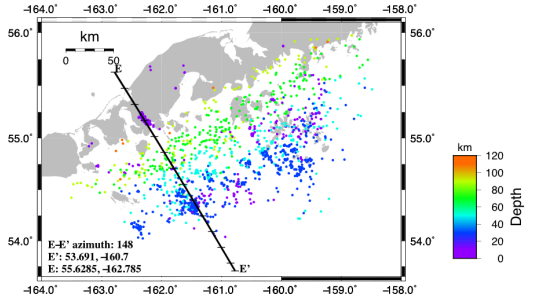
km
0 50
E
E-E' azimuth: 148
E': 53.691, -160.7
E: 55.6285, -162.785
km
120
100
80
60
40
20
0
Depth

VIII.2 DAMP increasing: 100, 200, 300, 400

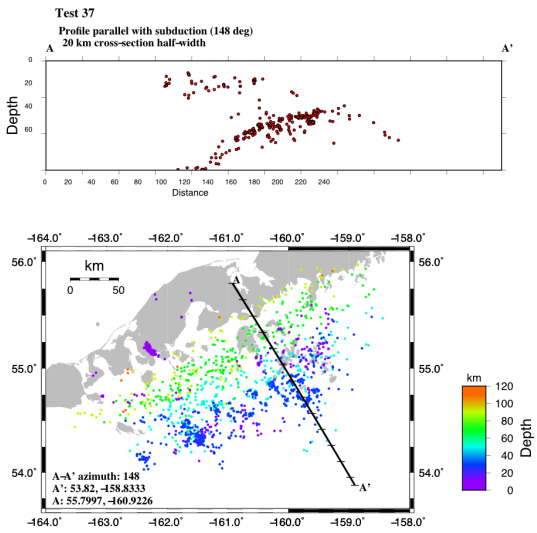
Test 37
Profile parallel with subduction (148 deg)
20 km cross-section half-width
A
A'
Depth
Distance
km
0
50
A-A' azimuth: 148
A': 53.82, -158.8333
A: 55.7997, -160.9226
Depth

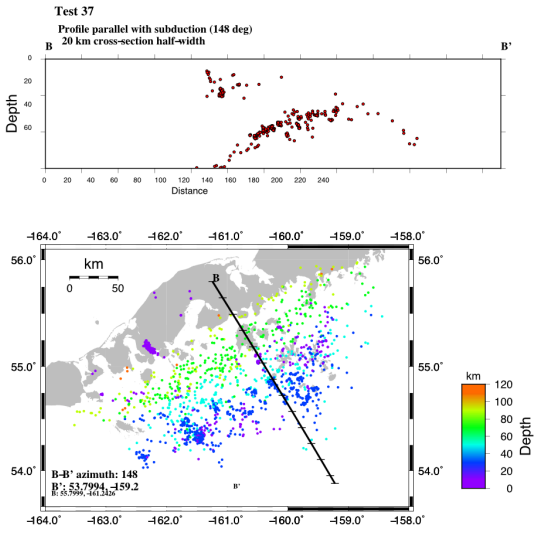
Test 37
Profile parallel with subduction (148 deg)
20 km cross-section half-width
B
B'
Depth
Distance
km
0
50
B-B' azimuth: 148
B': 53.7994, -159.2
B: 55.7999, -161.2426
Depth

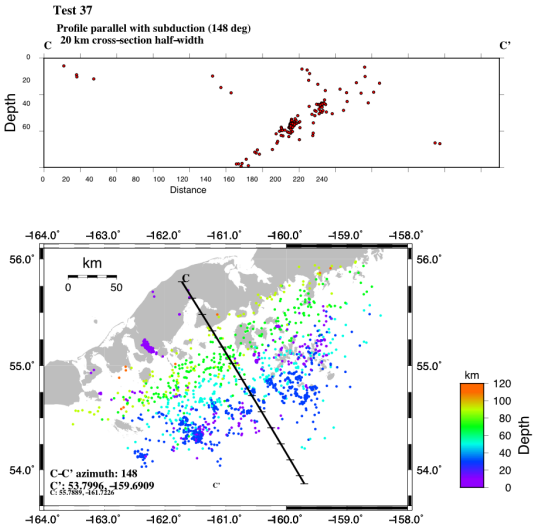
Test 37
Profile parallel with subduction (148 deg)
20 km cross-section half-width
C
C'
Depth
Distance
km
0
50
C-C' azimuth: 148
C': 53.7996, -159.6909
C: 55.7689, -161.7226
Depth

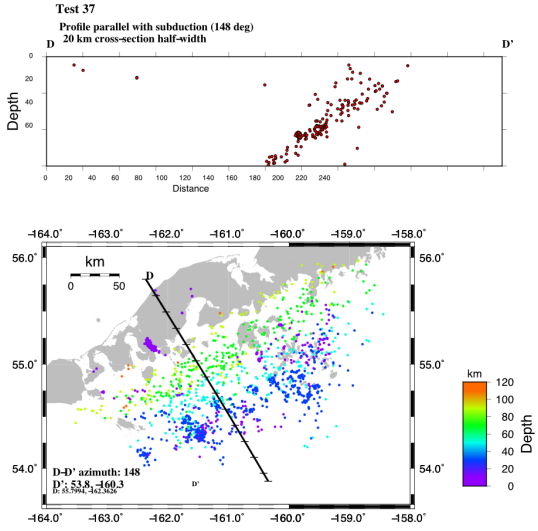
Test 37
Profile parallel with subduction (148 deg)
20 km cross-section half-width
D
D'
Depth
Distance
km
0
50
D-D' azimuth: 148
D': 53.8, -160.3
D: 55.7994, -162.3626
Depth

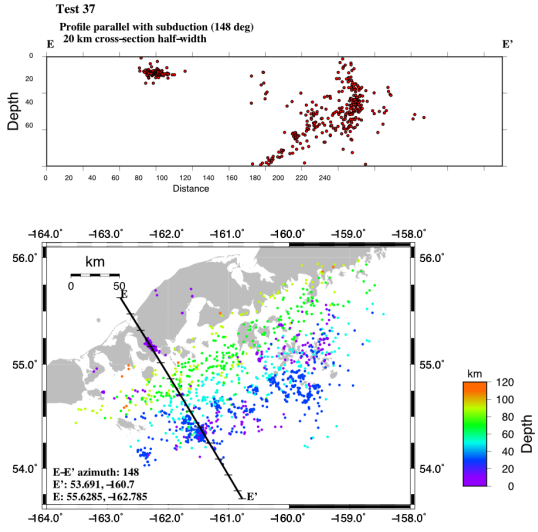
Test 37
Profile parallel with subduction (148 deg)
20 km cross-section half-width
E
E'
Depth
Distance
km
0
50
E-E' azimuth: 148
E': 53.691, -160.7
E: 55.6285, -162.785
Depth

APPENDIX C

Velocity Model 10% Faster

Plots and histograms for Segments 1 – 6

I. Map view showing horizontal change in locations from 10% faster velocity model for Segments 1 – 6

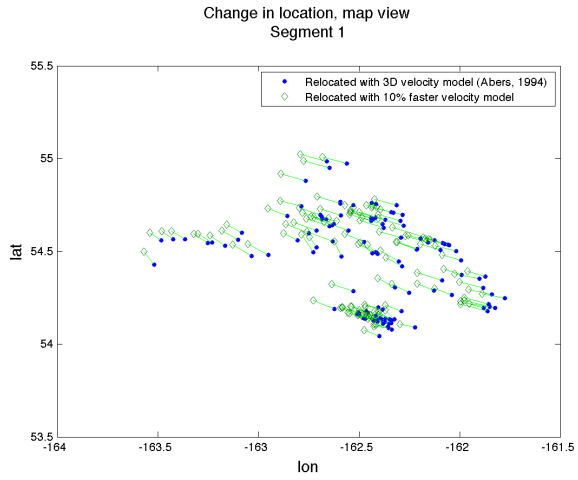
Change in location, map view
Segment 1
Relocated with 3D velocity model (Abers, 1994)
Relocated with 10% faster velocity model
lat
lon
55.5
55
54.5
54
53.5
-164
-163.5
-163
-162.5
-162
-161.5

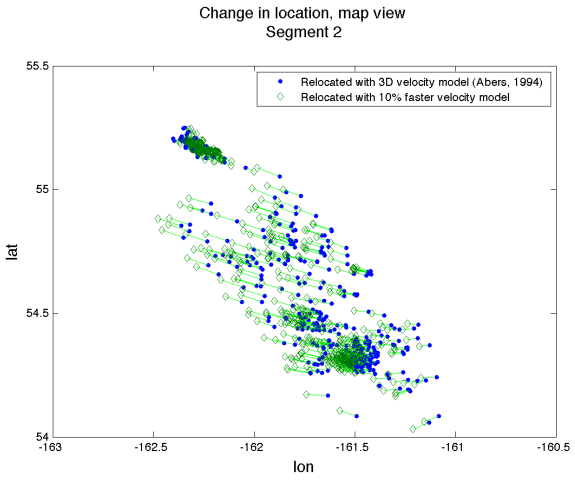
Change in location, map view
Segment 2
Relocated with 3D velocity model (Abers, 1994)
Relocated with 10% faster velocity model
lat
lon
55.5
55
54.5
54
-163
-162.5
-162
-161.5
-161
-160.5

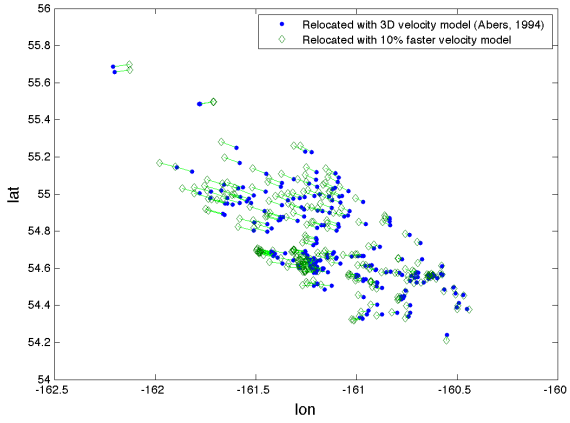
Change in location, map view
Segment 3
Relocated with 3D velocity model (Abers, 1994)
Relocated with 10% faster velocity model
lat
lon
56
55.8
55.6
55.4
55.2
55
54.8
54.6
54.4
54.2
54
-162.5
-162
-161.5
-161
-160.5
-160

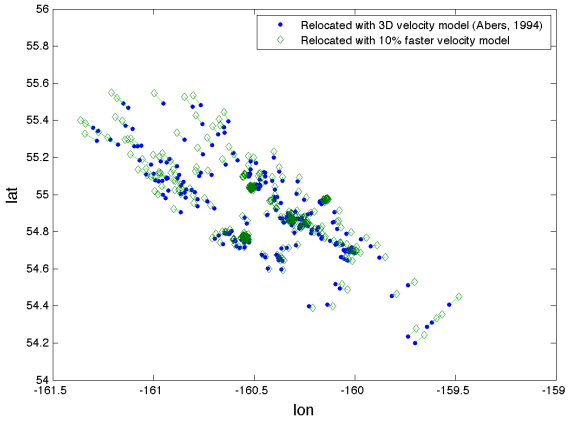
Change in location, map view
Segment 4
Relocated with 3D velocity model (Abers, 1994)
Relocated with 10% faster velocity model
lat
lon
56
55.8
55.6
55.4
55.2
55
54.8
54.6
54.4
54.2
54
-161.5
-161
-160.5
-160
-159.5
-159

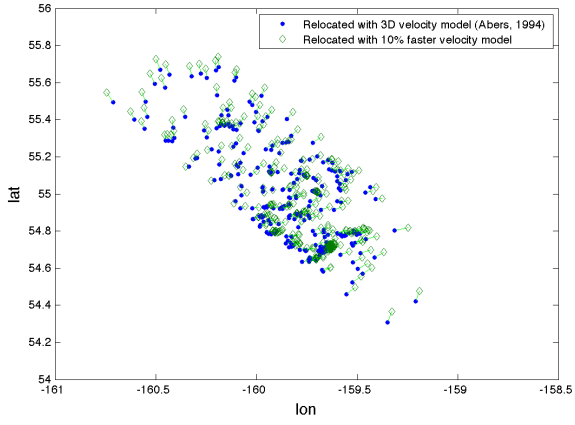
Change in location, map view
Segment 5
Relocated with 3D velocity model (Abers, 1994)
Relocated with 10% faster velocity model
lat
lon
56
55.8
55.6
55.4
55.2
55
54.8
54.6
54.4
54.2
54
-161
-160.5
-160
-159.5
-159
-158.5

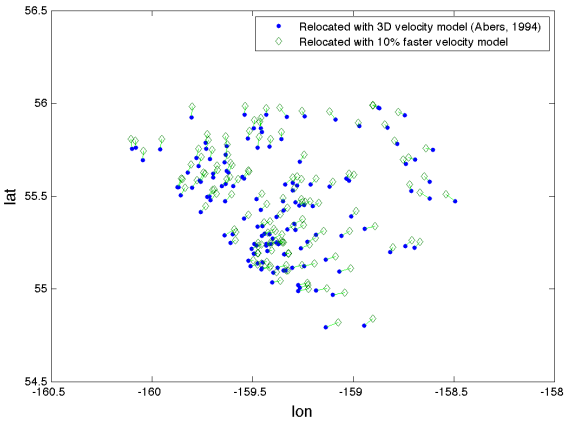
Change in location, map view
Segment 6
Relocated with 3D velocity model (Abers, 1994)
Relocated with 10% faster velocity model
lat
lon
56.5
56
55.5
55
54.5
-160.5
-160
-159.5
-159
-158.5
-158

II. Cross-section with vertical changes in locations 10% faster velocity model for Segments 1 – 6

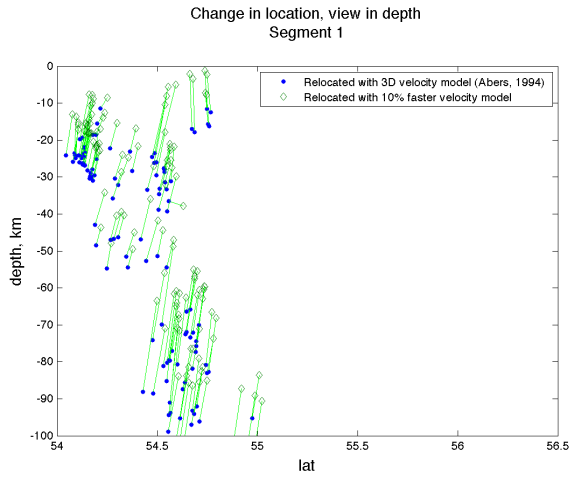
Change in location, view in depth
Segment 1
Relocated with 3D velocity model (Abers, 1994)
Relocated with 10% faster velocity model
depth, km
lat

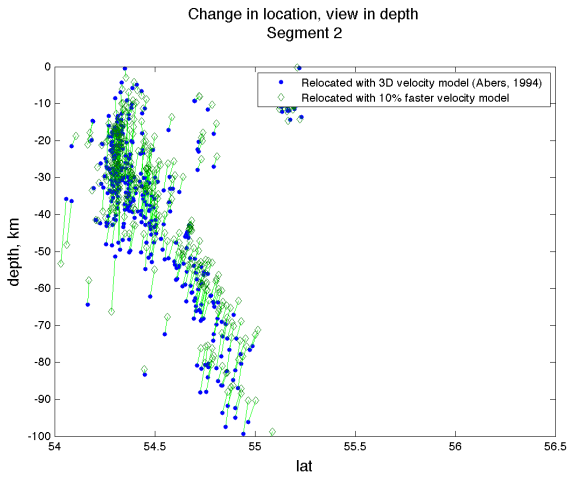
Change in location, view in depth
Segment 2
Relocated with 3D velocity model (Abers, 1994)
Relocated with 10% faster velocity model
depth, km
lat

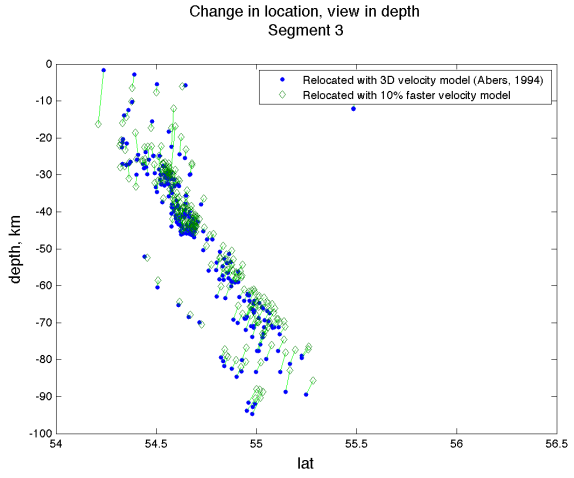
Change in location, view in depth
Segment 3
Relocated with 3D velocity model (Abers, 1994)
Relocated with 10% faster velocity model
depth, km
lat

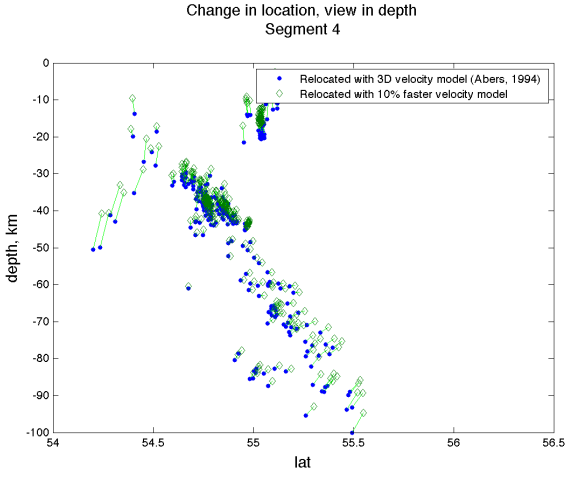
Change in location, view in depth
Segment 4
Relocated with 3D velocity model (Abers, 1994)
Relocated with 10% faster velocity model
depth, km
lat

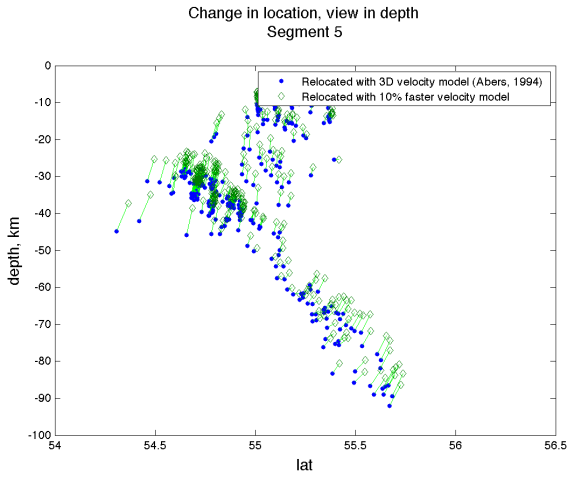
Change in location, view in depth
Segment 5
Relocated with 3D velocity model (Abers, 1994)
Relocated with 10% faster velocity model
depth, km
lat

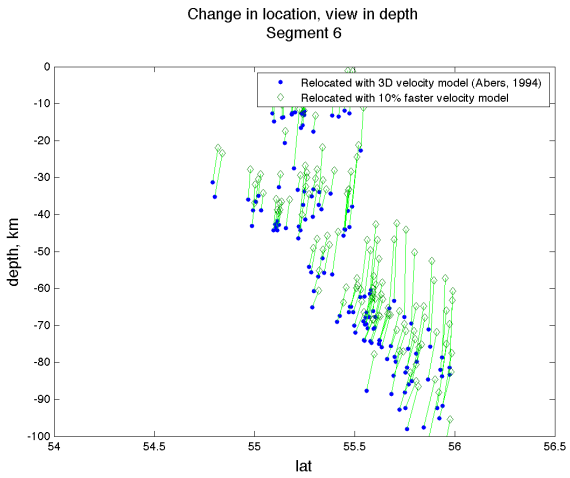
Change in location, view in depth
Segment 6
Relocated with 3D velocity model (Abers, 1994)
Relocated with 10% faster velocity model
depth, km
lat

III. Histograms of the total distances of location change from 10% faster velocity model for Segments 1 – 6

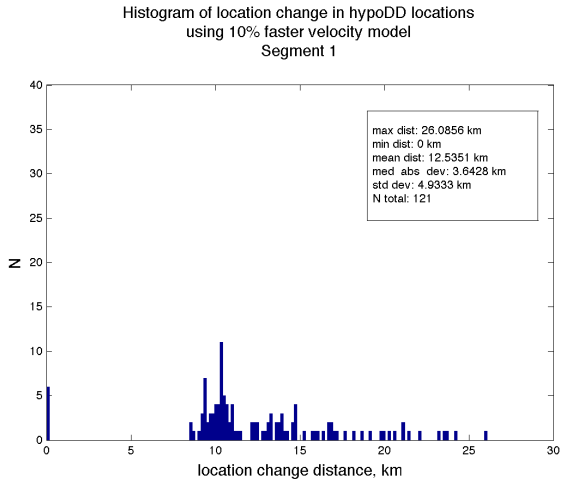
Histogram of location change in hypoDD locations
using 10% faster velocity model
Segment 1
max dist: 26.0856 km
min dist: 0 km
mean dist: 12.5351 km
med abs dev: 3.6428 km
std dev: 4.9333 km
N total: 121
N
location change distance, km

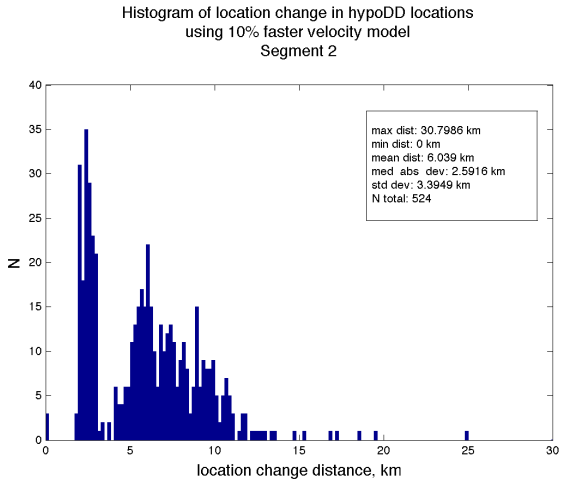
Histogram of location change in hypoDD locations
using 10% faster velocity model
Segment 2
max dist: 30.7986 km
min dist: 0 km
mean dist: 6.039 km
med abs dev: 2.5916 km
std dev: 3.3949 km
N total: 524
N
location change distance, km

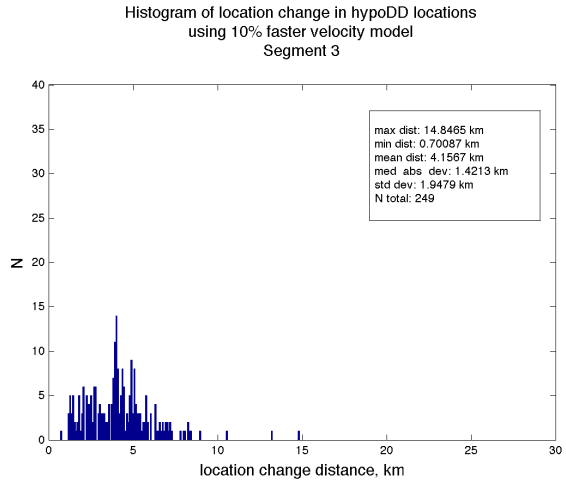
Histogram of location change in hypoDD locations
using 10% faster velocity model
Segment 3
max dist: 14.8465 km
min dist: 0.70087 km
mean dist: 4.1567 km
med abs dev: 1.4213 km
std dev: 1.9479 km
N total: 249
N
location change distance, km

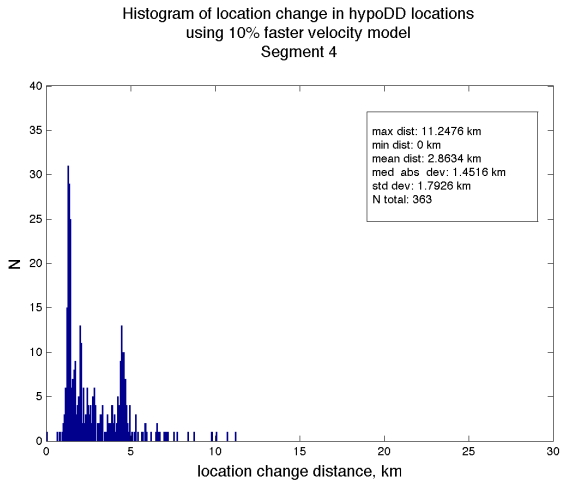
Histogram of location change in hypoDD locations
using 10% faster velocity model
Segment 4
max dist: 11.2476 km
min dist: 0 km
mean dist: 2.8634 km
med abs dev: 1.4516 km
std dev: 1.7926 km
N total: 363
N
location change distance, km

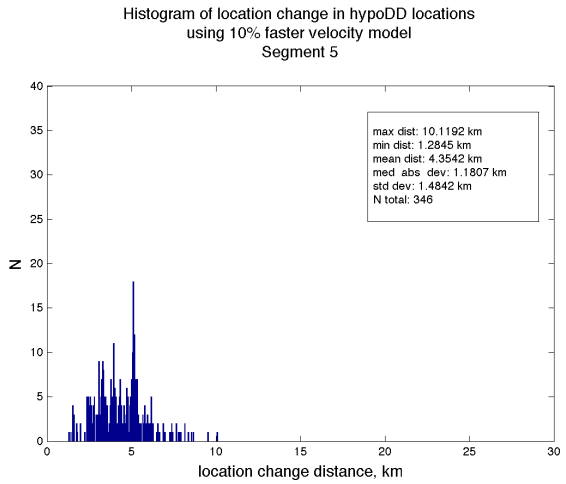
Histogram of location change in hypoDD locations
using 10% faster velocity model
Segment 5
max dist: 10.1192 km
min dist: 1.2845 km
mean dist: 4.3542 km
med abs dev: 1.1807 km
std dev: 1.4842 km
N total: 346
N
location change distance, km

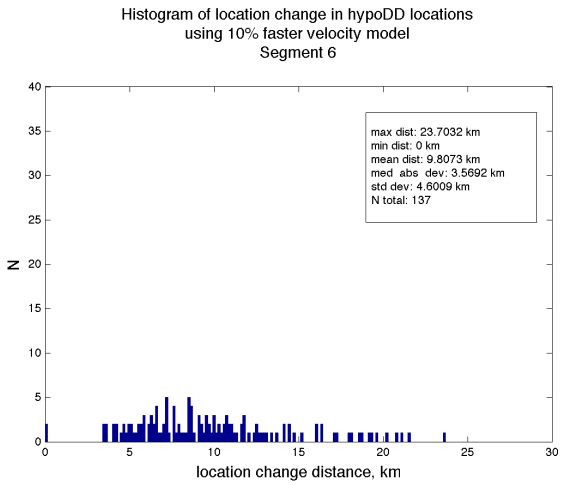
Histogram of location change in hypoDD locations
using 10% faster velocity model
Segment 6
max dist: 23.7032 km
min dist: 0 km
mean dist: 9.8073 km
med abs dev: 3.5692 km
std dev: 4.6009 km
N total: 137
N
location change distance, km

IV. Histograms of the horizontal distances of location change 10% faster velocity model for Segments 1 – 6

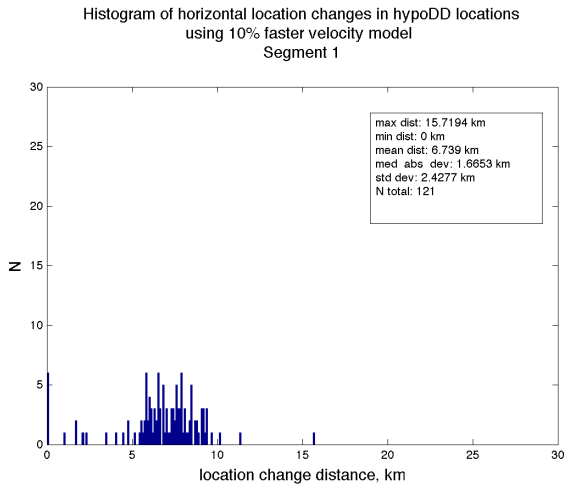
Histogram of horizontal location changes in hypoDD locations
using 10% faster velocity model
Segment 1
max dist: 15.7194 km
min dist: 0 km
mean dist: 6.739 km
med abs dev: 1.6653 km
std dev: 2.4277 km
N total: 121
N
location change distance, km

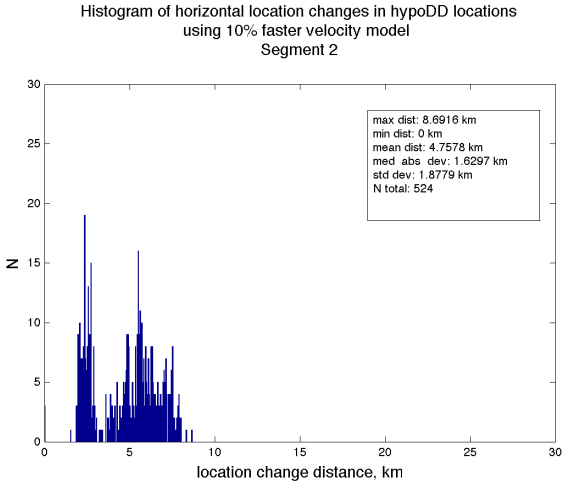
Histogram of horizontal location changes in hypoDD locations
using 10% faster velocity model
Segment 2
max dist: 8.6916 km
min dist: 0 km
mean dist: 4.7578 km
med abs dev: 1.6297 km
std dev: 1.8779 km
N total: 524
N
location change distance, km

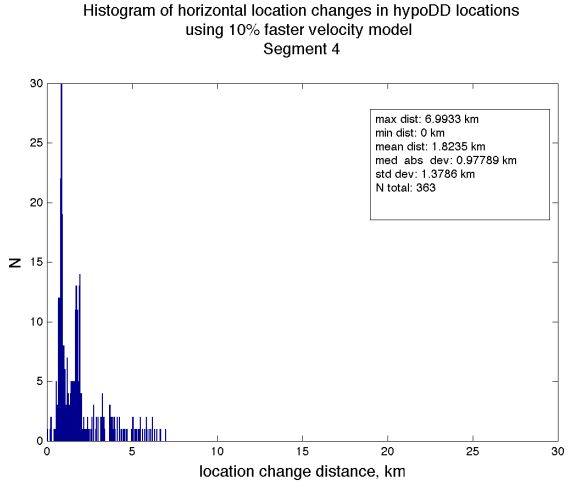
Histogram of horizontal location changes in hypoDD locations
using 10% faster velocity model
Segment 4
max dist: 6.9933 km
min dist: 0 km
mean dist: 1.8235 km
med abs dev: 0.97789 km
std dev: 1.3786 km
N total: 363
N
location change distance, km

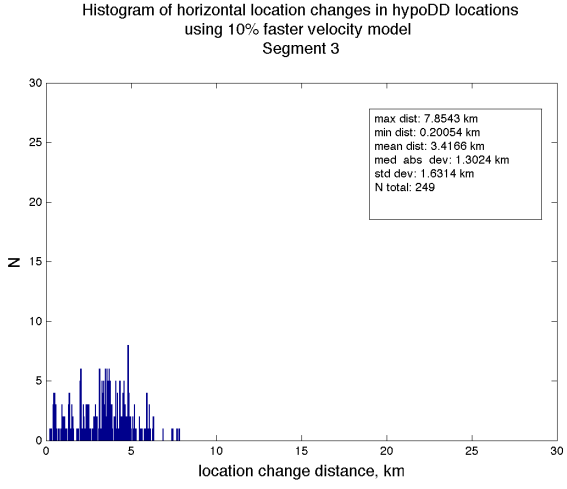
Histogram of horizontal location changes in hypoDD locations
using 10% faster velocity model
Segment 3
max dist: 7.8543 km
min dist: 0.20054 km
mean dist: 3.4166 km
med abs dev: 1.3024 km
std dev: 1.6314 km
N total: 249
N
location change distance, km

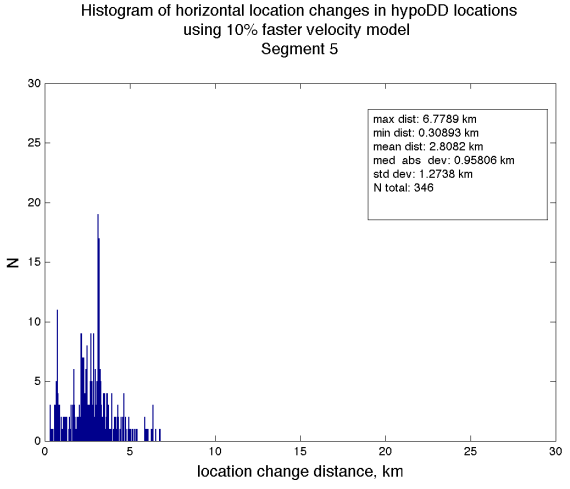
Histogram of horizontal location changes in hypoDD locations
using 10% faster velocity model
Segment 5
max dist: 6.7789 km
min dist: 0.30893 km
mean dist: 2.8082 km
med abs dev: 0.95806 km
std dev: 1.2738 km
N total: 346
N
location change distance, km

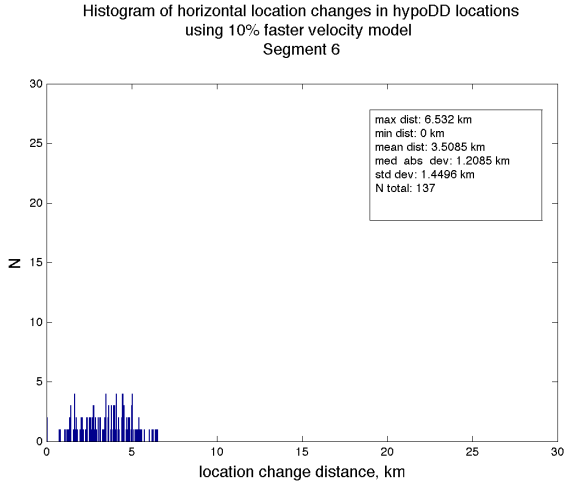
Histogram of horizontal location changes in hypoDD locations
using 10% faster velocity model
Segment 6
max dist: 6.532 km
min dist: 0 km
mean dist: 3.5085 km
med abs dev: 1.2085 km
std dev: 1.4496 km
N total: 137
N
location change distance, km

V. Histograms of the vertical distances of location change from 10% faster velocity model output for Segments 1 – 6

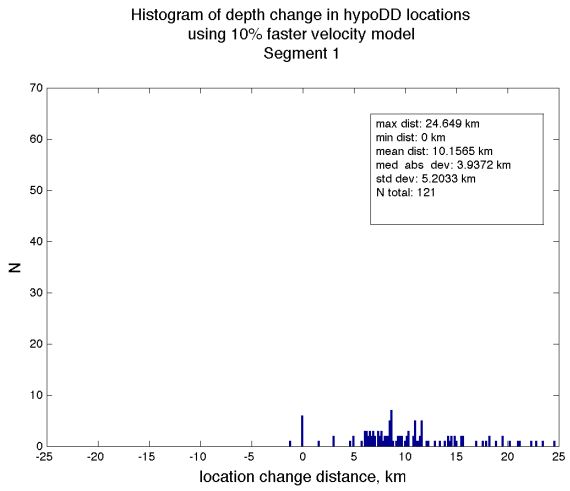
Histogram of depth change in hypoDD locations
using 10% faster velocity model
Segment 1
max dist: 24.649 km
min dist: 0 km
mean dist: 10.1565 km
med abs dev: 3.9372 km
std dev: 5.2033 km
N total: 121
N
location change distance, km

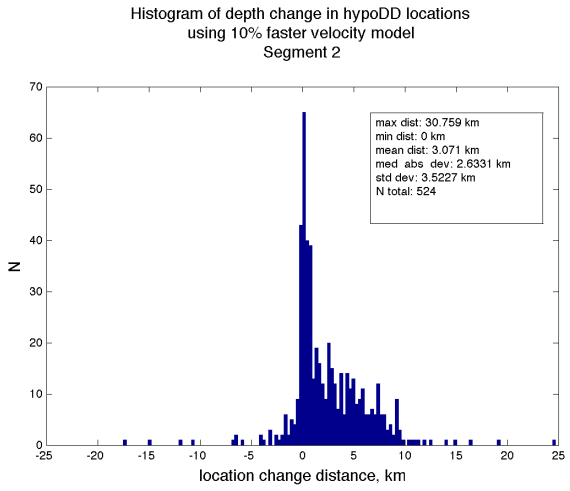
Histogram of depth change in hypoDD locations
using 10% faster velocity model
Segment 2
max dist: 30.759 km
min dist: 0 km
mean dist: 3.071 km
med abs dev: 2.6331 km
std dev: 3.5227 km
N total: 524
N
location change distance, km

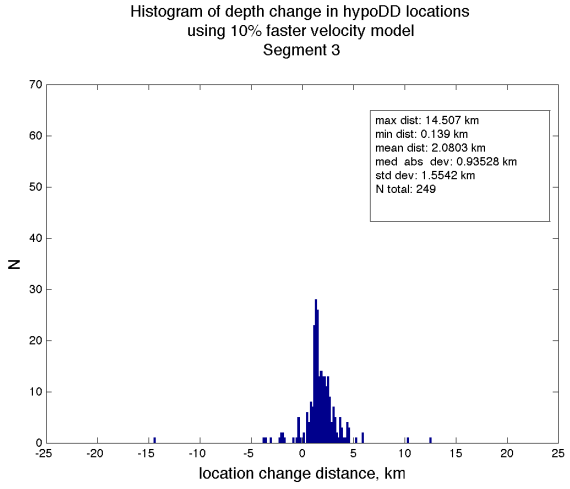
Histogram of depth change in hypoDD locations
using 10% faster velocity model
Segment 3
max dist: 14.507 km
min dist: 0.139 km
mean dist: 2.0803 km
med abs dev: 0.93528 km
std dev: 1.5542 km
N total: 249
N
location change distance, km

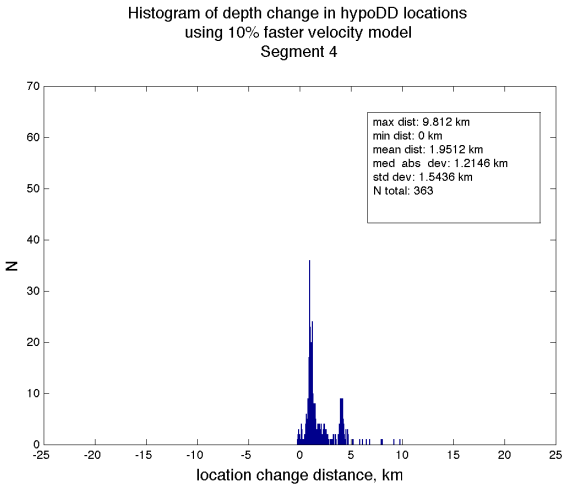
Histogram of depth change in hypoDD locations
using 10% faster velocity model
Segment 4
max dist: 9.812 km
min dist: 0 km
mean dist: 1.9512 km
med abs dev: 1.2146 km
std dev: 1.5436 km
N total: 363
N
location change distance, km

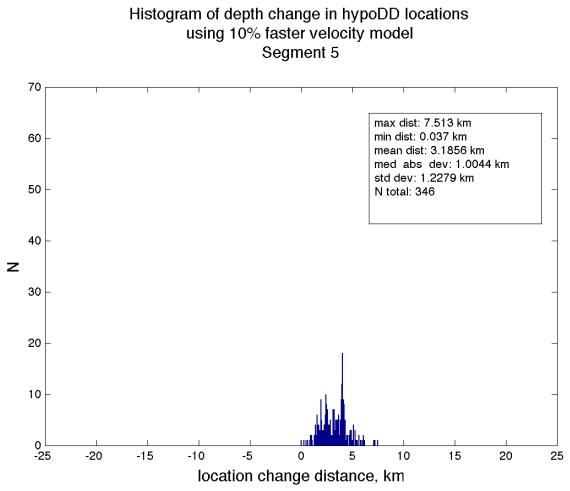
Histogram of depth change in hypoDD locations
using 10% faster velocity model
Segment 5
max dist: 7.513 km
min dist: 0.037 km
mean dist: 3.1856 km
med abs dev: 1.0044 km
std dev: 1.2279 km
N total: 346
N
location change distance, km

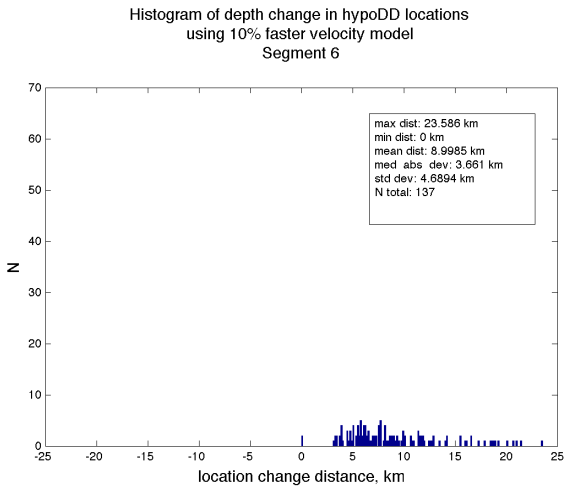
Histogram of depth change in hypoDD locations
using 10% faster velocity model
Segment 6
max dist: 23.586 km
min dist: 0 km
mean dist: 8.9985 km
med abs dev: 3.661 km
std dev: 4.6894 km
N total: 137
N
location change distance, km

APPENDIX D

Velocity Model 10% Slower

Plots and histograms for Segments 1 – 6

I. Map view showing horizontal change in locations from 10% slower velocity model for Segments 1 – 6

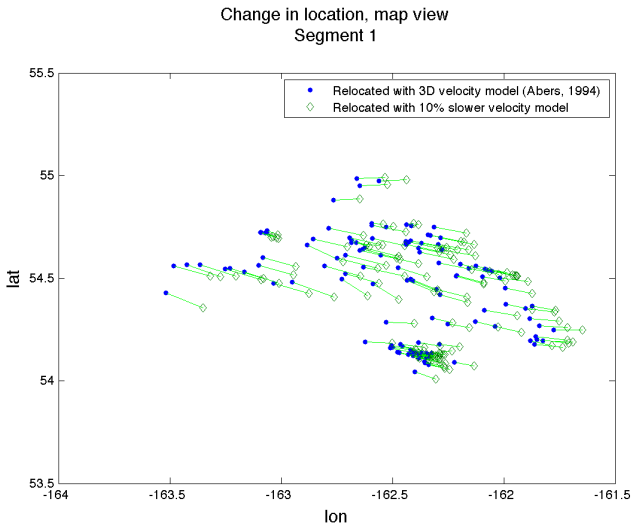
Change in location, map view
Segment 1
Relocated with 3D velocity model (Abers, 1994)
Relocated with 10% slower velocity model
lat
lon
55.5
55
54.5
54
53.5
-164
-163.5
-163
-162.5
-162
-161.5

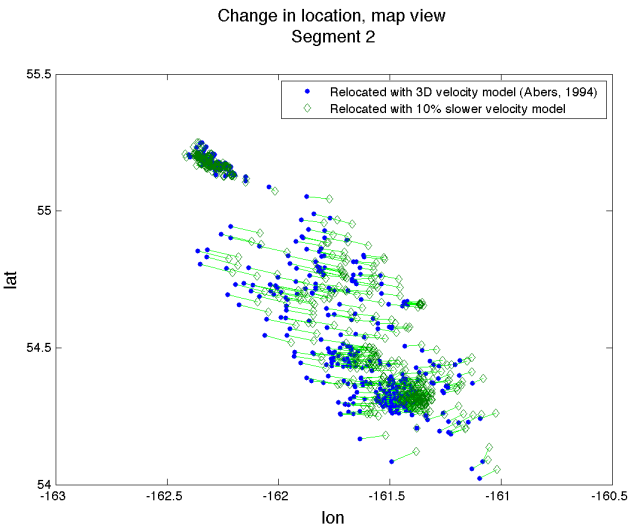
Change in location, map view
Segment 2
Relocated with 3D velocity model (Abers, 1994)
Relocated with 10% slower velocity model
lat
lon
55.5
55
54.5
54
-163
-162.5
-162
-161.5
-161
-160.5

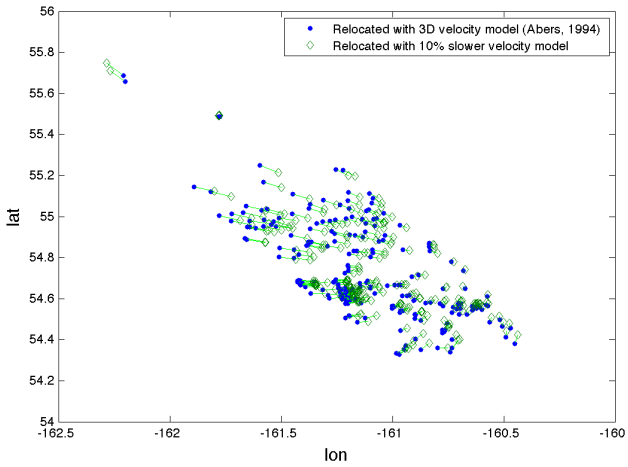
Change in location, map view
Segment 3
Relocated with 3D velocity model (Abers, 1994)
Relocated with 10% slower velocity model
lat
lon
56
55.8
55.6
55.4
55.2
55
54.8
54.6
54.4
54.2
54
-162.5
-162
-161.5
-161
-160.5
-160

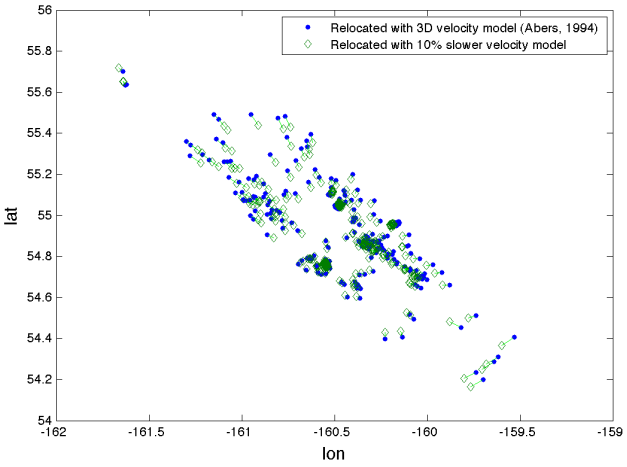
Change in location, map view
Segment 4
Relocated with 3D velocity model (Abers, 1994)
Relocated with 10% slower velocity model
lat
lon
56
55.8
55.6
55.4
55.2
55
54.8
54.6
54.4
54.2
54
-162
-161.5
-161
-160.5
-160
-159.5
-159

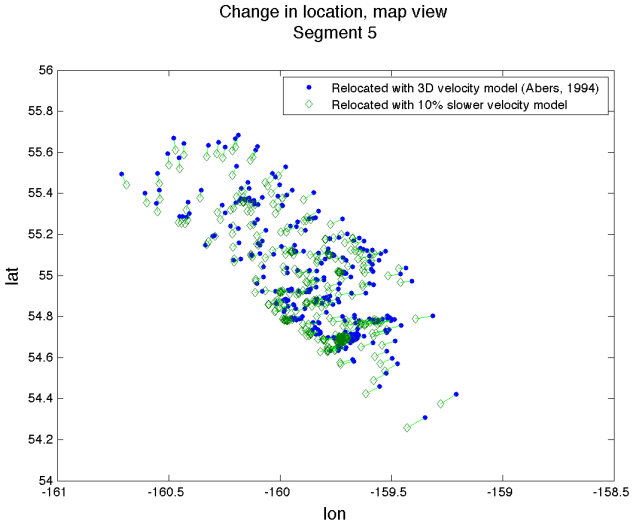
Change in location, map view
Segment 5
Relocated with 3D velocity model (Abers, 1994)
Relocated with 10% slower velocity model
lat
lon
56
55.8
55.6
55.4
55.2
55
54.8
54.6
54.4
54.2
54
-161
-160.5
-160
-159.5
-159
-158.5

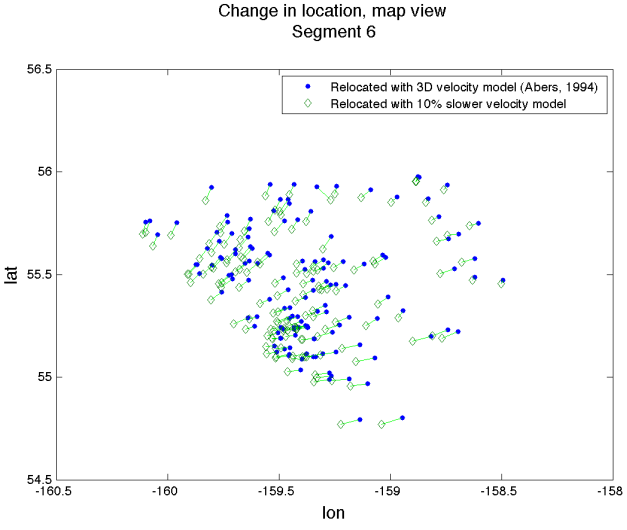
Change in location, map view
Segment 6
Relocated with 3D velocity model (Abers, 1994)
Relocated with 10% slower velocity model
lat
lon
56.5
56
55.5
55
54.5
-160.5
-160
-159.5
-159
-158.5
-158

II. Cross-section with vertical changes in locations 10% slower velocity model for Segments 1 – 6

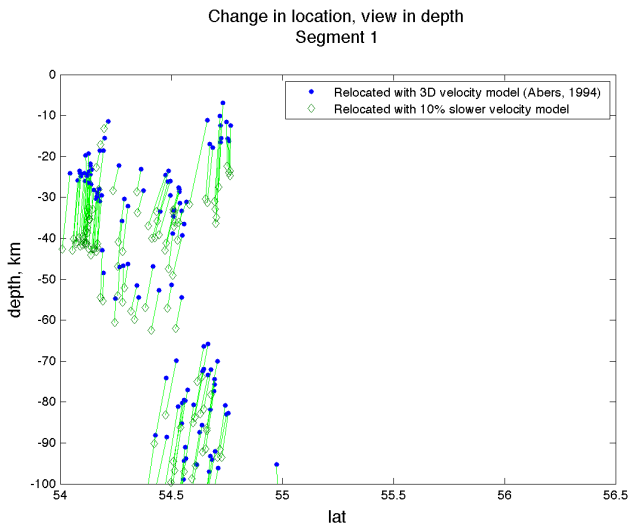
Change in location, view in depth
Segment 1
Relocated with 3D velocity model (Abers, 1994)
Relocated with 10% slower velocity model
depth, km
lat

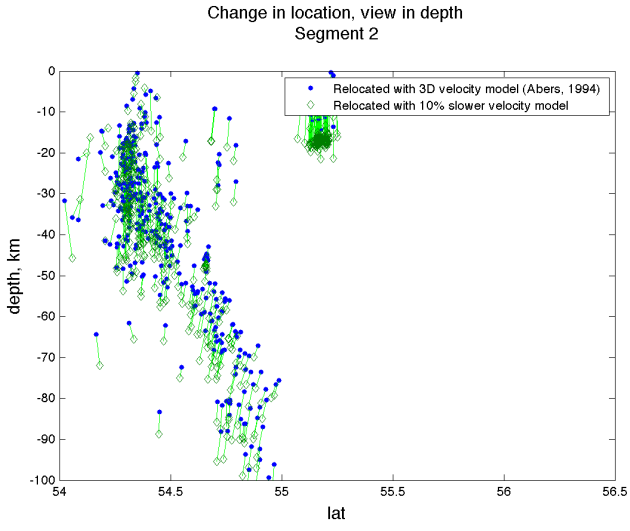
Change in location, view in depth
Segment 2
Relocated with 3D velocity model (Abers, 1994)
Relocated with 10% slower velocity model
depth, km
lat

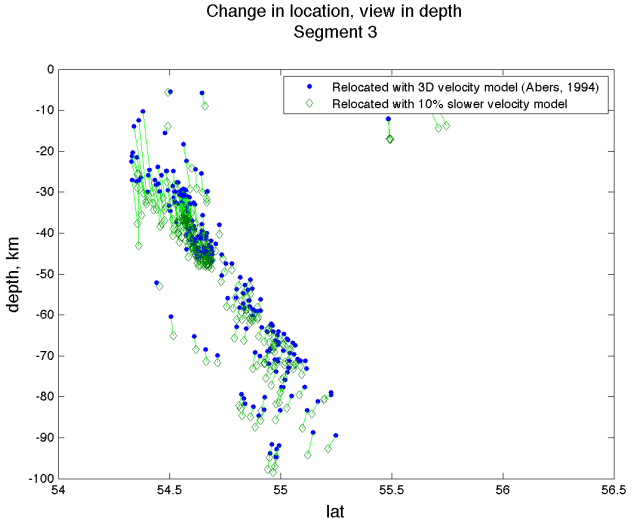
Change in location, view in depth
Segment 3
Relocated with 3D velocity model (Abers, 1994)
Relocated with 10% slower velocity model
depth, km
lat

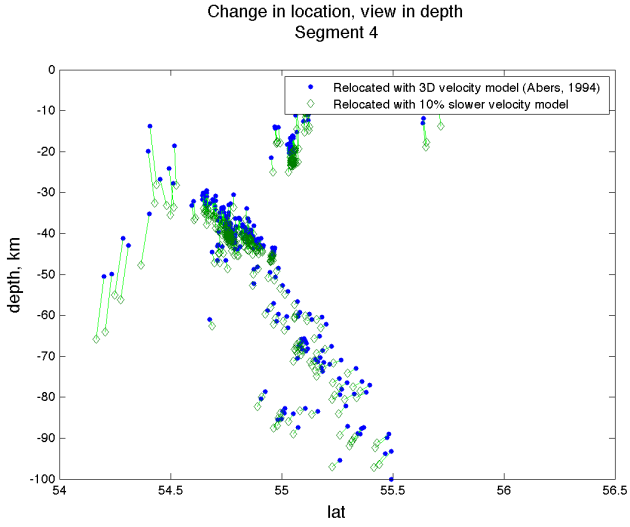
Change in location, view in depth
Segment 4
Relocated with 3D velocity model (Abers, 1994)
Relocated with 10% slower velocity model
depth, km
lat

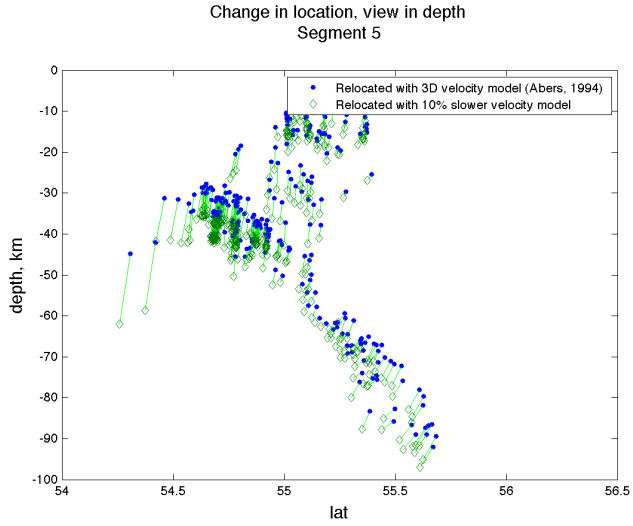
Change in location, view in depth
Segment 5
Relocated with 3D velocity model (Abers, 1994)
Relocated with 10% slower velocity model
depth, km
lat

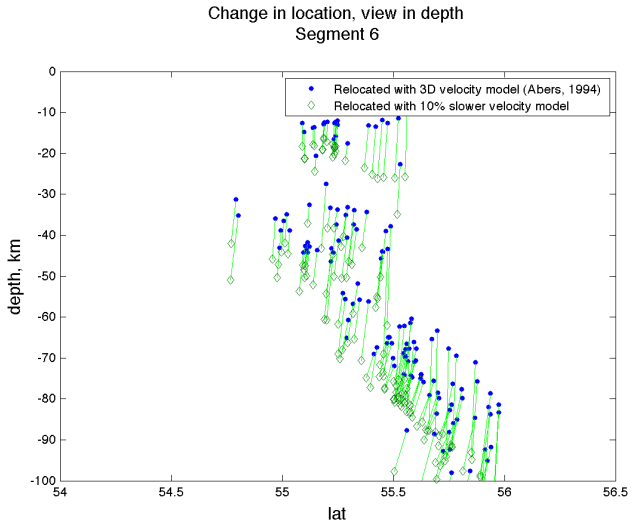
Change in location, view in depth
Segment 6
Relocated with 3D velocity model (Abers, 1994)
Relocated with 10% slower velocity model
depth, km
lat

III. Histograms of the total distances of location change from 10% slower velocity model for Segments 1 – 6

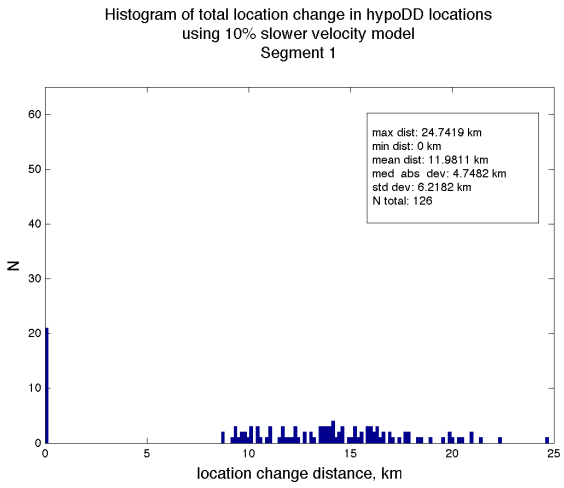
Histogram of total location change in hypoDD locations
using 10% slower velocity model
Segment 1
max dist: 24.7419 km
min dist: 0 km
mean dist: 11.9811 km
med abs dev: 4.7482 km
std dev: 6.2182 km
N total: 126
N
location change distance, km

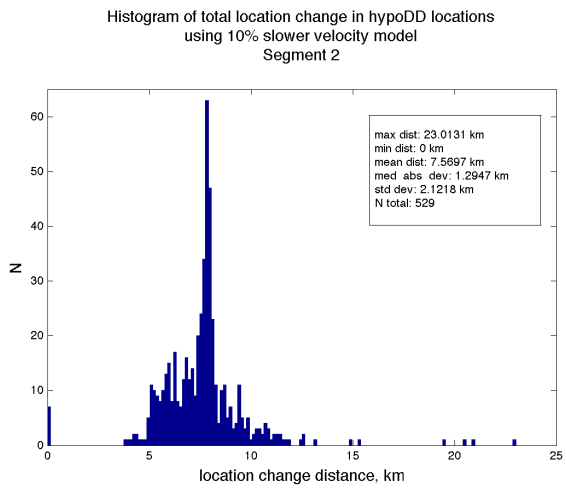
Histogram of total location change in hypoDD locations
using 10% slower velocity model
Segment 2
max dist: 23.0131 km
min dist: 0 km
mean dist: 7.5697 km
med abs dev: 1.2947 km
std dev: 2.1218 km
N total: 529
N
location change distance, km

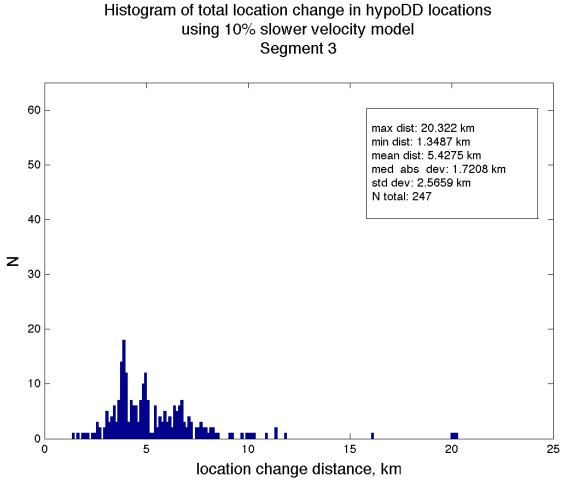
Histogram of total location change in hypoDD locations
using 10% slower velocity model
Segment 3
max dist: 20.322 km
min dist: 1.3487 km
mean dist: 5.4275 km
med abs dev: 1.7208 km
std dev: 2.5659 km
N total: 247
N
location change distance, km

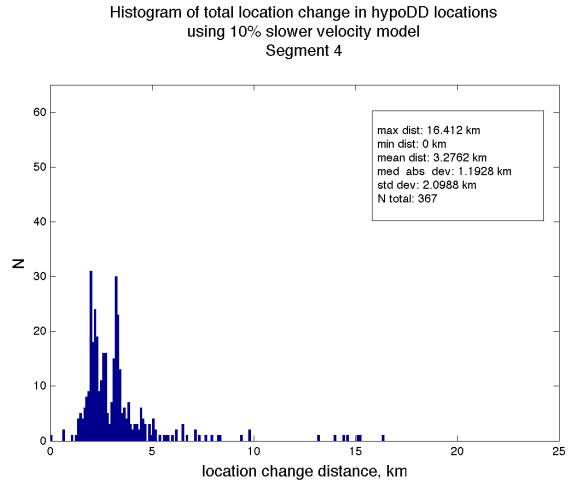
Histogram of total location change in hypoDD locations
using 10% slower velocity model
Segment 4
max dist: 16.412 km
min dist: 0 km
mean dist: 3.2762 km
med abs dev: 1.1928 km
std dev: 2.0988 km
N total: 367
N
location change distance, km

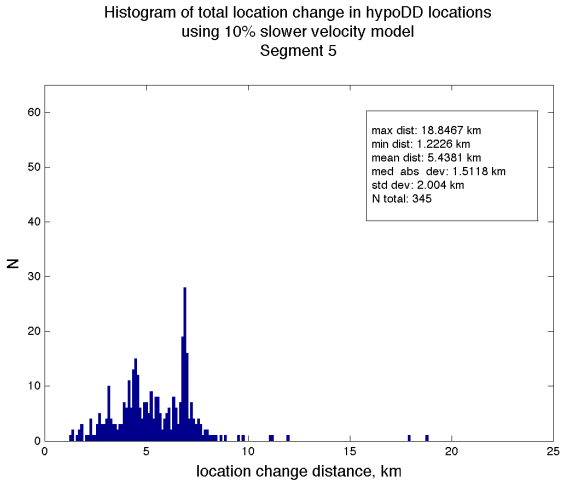
Histogram of total location change in hypoDD locations
using 10% slower velocity model
Segment 5
max dist: 18.8467 km
min dist: 1.2226 km
mean dist: 5.4381 km
med abs dev: 1.5118 km
std dev: 2.004 km
N total: 345
N
location change distance, km

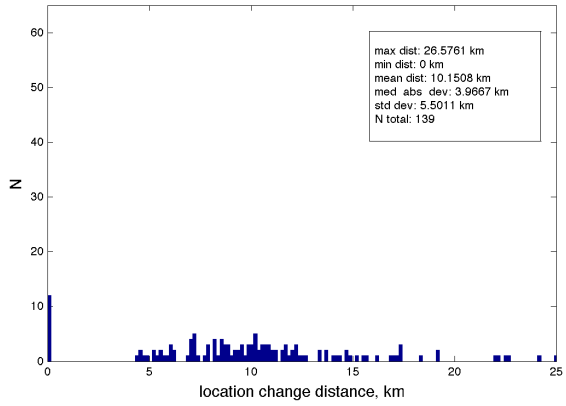
Histogram of total location change in hypoDD locations
using 10% slower velocity model
Segment 6
max dist: 26.5761 km
min dist: 0 km
mean dist: 10.1508 km
med abs dev: 3.9667 km
std dev: 5.5011 km
N total: 139
N
location change distance, km

IV. Histograms of the horizontal distances of location change 10% slower velocity model for Segments 1 – 6

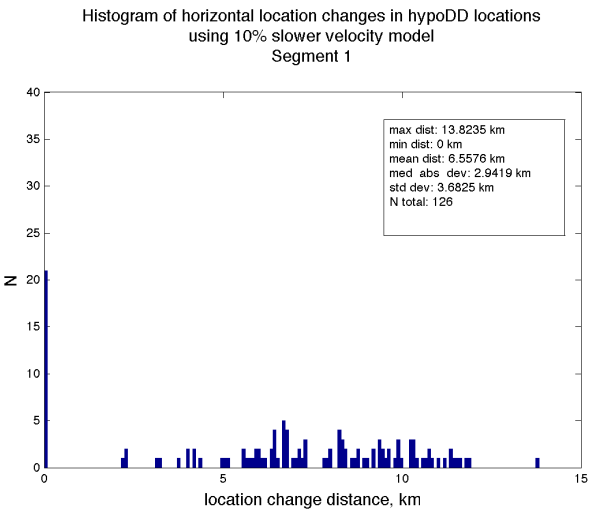
Histogram of horizontal location changes in hypoDD locations
using 10% slower velocity model
Segment 1
max dist: 13.8235 km
min dist: 0 km
mean dist: 6.5576 km
med abs dev: 2.9419 km
std dev: 3.6825 km
N total: 126
N
location change distance, km

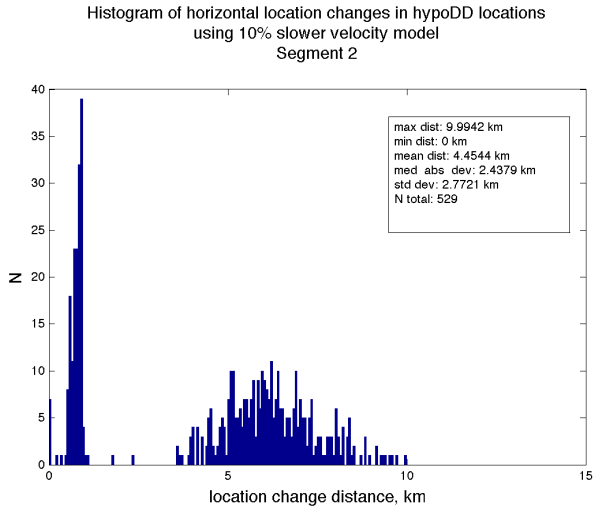
Histogram of horizontal location changes in hypoDD locations
using 10% slower velocity model
Segment 2
max dist: 9.9942 km
min dist: 0 km
mean dist: 4.4544 km
med abs dev: 2.4379 km
std dev: 2.7721 km
N total: 529
N
location change distance, km

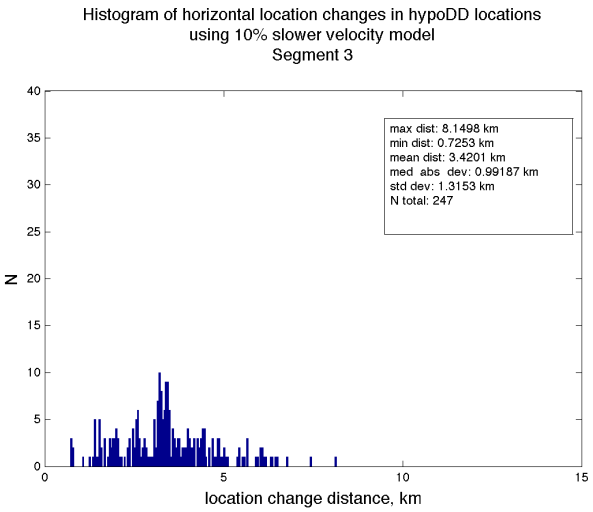
Histogram of horizontal location changes in hypoDD locations
using 10% slower velocity model
Segment 3
max dist: 8.1498 km
min dist: 0.7253 km
mean dist: 3.4201 km
med abs dev: 0.99187 km
std dev: 1.3153 km
N total: 247
N
location change distance, km

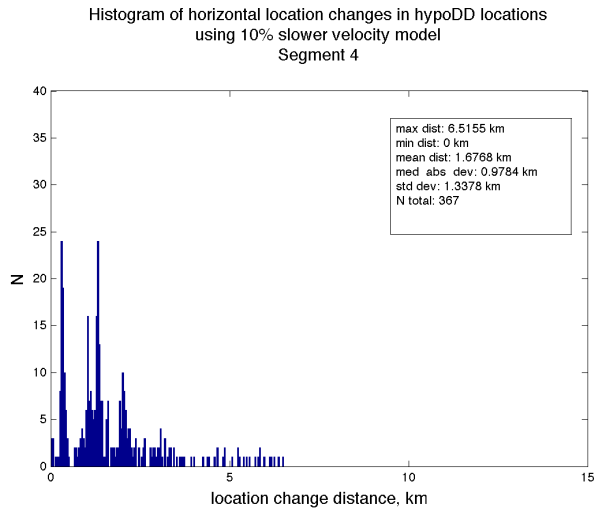
Histogram of horizontal location changes in hypoDD locations
using 10% slower velocity model
Segment 4
max dist: 6.5155 km
min dist: 0 km
mean dist: 1.6768 km
med abs dev: 0.9784 km
std dev: 1.3378 km
N total: 367
N
location change distance, km

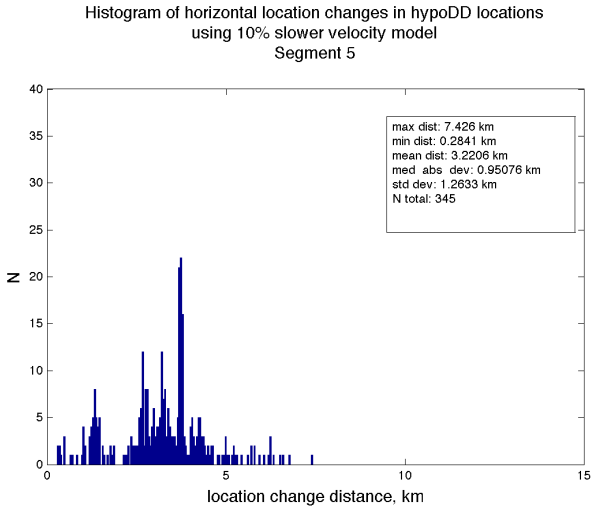
Histogram of horizontal location changes in hypoDD locations
using 10% slower velocity model
Segment 5
max dist: 7.426 km
min dist: 0.2841 km
mean dist: 3.2206 km
med abs dev: 0.95076 km
std dev: 1.2633 km
N total: 345
N
location change distance, km

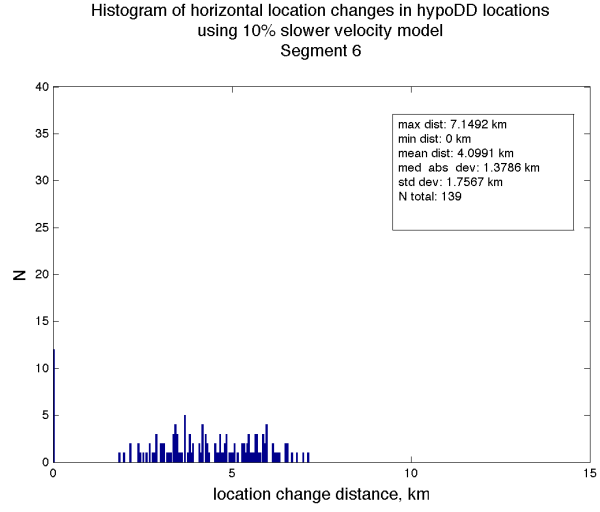
Histogram of horizontal location changes in hypoDD locations
using 10% slower velocity model
Segment 6
max dist: 7.1492 km
min dist: 0 km
mean dist: 4.0991 km
med abs dev: 1.3786 km
std dev: 1.7567 km
N total: 139
N
location change distance, km

V. Histograms of the vertical distances of location change from 10% slower velocity model output for Segments 1 – 6

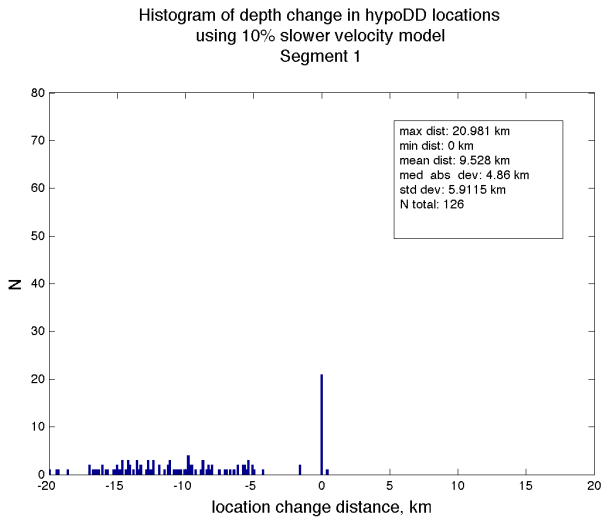
Histogram of depth change in hypoDD locations
using 10% slower velocity model
Segment 1
max dist: 20.981 km
min dist: 0 km
mean dist: 9.528 km
med abs dev: 4.86 km
std dev: 5.9115 km
N total: 126
N
location change distance, km

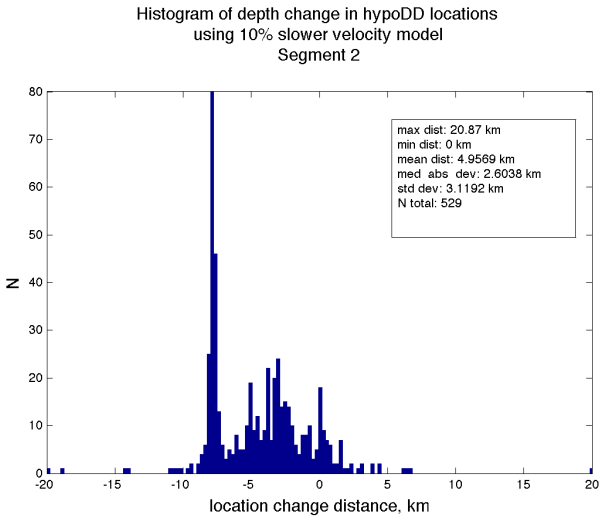
Histogram of depth change in hypoDD locations
using 10% slower velocity model
Segment 2
max dist: 20.87 km
min dist: 0 km
mean dist: 4.9569 km
med abs dev: 2.6038 km
std dev: 3.1192 km
N total: 529
N
location change distance, km

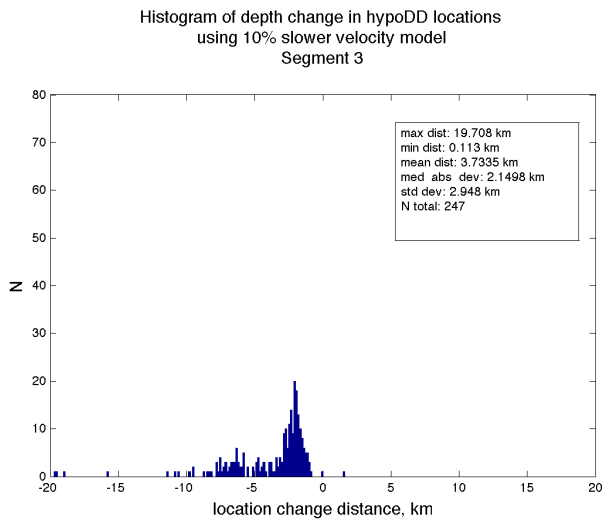
Histogram of depth change in hypoDD locations
using 10% slower velocity model
Segment 3
max dist: 19.708 km
min dist: 0.113 km
mean dist: 3.7335 km
med abs dev: 2.1498 km
std dev: 2.948 km
N total: 247
N
location change distance, km

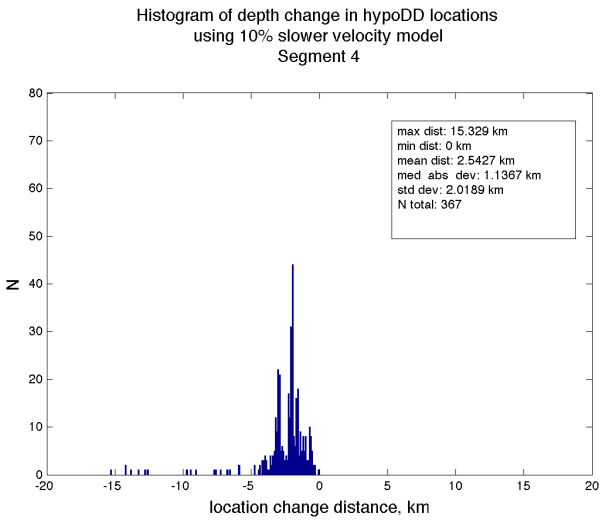
Histogram of depth change in hypoDD locations
using 10% slower velocity model
Segment 4
max dist: 15.329 km
min dist: 0 km
mean dist: 2.5427 km
med abs dev: 1.1367 km
std dev: 2.0189 km
N total: 367
N
location change distance, km

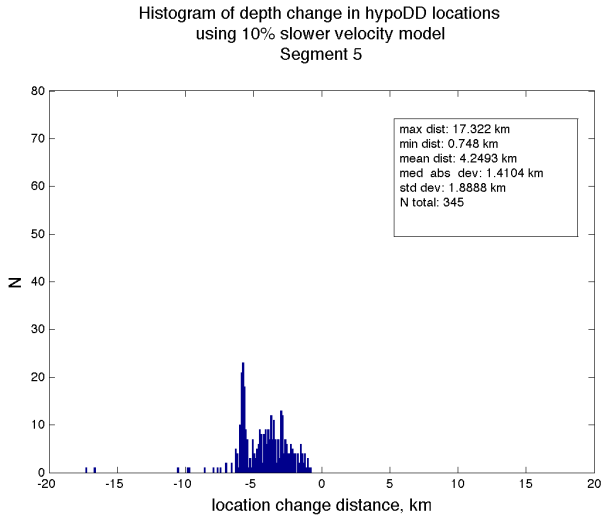
Histogram of depth change in hypoDD locations
using 10% slower velocity model
Segment 5
max dist: 17.322 km
min dist: 0.748 km
mean dist: 4.2493 km
med abs dev: 1.4104 km
std dev: 1.8888 km
N total: 345
N
location change distance, km

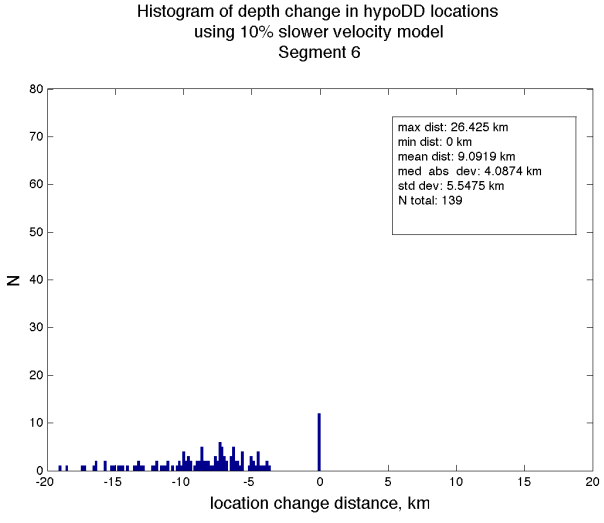
Histogram of depth change in hypoDD locations
using 10% slower velocity model
Segment 6
max dist: 26.425 km
min dist: 0 km
mean dist: 9.0919 km
med abs dev: 4.0874 km
std dev: 5.5475 km
N total: 139
N
location change distance, km

Citations

Abers, G.A., 1992, Relationship between shallow- and intermediate-depth seismicity in the eastern Aleutian subduction zone, *Geophys. Res. Lett.,* 19, 2019-2022.

Abers, G.A., 1994. Three-dimensional inversion of regional P and S arrival times in the East Aleutians and sources of subduction zone gravity highs, *J. Geophys. Res.* 99, 4395-4412.

Abers, G.A., J. Beavan, S. Horton, S. Jaume, and E. Triep, 1995a. Large accelerations and tectonic setting of the May 1993 Shumagin Islands earthquake sequence*, Bull. Seismol. Soc. Am.* 85, 1730-1738.

Abers, G.A., X. Hu, and L.R. Sykes, 1995b. Source scaling of earthquakes in the Shumagin region, Alaska: time-domain deconvolution of regional waveforms, *Geophys. J. Int.* 123, 41-58.

Amante, C. and B.W. Eakins, 2009. ETOPO1 1 Arc-Minute Global Relief Model: Procedures, Data Sources and Analysis. NOAA Technical Memorandum NESDIS NGDC-24. National Geophysical Data Center, NOAA. doi:10.7289/V5C8276M [accessed February 2016]

Bécel, A., Shillington, D.J., Nazimova, M.R., Webb, S.C., and H. Kuehn, 2015. Origin of dipping structures in fast-spreading oceanic lower crust offshore Alaska imaged by multichannel seismic data, *Earth and Planetary Sc. Let*., 424, 26-37.

Bécel, A., Shillington, D.J., Delescluse, M., Nedimović, M.R., Abers, G.A., Saffer, D.M., Webb, S.C., Keranen, K.M., Roche, H.-P., Li, J., and H. Kuehn, 2017. Tsunamigenic structures in a creeping section of the Alaska subduction zone, *Nature Geoscience, in review.*

Boyd, T. M., J.J. Taber, A. L. Lerner-Lam, and J. Beavan, 1988. Seismic rupture and arc segmentation within the Shumagin Islands seismic gap, Alaska, *Geophys. Res. Lett.,* 15, 201-204.

Bruns, T.R., von Huene, R., Culotta, R.D., and S.D. Lewis, 1985, Summary geologic report for the Shumagin Outer Continental Shelf (OCS) planning area, Alaska: U.S. Geological Survey Open-File Report 85-32, 58 p.

Bruns, T. and P. Carlson, 1987. Geology and petroleum potential of the southeast (Alaska) continental margin. Circum-Pacific Council for Energy and Mineral Resources 2009 – Geology and Resource Potential of the Western North America and Adjacent Ocean Basins--Beaufort Sea to Baja California, Chapter eight, Volume 6, 1987.

Bufe, C.G., Nishenko, S.P., and D.J. Varnes, 1994. Seismicity trends and potential for large earthquakes in the Alaska-Aleutian region, *Pure and Applied Geophysics*, 142 (1), 83-99.

Davies, J.N., and L.S. House, 1979. Aleutian subduction zone seismicity, volcano-trench

separation and their relation to great thrust-type earthquakes, *J. Geophys. Res.,* 84, 4583-4591.

Davies, J., Sykes, L., House, L., and K. Jacob 1981, Shumagin Seismic Gap, Alaska Peninsula: History of Great Earthquakes, Tectonic Setting, and Evidence for High Seismic Potential*, J. Geophys. Res.,* 86, 3821-3855.

Deichmann, N., and M. Garcia-Fernandez, 1992. Rupture geometry from high-precision relative hypocenter locations of microearthquake clusters, *Geophys. J. Int.* 110, 501-517.

DeMets, C., R.G. Gordon, D.F. Argus, and S. Stein, 1994. Effect of recent revisions to the geomagnetic reversal time scale on estimates of current plate motions, *Geophys. Res. Lett.*, 21, 2191-2194.

Dodge, D.A., G.C. Beroza, and W.L. Ellsworth, 1995. Foreshock sequence of the 1992 Landers, California earthquake and its implications for earthquake nucleation, *J. Geophys. Res.* 100, 9865–9880.

Dunn, M., Horton, S., DeShon, H., and C. Powell, 2010, High-resolution Earthquake Relocation in the New Madrid Seismic Zone*, Seis. Res. Lett*. 81 (2), 406-413. doi: 10.1785/gssrl.81.2.406

Estabrook, C.H. and T.M. Boyd, 1992. The Shumagin Islands, Alaska earthquake of May 31, 1917, *Bull. Seism. Soc. Am*., 82, 755-773.

Fournier, T.J., and J.T. Freymueller, 2007, Transition from locked to creeping subduction in the Shumagin region, Alaska*, Geophys. Res. Lett.,* 34 (L06303), doi: 06310.01029/02006GL029073.

Fréchet, J., 1985. Sismogenèse et doublets sismiques, Thèse d'Etat, Université Scientifique et Médicale de Grenoble, 206 pp.

Frémont, M.-J., and S.D. Malone 1987. High precision relative locations of earthquakes at Mount St. Helens, Washington, *J. Geophys. Res*. 92 (10), 233–10,236.

French, S.W., Warren, L.M., Fischer, K.M., Abers, G.A., Strauch, W., Porti, J.M., and V. Gonzalez, 2010. Constraints on upper plate deformation in the Nicaraguan subduction zone from earthquake relocation and directivity analysis, *Geochem. Geophys. Geosyst.*, 11 (3), Q03S20, doi:10.1029/2009GC002841

Freymueller, J.T., Woodard, H., Cohen, S.C., Cross, R., Elliott, J., Larsen, C.F., Hreinsdottir, S., and C. Zweck, 2008. Active Deformation Processes in Alaska, Based on 15 Years of GPS Measurements, in Active Tectonics and Seismic Potential of Alaska, Geophysical Monograph Series, edited by J. T. Freymueller, *et al*., pp. 1-42, AGU.

Fuchs, V., 1982. *Of Ice and Men: The Story of the British Antarctic Survey 1943-73*. Nelson, 383 pp.

Geller, R.J. and C.S. Mueller, 1980. Four similar earthquakes in central California, *Geophys.*

Res. Lett., 7 (10), 821-824.

Got, J.-L., Frechet, J., and F.W. Klein, 1994. Deep fault plane geometry inferred from multiplet relative relocation beneath the south flank of Kilauea, *J. Geophys. Res.,* 99 (B8), 15375 - 15386.

Hauksson, E., and P. Shearer, 2005. Southern California hypocenter relocation with waveform cross-correlation, part 1: Results using the double-difference method, *Bull. Seism. Soc. Am.* 95, 896–903.

Hicks, S. P., and A. Reitbrock, 2015. Seismic slip on an upper-plate normal fault during a large subduction megathrust rupture, *Nat. Geo*., 8, 955-960, doi:10.1038/ngeo2585.

Hill, E.M., Borrero, J.C., Huang, Z., Qiu, Q., Banerjee, P., Natawidjaja, D.H., Elosegui, P., Fritz, H.M., Suwargadi, B.W., Pranantyo, I.R., Li, L., Macpherson, K.A., Skanavis, V., Synolakis, C.E., and K. Sieh, 2012. The 2010 Mw 7.8 Mentawai earthquake: Very shallow source of a rare tsunami earthquake determined from tsunami field survey and near-field GPS data, *J. Geophys. Res*., 117 (B06402), doi:10.1029/2012JB009159.

House, L.S. and J. Boatwright, 1980. Investigation of two high stress drop earthquakes in the Shumagin seismic gap, Alaska, *J. Geophys. Res*., 85, 7151-7165.

Hudnut, K.W., and J.J. Taber, 1987. Transition from double to single Wadati-Benioff seismic zone in the Shumagin Islands, Alaska, *Geophys. Res. Lett*., 14, 143-146.

Hsu, Y.-J., Simons, M., Avouac, J.-P., Galetzka, J., Sieh, K., Chlieh, M., Natawidjaja, D., Prawirodirdjo, L., and Y. Bock, 2006. Frictional afterslip following the 2005 Nias-Simeulue earthquake, Sumatra, *Science*, 312, 1921–1926

Hyndman, R., Yamano, M., and D. Oleskevich, 1997. The seismogenic zone of subduction thrust faults. *The Island Arc*, 6, 244-260.

Iinuma, T., Hino, R., Kido, M., Inazu, D. Osada, Y., Ito, Y., Ohzono, M., Tsushima, H., Suzuki, S., Fujimoto, H., and S. Miura, 2012. Coseismic slip distribution of the 2011 off the Pacific Coast of Tohoku Earthquake (M9.0) refined by means of seafloor geodetic data, *J. Geophys. Res*., 117 (B07409), doi:10.1029/2012JB009186.

Jarvis A., Reuter, H.I., Nelson, A., and E. Guevara, 2008. Hole-filled seamless SRTM data V4, International Centre for Tropical Agriculture (CIAT), available from http://srtm.csi.cgiar.org.

Kanamori, H., 1997. The energy release in great earthquakes, J. *Geophys. Res.,* 82, 2981-2987.

Kido, M., Osada, Y., Fujimoto, H., Hino, R., and Y. Ito, 2011. Trench-normal variation in observed seafloor displacements associated with the 2011 Tohoku-Oki earthquake *Geophys. Res. Lett*., 38 (L24303), doi:10.1029/2011GL050057.

Kelleher, J.A., 1970. Space-time seismicity of the Alaska-Aleutian seismic zone, *J. Geophys. Res.*, 75, 5745-5756.

Lander, J.F., and P.A. Lockridge, 1989. United States Tsunamis (Including United States Possessions) 1690-1988. Natl. Geophys. Data Center Publ. 41-2, Natl. Ocean. Atmos. Admin., Boulder, CO.

Lees, J.M., 1998. Multiplet analysis at Coso geothermal, *Bull. Seis. Soc. Am*. 88, 1127–1143.

Li, J., Shillington, D.J., Bécel, A., Nedimović, MR., Webb, S.C., Saffer, D.M., Keranen, K.M., and H. Kuehn, 2015. Downdip variations in seismic reflection character: Implications for fault structure and seismogenic behavior in the Alaska subduction zone, *J. Geophys. Res. Solid Earth*, 120, doi:10.1002/2015JB012338.

Lockridge, P.A., and R.H. Smith, 1984. Tsunamis in the Pacific basin: 1900-1983, map, scale 1: 17,000,000, N*atl. Geophys. Data Cent.,* Boulder, Colo.

Lonsdale, P., 1988. Paleogene history of the Kula plate: Onshore evidence and onshore implications. *Geol. Soc. Am. Bull*. 10, 733754.

López, A.M., and E.A. Okal, 2006. A seismological reassessment of the source of the 1946 Aleutian "tsunami" earthquake. *Geophys. J. Intl.*, 165, 835-849. doi: 10.1111/j.1365-246X.2006.02899.x

Menke, W., 1999. Using waveform similarity to constrain earthquake locations, *Bull. Seism. Soc. Am*, 89 (4), 1143-1146.

Miller, T.P., McGimsey, R.G., Richter, D.H., Riehle, J.R., Nye, C.J., Yount, M.E., Dumoulin, J.A., 1998. Catalog of the historically active volcanoes of Alaska. U.S. Geol. Surv. Open-File Report 98-582.

Mori, J., 1983. Dynamic stress drops of moderate earthquakes of the Eastern Aleutians and their relation to a great earthquake, *Bull. Seism. Soc. Am.,* 73, 1077-1097.

Moriya, H., Niitsuma, H., and R. Baria, 2003. Multiplet-clustering analysis reveals structural details within the seismic cloud at the Soultz Geothermal Field, France, *Bull. Seism. Soc. Am.* 93, 1606–1620.

Nadeau, R.M., Foxall, W., and T.V. McEvilly, 1995. Clustering and periodic recurrence of microseismicities on the San Andreas fault at Parkfield, California, *Science,* 267, 503–507.

Newman, A.V., Schwartz, S.Y., Gonzalez, V., DeShon, H.R., Protti, J.M., and L.M. Doorman, 2002. Along-strike variability in the seismogenic zone below Nicoya Peninsula, Costa Rica, *Geophys. Res. Lett*., 29 (20), 1977, doi:10.1029/2002GL015409.

Nishenko, S.P. and K.H. Jacob, 1990. Seismic Potential of the Queen Charlotte-Alaska-Aleutian

Seismic Zone, *J. Geophys. Res.,* 95 (B3), 2511-2532.

Norabuena, E., Dixon, T.H., Schwartz, S., DeShon, H., Newman, A., Protti M., Gonzalez, V., Dorman, L., Flueh, E.R., Lundgren, P., Pollitz, F., and D. Sampson, 2004. Geodetic and seismic constraints on some seismogenic zone processes in Costa Rica, *J. Geophys. Res.,* 109 (B11403), doi:10.1029/2003JB002931

Okal, E.A., Synolakis, C.E., Fryer, G.J., Heinrich, P., Borerro, J.C., Ruscher, C., Arcas, D., Guille, G., Rousseau, D., 2002. A field survey of the 1946 Aleutian tsunami in the far feld. *Seism. Res. Lett*. 73, 490-503

Okal, E.A., and H. Hébert, 2007. Far-field simulation of the 1946 Aleutian tsunami, *Geophys. J. Int.,* 169, 1229-1238.

Pavlis, G.L., 1992. Appraising relative earthquake location errors, *Bull. Seism. Soc. Am.* 82, 836-859.

Phillips, W.S., 2000. Precise microearthquake locations and fluid flow in the geothermal reservoir at Soultz-sous-Forêts, France*, Bull. Seism. Soc. Am.* 90, 212–228.

Plafker, G., Moore, J.C. and G.R. Winkler, 1994. The Geology of Alaska (eds Plafker, G. & Berg, H. C.) *Geological Society of America*, 389-449.

Poupinet, G., Ellsworth W.L., and J. Fréchet, 1984. Monitoring velocity variations in the crust using earthquake doublets: an application to the Calaveras fault, California, *J. Geophys. Res.* 89, 5719–5731.

Ratchkovsky, N.A., Pujol, J., and N.N. Biswas, 1997. Relocation of Earthquakes in the Cook Inlet Area, South Central Alaska, Using the Joint Hypocenter Determination Method. *Bull. Seism. Soc. Am.* 87 (3), 620-636.

Reyners, M. and K.S. Coles, 1982. Fine structure of the dipping seismic zone and subduction mechanics in the Shumagin Islands, Alaska, *J. Geophys. Res.*, 87 (B1), 356-366.

Rubin, A.M., Gillard, D., and J.-L. Got, 1999. Streaks of microearthquakes along creeping faults. *Nature*, 400, 635-641.

Ruff, L.J., and B.W. Tichelaar, 1996. What controls the seismogenic plate interface in subduction zones?, in Subduction: Top to Bottom, vol. 96, 105–111, *American Geophysical Union*.

Savage, J.C., Lisowski, M., and W.H. Prescott, 1986. Strain accumulation in the Shumagin and Yakataga seismic gaps, Alaska. *Science* 231, 585–587

Schaff, D.P., Bokelman, G.H.R., Beroza, G.C., Waldhauser, F., and W.L. Ellsworth, 2002. High-resolution image of Calaveras Fault seismicity. *J. Geophys. Res.,* 107 (B9), 2186,

doi:10.1029/2001JB000633

Schaff, D.P., and G. C. Beroza, 2004. Coseismic and postseismic velocity changes measured by repeating earthquakes, *J. Geophys. Res*., 109 (B10302), doi:10.1029/2004JB003011.

Schaff, D.P., Bokelmann, G.H.R., Ellsworth, W.L., Zanzerkia, E., Waldhauser, F., and G.C. Beroza, 2004. Optimizing correlation techniques for improved earthquake location, *Bull. Seism. Soc. Am*. 94, 705–721.

Schaff, D.P., 2010. Improvements to detection capability by cross-correlating for similar events: a case study of the 1999 Xiuyan, China, sequence and synthetic sensitivity tests. *Geophys. J. Int.,* 180, 829–846, doi: 10.1111/j.1365-246X.2009.04446.x.

Schaff, D.P., and F. Waldhauser, 2005. Waveform cross-correlation-based differential travel-time measurements at the Northern California Seismic Network, *Bull. Seism. Soc. Am.* 95 (6), 2446-2461.

Sella, G.F., Dixon, T.H., and A. Mao, 2002. REVEL: A model for recent plate velocities from space geodesy, *J. Geophys. Res.,* 107 (B4), 2081, doi:10.1029/2000JB000033.

Shearer, P.M., 1997. Improving local earthquake locations using the L1 norm and waveform cross correlation: application to the Whittier Narrows, California, aftershock sequence, *J. Geophys. Res.* 102, 8269–8283.

Shepard, F.P., Macdonald, G.A., and D.C. Cox, 1950. The tsunami of April 1, 1946. *Bull. Scripps Inst. Oceanogr. Univ. Calif.* 5, 391-528

Shillington, D.J., Bécel, A., Nedimović, M.R., Kuehn, H., Webb, S.P., Abers, G.A., Keranen, K.M., Delescluse, M., and G.A. Mattei-Salicrup, 2015. Link between plate fabric, hydration and subduction zone seismicity in Alaska, *Nat. Geo*., 8, 961-965, doi: 10.1038/NGEO2586

Sun, T., Wang, K., Iinuma, T., Hino, R., He, J., Fujimoto, H., Kido, M., Osada, Y., Miura, S., Ohta, Y., and Y. Hu, 2014. Prevalence of viscoelastic relaxation after the 2011 Tohoku-oki earthquake, *Nature*, 514, 84–87, http://dx.doi.org/10.1038/nature13778

Syracuse, E.M., van Keken, P.E., and G.A. Abers, 2010. The global range of subduction zone thermal models, *Phys. Earth and Planetary Interiors*, 183, 73-90.

Syracuse, E.M., and G.A. Abers, 2006. Global compilation of variations in slab depth beneath arc volcanoes and implications, *Geochem. Geophys. Geosyst.,* 7, Q05017, doi:10.1029/2005GC001045.

Thio, H.K., Somerville, P., and Polet, J., 2010. Probabilistic tsunami hazard in California: Pacific Earthquake Engineering Research Center, PEER_ Report 2010–108, 61 p. Available online at http://peer.berkeley.edu/publications/peer_reports.html.

Vallier, T.L., Scholl, D.W., Fisher, M.A., Bruns, T.R., Wilson, F.H., von Huene, R., and A. J. Stevenson, 1994. Geologic framework of the Aleutian arc, Alaska, in Plafker, George, and Berg, H. C., eds., The Geology of Alaska: Geological Society of America, p. 367-388.

Von Huene, R., Miller, J.J., and W. Weinrebe, 2012. Subducting plate geology in three great earthquake ruptures of the western Alaska margin, Kodiak to Unimak, *Geosphere*, 8 (3), 628–644.

Waldhauser, F.,2001. hypoDD: A computer program to compute double-difference hypocenter locations, (updated: Version 2.1b, 2011), U.S. Geol. Surv. Open File Rep., 01-113, Menlo Park, California.

Waldhauser, F., and W.L. Ellsworth, 2000. A double-difference earthquake location algorithm: Method and application to the northern Hayward fault, California *Bull. Seism. Soc. Am.*, 90, 1353-1368.

Waldhauser, F., and W.L. Ellsworth, 2002. Fault structure and mechanics of the Hayward Fault, California, from double-difference earthquake locations, *J. Geophys. Res.* 107 (B3), 2054, doi:10.1029/2000JB000084

Waldhauser, F. and D.P. Schaff, 2008. Large-scale relocation of two decades of Northern California seismicity using cross-correlation and double-difference methods*, J. Geophys. Res*. 113, B08311, doi:10.1029/2007JB005479

Waldhauser, F., Schaff, D.P., Diehl, T., and E.R. Engdahl, 2012. Splay faults imaged by fluid-driven aftershocks of the 2004 Mw 9.2 Sumatra-Andaman earthquake. *Geology*, 40, (3), 243-246, doi:10.1130/G32420.1